Investigation of the Performance and Benefits of Lightweight SCC Prestressed Concrete Bridge Girders and SCC Materials

Dr. Paul H. Ziehl
Dr. Dimitris C. Rizos
Dr. Juan M. Caicedo
Francisco Barrios
Robert B. Howard
Alexander S. Colmorgan

submitted to:

The South Carolina Department of Transportation
and
The Federal Highway Administration

2009

This research was sponsored by the South Carolina Department of Transportation and the Federal Highway Administration. The opinions, findings and conclusions expressed in this report are those of the authors and not necessarily those of the SCDOT or FHWA. This report does not comprise a standard, specification or regulation.

Department of Civil and Environmental Engineering
300 Main Street
Columbia, SC 29208
(803) 777 3614
cee@engr.sc.edu

Report No. FHWA-SC-09-02
CEE-SG-0662-01

Technical Report Documentation Page

1. Report No. FHWA-SC-09-02	2. Government Accession No.	3. Recipient's Catalog No.
4. Title and Subtitle Investigation of the Performance and Benefits of Lightweight SCC Prestressed Concrete Bridge Girders and SCC Materials		5. Report Date October 2009 6. Performing Organization Code
7. Author(s) P. Ziehl, D. Rizos, J. Caicedo, F. Barrios, R. Howard, and A. Colmorgan		8. Performing Organization Report No. *CEE-SG-0662-01*
9. Performing Organization Name and Address University of South Carolina Department of Civil and Environmental Engineering 300 Main Street Columbia, SC 29208		10. Work Unit No. (TRAIS) 11. Contract or Grant No. SPR 662
12. Sponsoring Agency Name and Address South Carolina Department of Transportation Office of Materials and Research 1406 Shop Road Columbia, South Carolina 29201		13. Type of Report and Period Covered Final Report September 2005 to September 2009 14. Sponsoring Agency Code

Supplementary Notes:

Prepared for the SCDOT in cooperation with the Federal Highway Administration

16. Abstract

Self-Consolidating Concrete (SCC), also known as self-compacting concrete, is a highly flowable concrete that is capable of filling formwork without using conventional vibration techniques while maintaining its cohesiveness. Currently SCC is used in many commercial applications and is gaining acceptance from many state DOTs for use in precast prestressed bridge girders. SCC is advantageous for many reasons including: (i) the number of workers required and the noise produced by mechanical vibration is reduced significantly; (ii) the safety hazards of workers on top of the girders is eliminated; (iii) the surface finish of the concrete can be more smooth than that of conventional concrete; (iv) formwork damage from mechanical vibration is reduced, increasing the life of the forms; (v) reinforcing bar configurations are not damaged; (vi) improved bond of concrete to prestressed strands could reduce strand end-slip and the top bar effect; and (vii) SCC is able to fill complicated shapes and congested reinforcement areas better than vibrated concrete.

This research report addresses the design and resulting properties of normal weight mix designs that were developed at the University of South Carolina and the testing of full-scale lightweight concrete AASHTO Type III girders. Both aspects address material testing for properties in the fresh and hardened states. Fresh properties include slump spread, filling ability, passing ability, and air content. Hardened properties include compressive strength, modulus of elasticity, creep, shrinkage, chloride permeability, and freeze-thaw durability. Testing of the girders includes transfer length, end-slip, midspan deflections, midspan strains, and internal curing temperatures. Summaries and conclusions are provided along with recommended guidelines for implementation.

17. Key Words *high-performance concrete, lightweight concrete, prestressed concrete bridge girders, structural testing, transfer length, flexural strength*	18. Distribution Statement No restriction		
19. Security Classif. (of this report) Unclassified	20. Security Classif. (of this page) Unclassified	21. No. of Pages 182	22. Price

Form DOT F 1700.7 (8-72) **Reproduction of completed page authorized**

PRINTING

This report was printed as follows:

Cost: $ 133.75

Total number of documents: 50

Cost per unit: $ 2.68

ACKNOWLEDGEMENTS

The authors thank the SCDOT for sponsorship of this research and especially the timely and helpful input of the Steering Committee: Merrill Zwanka (Chairman), Mike Sanders, Terry Swygert, Aly Hussein, Bill Mattison, David Meetze, Bener Amado, Herb Cooper, and Ken Johnson (FHWA).

The authors also thank all the companies that contributed materials and time to make this project possible. This includes Florence Concrete Products, North Carolina Stalite, Holcim Cement Company, Euclid Chemical Company, Boral Material Technologies, Hardaway Concrete, Ready-mix Concrete Company, Glasscock Sand, and W.R. Grace and Company. The technical input of Reid Castrodale and Jody Wall are especially appreciated. The input of J. R. Parimuha of Florence Concrete Products and Richard Potts of Standard Concrete Products is also gratefully acknowledged. The authors would also like to thank Blake Stassney of the University of Texas, Austin for input related to the creep frames.

The authors would also like to thank their associates Avery Fox, Brad Tune, Zhiwei Liu, Yizhuo Chen, Justin Inman, David Harris, Shawn Sweigart, Daniel Learn, and Heramb Haldankar for all of their hard work and help throughout the duration of this project.

ABSTRACT

Self-Consolidating Concrete (SCC), also known as self-compacting concrete, is a highly flowable concrete that is capable of filling formwork without using conventional vibration techniques while maintaining its cohesiveness. Currently SCC is used in many commercial applications and is gaining acceptance from many state DOTs for use in precast prestressed bridge girders. SCC is advantageous for many reasons including: (i) the number of workers required and the noise produced by mechanical vibration is reduced significantly; (ii) the safety hazards of workers on top of the girders is eliminated; (iii) the surface finish of the concrete can be more smooth than that of conventional concrete; (iv) formwork damage from mechanical vibration is reduced, increasing the life of the forms; (v) reinforcing bar configurations are not damaged; (vi) improved bond of concrete to prestressed strands could reduce strand end-slip and the top bar effect; and (vii) SCC is able to fill complicated shapes and congested reinforcement areas better than vibrated concrete.

This research report addresses the design and resulting properties of normal weight mix designs that were developed at the University of South Carolina and the testing of full-scale lightweight concrete AASHTO Type III girders. Both aspects address material testing for properties in the fresh and hardened states. Fresh properties include slump spread, filling ability, passing ability, and air content. Hardened properties include compressive strength, modulus of elasticity, creep, shrinkage, chloride permeability, and freeze-thaw durability. Testing of the girders includes transfer length, end-slip, midspan deflections, midspan strains, and internal curing temperatures. Summaries and conclusions are provided along with recommended guidelines for implementation.

TABLE OF CONTENTS

Page No.

COPYRIGHT i
ACKNOWLEDGEMENTS ii
ABSTRACT iii
TABLE OF CONTENTS iv
LIST OF TABLES vi
LIST OF FIGURES vii
LIST OF SYMBOLS AND ABBREVIATIONS xi

CHAPTER 1 – INTRODUCTION 1
1.1 Background 1
1.2 Definition of Self-Consolidating Concrete (SCC) 2
1.3 SCC for Bridge Girders 3
1.4 Objectives 3
1.5 Organization 4

CHAPTER 2 – LITERATURE REVIEW 5
2.1 Introduction 5
2.2 Materials Considerations for Normal Weight SCC 6
2.3 Benefits of SCC versus Conventional Concrete 16
2.4 Materials Considerations for SCLC 17
2.5 Considerations for Girders Fabricated with SCLC 22

CHAPTER 3 – DEVELOPMENT OF MIX DESIGNS 44
3.1 Introduction 44
3.2 Concrete Constituents 44
3.3 Laboratory Mix Design Studies 46
3.4 Curing Procedures 48
3.5 Mix Designs for Companion Specimens (AASHTO Type III Girders) 48

CHAPTER 4 – MATERIAL CHARACTERIZATION PROCEDURES 64
4.1 Introduction 64
4.2 Fresh Properties 64
4.3 Hardened Properties 64

CHAPTER 5 – GIRDER FABRICATION AND INSTRUMENTATION 77
5.1 Introduction 77
5.2 Fabrication of Girders 77
5.3 Fresh Property Tests Conducted 80

CHAPTER 6 – LOADING OF GIRDERS 96
6.1 Introduction 96
6.2 Specimen Details 96

6.3 Test Setup....96
6.4 Instrumentation....97
6.5 Load Testing Procedure....98

CHAPTER 7 – RESULTS AND PERFORMANCE....111
7.1 Introduction....111
7.2 Material Performance....111
7.3 Girder Performance....117

CHAPTER 8 – SUMMARY AND CONCLUSIONS....157
8.1 Introduction....157
8.2 Fresh Properties....157
8.3 Hardened Properties....158
8.4 Full-scale Girders....162

CHAPTER 9 – RECOMMENDATIONS AND GUIDELINES....165
9.1 Introduction....165
9.2 Guidelines....165
9.3 Design Considerations....169

REFERENCES....174

APPENDIX....182

LIST OF TABLES

Table 2.1 Test methods for fresh SCC properties (PCI, 2003a) 26
Table 2.2 Slump flow parameter determination (PCI, 2003a) 27
Table 2.3 L-box ratio parameter determination (PCI, 2003a) 28
Table 2.4 U-box ranking parameter determination (PCI, 2003a) 29
Table 2.5 Performance grades for high performance structural concrete (FHWA, 2005) 30
Table 2.6 Values from α and β constants for equation 2.1 (ACI 318-02) 31
Table 2.7 Modulus of elasticity comparison - SCC and HESC (Naito et. al., 2005) 31
Table 2.8 Mix proportions from Raghaven et. al. (2002) 32

Table 3.1 Approved coarse aggregate sources (SCDOT, 2007) 50
Table 3.2 Approved fine aggregate sources (SCDOT, 2007) 51
Table 3.3a Source of materials for USC laboratory mixes 52
Table 3.3b Source of materials for fabricator mixes (Florence Concrete Products) 53
Table 3.4a U.SC trial mixes - 1 of 2 54
Table 3.4b U.SC trial Mixes - 2 of 2 55
Table 3.4c Fabricator mix designs (Florence Concrete Products) 56
Table 3.5 Final mix matrix – laboratory and producer (FCP) mixes 57

Table 7.1 Compressive strength and E_c data, Batch No. 1 123
Table 7.2 Compressive strength and E_c data, Batch No. 2 123
Table 7.3 Compressive Strength and E_c data, Batch No. 3 123
Table 7.4 Compressive strength and E_c data, SCLC 124
Table 7.5 Compressive Strength and E_c data, HESLC 124
Table 7.6 Suggested lightweight concrete mix design 125
Table 7.7 Tensile strength data, SCLC 126
Table 7.8 Tensile strength data, HESLC 126
Table 7.9 Rapid chloride permeability data 126
Table 7.10 CLT evaluation - SCLC girder No. 1 127
Table 7.11 CLT evaluation – SCLC girder No. 2 (fatigue girder) 128
Table 7.12 CLT evaluation – HESLC girder 129
Table 7.13 24h load test deflection data (all girders) 130
Table 7.14 24h load test evaluation (all girders) 130

LIST OF FIGURES

Figure 2.1 Surface chemistry of cement particles and super-plasticizers (SCI, 2003) .33
Figure 2.2 Blocking of concrete by aggregate arching 33
Figure 2.3 Spread test and impervious surface 34
Figure 2.4a VSI rating 0 (PCI, 2003a).....35
Figure 2.4b VSI rating 1 (PCI, 2003a).....35
Figure 2.4c VSI rating 2 (PCI, 2003a).....36
Figure 2.4d VSI rating 3 (PCI, 2003a).....36
Figure 2.5 L-box testing apparatus 37
Figure 2.6 Compressive strength gain (Naito et. al., 2005) 38
Figure 2.7a Compressive strength versus concrete age (Bailey, 2005) 39
Figure 2.7b Modulus of elasticity versus concrete age (Bailey, 2005).....39
Figure 2.8a Creep strain response (Raghaven, 2002) 40
Figure 2.8b Drying shrinkage at 28 days (Raghaven, 2002) 40
Figure 2.9a Creep response (Naito et al., 2005) 41
Figure 2.9b Shrinkage response (Naito et al., 2005).....41
Figure 2.10 V-funnel test 42
Figure 2.11 Wet seive segregation test 42
Figure 2.12 Column segregation test 43

Figure 3.1 Sieve analysis of #67 coarse aggregate 58
Figure 3.2 Sieve analysis of FA-10 fine aggregate.....58
Figure 3.3 Sieve analysis of #789 coarse aggregate 59
Figure 3.4a Coarse aggregate storage bin 60
Figure 3.4b Fine aggregate storage bin.....60
Figure 3.5 2.5 cu. ft. mixer in U.SC laboratory 61
Figure 3.6 6 cu. ft. mixer in U.SC laboratory 61
Figure 3.7a Small syringe for admixture measurement 62
Figure 3.7b Large syringe for admixture measurement.....62
Figure 3.8 Long-term temperature curing data 63
Figure 3.9 Long-term relative humidity curing data.....63

Figure 4.1 Compressive loading apparatus 72
Figure 4.2 Schematic of creep frames.....73
Figure 4.3 Railcar springs at base of creep frame.....74
Figure 4.4 Mechanical strain gage and creep specimen 74
Figure 4.5 Digital length comparator test setup.....75
Figure 4.6 Permeability sample preparation 75
Figure 4.7 Rapid chloride permeability test setup 76
Figure 4.8 Freeze-thaw chamber.....76

Figure 5.1 Dimensions of AASHTO type III girder 82
Figure 5.2 Prestressing strand layout 82
Figure 5.3 Reinforcement pattern 83
Figure 5.4 Reinforcing bar and girder appearance upon arrival 83

Figure 5.5 Vibrating-wire strain gage inside girder....84
Figure 5.6 Sister bar strain gage....84
Figure 5.7 Temperature gage (SmartButton)....85
Figure 5.8 Temperature gage installation layout....86
Figure 5.9 Internal instrumentation layout....86
Figure 5.10 Transfer length measurement....86
Figure 5.11 Demec point layout....87
Figure 5.12 Demec points for transfer length calculations....87
Figure 5.13 Endslip measurement (from *FHWA SA-96-075*)....88
Figure 5.14 Endslip measurement....89
Figure 5.15 Camber measurement technique....89
Figure 5.16 Piano wire attachment....89
Figure 5.17 Typical girder end and anchor bolt placement....90
Figure 5.18 Weight for camber measurement....90
Figure 5.19 Anchor bolt for camber measurement....91
Figure 5.20 De-tensioning sequence....91
Figure 5.21 Cut prestressing strands (top flange)....92
Figure 5.22 Cut prestressing strands (bottom flange)....92
Figure 5.23 Slump cone....93
Figure 5.24 Spread test (prior)....93
Figure 5.25 Spread test (subsequent)....94
Figure 5.26 U-box apparatus....94
Figure 5.27 L-box apparatus....95
Figure 5.28 Air content apparatus....95

Figure 6.1 Girder and deck dimensions for parallel test program....103
Figure 6.2 Deck dimensions for current test program....103
Figure 6.3 Roller connection (simply supported)....104
Figure 6.4 Test setup in laboratory (lightweight girder left, normal weight girder right)....104
Figure 6.5 Test setup in laboratory (both girders lightweight)....105
Figure 6.6 Static loading apparatus....105
Figure 6.7 Hydraulic rams and plates....106
Figure 6.8 Electric pump....106
Figure 6.9 Girder internal instrumentation....107
Figure 6.10 External instrumentation (elevation view)....108
Figure 6.11 External instrumentation (viewed from below)....108
Figure 6.12 Cracks marked during load holds....109
Figure 6.13 Loading profile for CLT method....109
Figure 6.14 Load profile for SCLC No. 1 and HESC girders....110
Figure 6.15 Load profile for SCLC girder No. 2 (after fatigue loading)....110

Figure 7.1 Compressive strength gain with time....131
Figure 7.2 Predicted vs. measured E_c at 28 days....132
Figure 7.3 Predicted vs. measured E_c at 28 days....132
Figure 7.3 Shrinkage vs. time, Batch No. 1....133

Figure 7.4 Shrinkage vs. time, Batch No. 2 133
Figure 7.6 Shrinkage vs. time, Batch No. 3 133
Figure 7.7 Shrinkage vs. time, SCC 134
Figure 7.8 Shrinkage vs. time, HESC 134
Figure 7.9 Creep strain vs. time, Batch No. 1 135
Figure 7.10 Creep strain vs. time, Batch No. 2 135
Figure 7.11 Creep strain vs. time, SCC 136
Figure 7.12 Creep strain vs. time, HESC 136
Figure 7.13 Freeze-thaw degradation, Batch No. 1 137
Figure 7.14 Freeze-thaw degradation, Batch No. 2 137
Figure 7.15 Freeze-thaw weight changes, Batch Nos. 1 - 3 138
Figure 7.16 Freeze-thaw setup and specimens 138
Figure 7.17 Sample chloride permeability readout 139
Figure 7.18a Temperature profile – TG1 140
Figure 7.18b Temperature profile – TG2 140
Figure 7.19a End slip – SCLC girder No. 1 141
Figure 7.19b End slip – SCLC girder No. 2 141
Figure 7.19c End slip – HESLC girder 141
Figure 7.20a Transfer length – SCLC girder No. 1 142
Figure 7.20b Transfer length – SCLC girder No. 2 142
Figure 7.20c Transfer length – HESLC girder 142
Figure 7.21 Camber – all girders 143
Figure 7.22 Prestress losses – all girders 143
Figure 7.23 CLT method, load vs. displacement (all girders) 144
Figure 7.24a CLT method, repeatability (SCLC girder No. 1) 145
Figure 7.24b CLT method, permanency (SCLC girder No. 1) 145
Figure 7.24c CLT method, deviation from linearity (SCLC girder No. 1) 145
Figure 7.25a CLT method, repeatability (SCLC girder No. 2) 146
Figure 7.25b CLT method, permanency (SCLC girder No. 2) 146
Figure 7.25c CLT method, deviation from linearity (SCLC girder No. 2) 146
Figure 7.26a CLT method, repeatability (HESLC girder) 147
Figure 7.26b CLT method, permanency (HESLC girder) 147
Figure 7.26c CLT method, deviation from linearity (HESLC girder) 147
Figure 7.27a Load vs. displacement (SCLC girder No. 2) 148
Figure 7.27b Load vs. strain (SCLC girder No. 2) 148
Figure 7.28 24h load test – displacement vs. time 149
Figure 7.29 24h load test – evaluation criteria 149
Figure 7.30 Load vs. displacement to failure (all girders) 150
Figure 7.31a Failure mode - SCLC girder No. 1 151
Figure 7.31b Failure mode - SCLC girder No. 1 151
Figure 7.32a Failure mode - HESLC girder 152
Figure 7.32b Failure mode - HESLC girder 152
Figure 7.33a Failure mode - SCLC girder No. 2 (fatigue girder) 153
Figure 7.33b Failure mode - SCLC girder No. 2 (fatigue girder) 153
Figure 7.33c Failure mode - SCLC girder No. 2 (fatigue girder) 154

Figure 7.33d Failure mode - SCLC girder No. 2 (fatigue girder).....154
Figure 7.33e Failure mode - SCLC girder No. 2 (fatigue girder).....155
Figure 7.33f Demolition - SCLC girder No. 2 (fatigue girder) 155
Figure 7.33g Demolition - SCLC girder No. 2 (fatigue girder).....156

LIST OF SYMBOLS AND ABBREVIATIONS

γ_c = product of applicable correction factors for creep
γ_{sh} = product of applicable correction factors for shrinkage
ΔL_x = the length change of a specimen at any age (percent)
ε_2 = the strain produced by the stress S_2
ε_{cr} = creep strain
ε_{tot} = total strain
ε_e = elastic strain
ε_{sh} = shrinkage strain
$\varepsilon_{sh\,t}$ = the total shrinkage at any time *t* after shrinkage is considered
$\varepsilon_{sh\,u}$ = the ultimate shrinkage strain
Ψ = creep coefficient
$\mu\varepsilon$ = micro-strain (strain x 10^6)
ν_u = ultimate creep coefficient
ν_t = creep coefficient at time t (ratio of creep strain to initial strain)
f'_c = concrete compressive strength at given time (in days)
f'_{ci} = concrete compressive strength at strand release
f_{ct} = concrete tensile strength
k = spring constant (in relation to creep frames)
k_f = concrete strength factor
k_s = size factor
k_{hs} = humidity factor for shrinkage
k_{td} = time development factor
t = time (measured in days)
24h LT = 24 hour load test
AE = air entrainer (also air entraining/air entrainment)
AEA = air entraining admixture
ASTM = American Society for Testing and Materials
CLT = cyclic load test
CRD = the difference between the comparator reading of the specimen and the reference bar at any age (in.)
$CRD_{initial}$ = initial value of CRD (in.)
D_s = dead load due to superimposed loads
D_w = dead load due to self weight
DWT = draw wire transducer
E'_c = effective modulus of concrete (for prediction of creep)
E_c = modulus of concrete
EFCA = The European Guidelines for Self-Compacting Concrete, Specification, Production and Use
EFNARC = European Federation of Producers and Applicators of Specialist Products for Structures
FHWA = Federal Highway Administration
G = gage length (in.)
GGBFS = ground granulated blast furnace slag

H = relative humidity (percent)
HESC = high early strength concrete (normal weight)
HESLC = high early strength lightweight concrete
HESLC girder = high early strength lightweight concrete girder
HLSCC = high strength lightweight self consolidating concrete
HPC = high performance concrete
HRWR = high range water reducer
HSLC = high strength lightweight concrete
HSNWC = high strength normal weight concrete
I_R = index of repeatability (or repeatability index)
IBC = International Building Code
JSCE = Japanese Society of Civil Engineering
K1 = adjustment factor related to prediction of E_c (refer to governing document as described in report)
K2 = adjustment factor related to prediction of E_c (refer to governing document as described in report)
L = live loads not including construction or environmental loads
L_r = live loads during maintenance due to workers and equipment
LC = lightweight concrete or lightweight coarse aggregate (dependent on use)
LF = lightweight fine aggregate
LVDT = linear variable displacement transducer
LWA = lightweight aggregate
LWAC = lightweight aggregate concrete
NC = normal concrete (normal in terms of weight, also non-self compacting)
PC = prestressed concrete
PCI = Precast/Prestressed Concrete Institute
P_{max} = maximum applied load (in relation to creep frames)
R = rain load
RC = reinforced concrete
RCPT = rapid chloride permeability test
S = snow load (in relation to test load magnitude for CLT and 24h LT methods)
S = maximum travel distance (in relation to creep frames)
S = surface area (in relation to prediction of creep and shrinkage)
S_1 = the stress in psi that corresponds to a strain of $50x10^{-6}$
S_2 = 40 % of the ultimate strength of the concrete (psi)
S_T : Settlement value at given time t
S_{T-5}: Settlement value at time T - 5 min.
SB = sister bar
SCC = self consolidating concrete (normal weight)
SCDOT = South Carolina Department of Transportation
SCLC girder No. 1 = self consolidating lightweight concrete girder, specimen no. 1
SCLC girder No. 2 = self consolidating lightweight concrete girder, specimen no. 2
SR = segregation ratio
STR = relative settlement per hour
T_V = total time spent by the mix while flowing through the V-funnel apparatus

TG = temperature gage
V = volume
VMA = viscosity modifying admixture
WR = water reducer

CHAPTER 1
INTRODUCTION

1.1 Background

Proper concrete compaction is very important to the structural integrity and overall quality in hardened concrete. Therefore, normal concrete requires internal and external vibration to properly compact the concrete and ensure that it completely fills all voids in the formwork eliminating unwanted entrapped air. Self-Consolidating Concrete (SCC) eliminates the need for vibration since it is able to consolidate under its own weight due to its increased workability. SCC was first introduced in Japan in the late 1980s by researchers at the University of Tokyo. The need for this new type of concrete was brought about by problems associated with poor compaction due to a decrease in skilled laborers in Japan.

Potentially, SCC could reduce the number of workers required to place the concrete while adding other benefits and improving material properties. By using chemical admixtures, primarily super-plasticizers, and by decreasing the coarse-to-fine aggregate ratios the concrete is able to flow much better while preventing segregation. Also, since the water demand is reduced due to the use of super-plasticizers, the strength and possibly the durability can be increased.

Since its introduction SCC has been widely accepted in Japan and all over the world including the United States where it was introduced in the late 1990's. Although it was first introduced in the commercial market, state agencies have recently been gaining interest in the material for use in highway bridge construction. The reduction in required laborers could potentially save DOTs money by lowering production cost for the fabricator.

The rapid appearance of new materials, construction techniques and analysis methods poses a real challenge for engineers, designers and researchers in our society. Recent innovations in the concrete industry such as self-consolidating concrete (SCC) and its lightweight version (SCLC), as well as nano-flexible and self-cleaning concrete among others, have pushed harder for the development of new tools and methodologies that permit a quick implementation and the commercialization of these novel and promising materials. However, safe application of these technological advancements requires prior long and meticulous real scale testing in the lab or in-situ in order to guarantee the reliability of the system and to evaluate structural performance and response to service demands.

SCLC constitutes one of the many cases where the lack of guidance in the design codes (Bardhan-Roy, 1993) and the limited applicability of our current in-situ load testing procedures (Galati et al., 2008) do not allow an effective and detailed assessment of the material behavior. Moreover, acceptance criteria at hand have often been developed long in the past for specific engineering practices and materials which are no longer relevant to our current construction technology and necessities. Alternative load testing and

nondestructive evaluation methods which can avoid these pitfalls are under development by researchers and engineers worldwide. Nonetheless, there is a divergence of opinions about the sensitivity of the examination processes to changes in the nature of the material (metals, concrete, polymers, etc.), type of load (static or dynamic) and type of structure (bridges, buildings, tanks, etc).

1.2 Definition of Self-Consolidating Concrete (SCC)

In the United States the concrete industry understands SCC as "self-consolidating concrete" while the term "self compacting concrete" is generally accepted in all other parts of the world. This is only a matter of choice since compaction and consolidation can be used interchangeably. SCC is defined as a highly workable concrete that fills formwork without consolidation, and without undergoing significant segregation. Alternative definitions from two widely accepted SCC specifications can be seen below;

> **Self-Consolidating Concrete** - *"A highly workable concrete that can flow through densely reinforced or complex structural elements under its own weight and adequately fill voids without segregation or excessive bleeding without the need for vibration."*- from *Interim Guidelines for the Use of Self-Consolidating Concrete in Precast /Prestressed Concrete Institute Member Plants* (2003).
>
> **Self-Compacting Concrete –** *"Concrete that is able to flow and consolidate under its own weight, completely filling the formwork even in the presence of dense reinforcement, whilst maintaining homogeneity and without the need for any additional compaction."* - from *The European Guidelines for Self-Compacting Concrete – Specification, Production, and Use* (2005).

The requirements for SCC are similar to that of normal concrete in the hardened state. However, SCC in its hardened state should also classify as a High Performance Concrete (HPC) conforming to the requirements of the HPC Performance Criteria developed by the Federal Highway Administration (FHWA). The HPC Performance Criteria and testing methods will be discussed in later chapters. Additionally, in the fresh state the concrete mix must be examined and classified using different characteristics concerning the workability of the concrete. These fresh properties are generally known as filling ability, passing ability, and stability. PCI defines these properties as (PCI, 2003):

- ***Filling ability:*** "The ability of SCC to flow under its own weight (without vibration) into and completely fill all spaces within intricate formwork, containing obstacles, such as reinforcement."
- ***Passing ability:*** "The ability of SCC to flow through openings approaching the size of the mix coarse aggregate, such as the spaces between steel reinforcing bars, without segregation or blocking."
- ***Stability:*** "The ability of SCC to remain homogeneous during transport, placing, and after placement."

Generally, if these three requirements are met, then the concrete can be classified as a self-consolidating mix in the fresh state. Methods for testing these properties are still being developed and will be discussed in later chapters.

1.3 SCC for Bridge Girders

Due to the ease of construction and quality control in precast/prestressed girders, state DOTs often elect to use them on their bridges instead of steel or cast-in-place girders. These girders are fabricated at a precast plant under regulated conditions, and then carried to the bridge site where they are lifted into place and cast into the bridge system. Typically, precast plants have very strict quality control measures to ensure consistency and durability in all of their products. Also, the faster precast plants can get products off the production line and into the curing yards, the more economical they can be.

For these reasons, SCC may be a very good choice of concrete used in prestressed bridge girders and other bridge elements. Since precast plants already practice extensive quality control techniques, batching and mixing SCC would not be difficult. With SCC, there would be no need for extra laborers to vibrate the concrete and finishing should be minimal. This would shorten the turnover time for girders, and save the states additional money in the long run.

The use of lightweight concrete (110 – 125 pcf) for bridge girders likewise has several advantages. The most obvious is the reduction in shipping and erection costs when compared to girders fabricated with conventional weight concrete. This is becoming more important and girder designs are continually increasing in length to reduce construction costs. There may also be reason to believe that the durability of lightweight concrete may be equal to or in some cases superior to conventional concrete girders. This has been attributed to the similarity between the modulus of the lightweight aggregate and the cement paste itself, leading to fewer micro-cracks between these two components of the concrete mixture. Lightweight girders have some special considerations, including the potential for reduced stiffness and increased shrinkage when compared to conventional concrete girders.

1.4 Objectives

The primary objective of this project is to evaluate fresh and hardened properties of self-consolidating concrete, including self-consolidating lightweight concrete (SCLC), as it pertains to prestressed bridge girders using materials readily available in the State of South Carolina.

The freshly mixed SCC properties are characterized according to test procedures described in current literature on SCC and SCLC. The hardened properties investigated include mechanical properties and durability characteristics using the FHWA HPC (High Performance Concrete) performance grade criteria. The mechanical properties tested in this program were compressive strength (ASTM C39) and modulus of elasticity (ASTM C469). Durability characteristics studied pertain to creep (ASTM C512), shrinkage

(ASTM C157), chloride permeability (ASTM C1202), and freeze-thaw resistance (ASTM C666).

Three full-scale AASHTO Type III prestressed concrete girders [two SCLC and one high early strength lightweight concrete (HESLC)], were evaluated for immediate and long-term camber, end-slip, transfer length, stiffness, and behavior under static and fatigue loading.

1.5 Organization

This report presents an investigation of SCC and its properties for use in prestressed bridge girder construction in South Carolina. It consists of characterization of SCC and SCLC materials, characterization of full-scale lightweight concrete girders, and a recommended set of guidelines for the use of SCC and SCLC. Chapter 2 reviews the current literature on SCC, including SCLC, and discusses the properties and benefits in comparison to normal concrete. Chapter 3 presents the development of mix designs for SCC, including SCLC, and describes the constituent materials used. Material characterization techniques and procedures are presented in Chapter 4. The girder fabrication and instrumentation procedures are described in Chapter 5, and the loading procedures for the girders are described in Chapter 6. The results and performance of both materials and girders are presented in Chapter 7. Finally, the conclusion to this research is in Chapter 8 followed by Chapter 9 which addresses guidelines.

CHAPTER 2
LITERATURE REVIEW

2.1 Introduction

There is a vast amount of literature on SCC with respect to material properties in the fresh and hardened states. The early research in this field was conducted at the Kochi University of Technology in Kochi Japan by researchers Okamura and Ouchi in the 1980s (Zia, 2005). Since then the idea of a high performance SCC has become a reality and is gaining acceptance among the civil engineering community. In the past decade, a number of agencies have hosted SCC conferences and workshops to promote the use of this innovative type of concrete. For instance, *The First North American Conference on the Design and Use of SCC* brought together over 300 participants from across the globe who shared their knowledge and experience on SCC.

Several major industry leaders such as PCI in the USA and EFNARC in Europe have developed specifications and guidelines for the use of SCC. Many State DOTs are also currently conducting research on SCC and developing their own specifications for use in highway structures. This chapter includes a review of the literature pertaining to the fresh (plastic) and hardened concrete properties, the tests that quantify them, and the current specifications on SCC.

Self consolidating lightweight concrete (SCLC) is one of the latest innovations in concrete technology. This new type of concrete was developed to offer enhanced durability due to its self-compaction ability and its low water-cement ratio. As with normal weight SCC, these special properties allow SCLC to penetrate through formwork areas with complex geometry as well as highly-congested reinforcing, minimizing voids in the mixture and hence providing a better quality in the construction of the structural members along with a reduction of labor. In addition, SCLC also has a further impact on the construction cost by reducing the total dead load of the structural members up to 25%, and requiring less maintenance than a similar steel structure (Bardhan-Roy, 1993). This may represent considerable savings in large scale construction that could not otherwise be attained with the use of standard self-consolidating concrete (SCC).

SCLC can achieve great strength and durability while offering excellent workability (Hwang and Hung, 2005), and its mechanical properties are in general either competitive or superior to those in conventional lightweight concrete (LC) and SCC (Lo et al., 2007). SCLC has already been implemented successfully in large scale bridge construction (Ohno et al., 1993; and Melby et al., 1996) and its manufacturing process and rational mix-design methods, as well as testing and acceptance criteria, have undergone substantial progress in recent years; nevertheless, SCLC structures remain rare due to the relative novelty of the material and the lack of guidance in the construction and building codes.

This chapter is divided into four main parts:

- Materials considerations for normal weight SCC
- Benefits of SCC versus conventional concrete
- Materials considerations for SCLC
- Considerations for girders fabricated with SCLC

2.2 Materials Considerations for Normal Weight SCC

Constituent Materials: High strengths in High Performance Concrete (HPC) are generally achieved by lowering the water/cement ratio of the concrete mix while using mineral admixtures or chemical admixtures to maintain the workability of the concrete. The same concept is applied to SCC except that the aggregate proportions are also adjusted to achieve maximum flowability while keeping the mix from segregating (separation of paste and aggregates). According to the Federal Highway Administration (FHWA, 2004) SCC can be designed as the "Powder-type", "VMA-type", or the "Combined-type". The powder-type of SCC uses increased powder content around 750 - 900 lbs/yd^3 along with super-plasticizers to achieve required strength and workability. The VMA type uses a smaller amount of powder and super-plasticizer, but introduces a viscosity modifying admixture to control segregation caused by increased fluidity. The combination method uses super-plasticizers, increased powder content, and a small amount of VMA to achieve the desired workability (Berke et al., 2003).

Aggregate gradation also plays an important role in the workability of SCC mixes. Khayat et al. (2003) studied the significance of aggregate packing density on the fresh properties of SCC. They tested 32 mixes using both discontinuously and continuously graded aggregates. The gradation of the fine and coarse aggregate combinations is quantified using the aggregate packing density. By definition, this is the volume of solids per unit volume (Quiroga, 2004). Khayat and his co-workers (Khayat et al., 2003) determined from this research that by optimizing the packing density, or improving the overall gradation of the combined aggregate system the viscosity of the cement paste could be reduced. Therefore, they could lower the amount of super-plasticizer needed to obtain the desired spread and, thus, lower material costs.

Concrete admixtures are additional ingredients in concrete that enhance the plastic and hardened properties of the material such as workability, setting time, chloride resistance, and air content. In general, there are two types of admixtures used in concrete production, i.e., mineral admixtures and chemical admixtures. The most common mineral admixtures used today are fly ash, silica fume, and ground granulated blast furnace slag (GGBFS). These materials improve quality of the concrete while also reducing the cement content and saving costs. Most SCC mixes employ some volume of fly ash and/or silica fume to increase the workability of the fresh concrete, and to reduce chloride permeability of the hardened material.

The replacement amounts for mineral admixtures are unique to each SCC application and should be evaluated to meet specific performance criteria. For example, in prestressed

applications it is common to see from 0 – 20 % replacement of cement with fly ash (Shadle, 2003). After evaluating seven SCC mixes of varying fly ash and accelerator dosages researchers have shown that a 10 % fly ash replacement with 24 oz/cwt of accelerator produced excellent strength and reduced cost by 6 % from the control SCC batch (Shadle, 2003).

Chemical admixtures are used for water-reduction, air-entrainment, acceleration, retardation, and viscosity modification. Water-reducers and viscosity modifiers are the key chemical admixtures that give SCC its self-leveling quality. The water-reducing agents in SCC are generally known as superplasticizers. These super-plasticizers cause dispersion of the cement particles, releasing the water molecules trapped in the cement conglomerations, and thus, improve workability. Super-plasticizer technology has been improving over the past few decades and continues to draw much attention among admixture experts. The current mechanisms that superplasticizers rely on are electrostatic repulsion, steric stabilization, or a combination of the two that is termed 'electro-steric stabilization'.

Figure 2.1 shows surface chemistry between super-plasticizers and cementitious materials. The most commonly used super-plasticizers in the concrete industry today are based on polycarboxylate ethers which rely on electrosteric stabilization for particle dispersion. Electrosteric stabilization combines two mechanisms by first introducing a negative charge to repel the cement particles from each other and then using steric stabilization to keep them apart. Steric stabilization occurs when the cement particles adsorb the polymer chains and give steric hindrance for the agglomeration of particles. The older super-plasticizers are mostly based on lignosulfonates which are a by-product of the paper industry. These introduce an electrostatic stabilization to the cement paste by imparting a negative charge around the cement particles as shown in Figure 2.1 (SCI, 2003).

Viscosity modifying admixtures (VMAs) are also used to enhance the rheology of fresh concrete. Typically VMAs are used to control segregation and increase the viscosity (resistance to fluid deformation) of the mix. When used in conjunction with HRWRs, viscosity modifiers can produce very stable, yet highly flowable concrete that can fill congested reinforcement and odd-shaped formwork.

VMAs can be in liquid or powder form, and are classified as Class A, B, C, D, or E according to their physical attributes (Khayat, 1998). The most common types used in SCC are water-soluble polysaccharides or acrylic-based polymers; that is Class A and C, respectively. The Class A VMAs consists of natural or synthetic polymers that increase the viscosity of the water, and thus, the viscosity of the fresh concrete. According to Khayat (1998) Class C VMAs enhance the inter-particle attraction by introducing superfine particles into the cement paste. Although these chemical VMAs are very effective in producing highly flowable and stable concrete, the increased cost that results has kept some concrete producers from using them. As with all other concrete admixtures, the need for VMAs and the dosage should be evaluated depending on each specific application and performance criteria.

Fresh Properties

SCC in its fresh or "plastic" state exhibits much different characteristics than conventional concrete. It should be able to flow under its own weight without the need for mechanical vibration, and completely fill formworks and surround any steel reinforcement or prestressing strands that exist in the forms. The requirement for concrete to be considered an SCC in the plastic state is that it must exhibit adequate filling ability, passing ability, and stability (segregation resistance).

For SCC to exhibit adequate filling ability it must be able to completely fill all parts of the formwork including areas of complex reinforcement under its own weight. According to Bailey et al. (2005) the deformation capacity of SCC correlates to the internal yield stress in the freshly mixed concrete. Therefore, for SCC to flow adequately, the yield stress of the mix must be reduced. This is achieved by reducing the inter-particle friction through the use of admixtures (super-plasticizers) and by increasing the paste content of the mix (Bailey et al., 2005). According to Bailey, two methods are available to ensure that the concrete will exhibit proper filling ability. By balancing the water/cement ratio with the superplasticizer dosage, it is possible to increase the deformability of the paste. Also, by reducing the amount of coarse aggregate and increasing the volume of paste, the inter-particle friction within the mix can be minimized (Bailey et al., 2005).

Passing ability is another property of freshly mixed SCC that describes its flowability through obstacles such as prestressed strands and steel reinforcement. Bailey et al. (2005) and EFCA (2005) suggest that the three parameters to consider when evaluating the passing ability of the concrete are the geometry and density of reinforcement, the stability of the fresh concrete, and the maximum aggregate size and content. These should be optimized so that the SCC has no blockage at the areas of congested reinforcement and should have no segregation. According to SCI (2004), blocking occurs in fresh concrete due to the change in the flow path around obstacles. When the size of the aggregate is large, relative to the smallest opening in the reinforcement, the aggregate particles can form an arch that can obstruct the flow of concrete. It is also suggested (SCI, 2004) that the shape of the aggregate and the content can affect the formation of aggregate arches around the rebar. For instance round river gravel would be less likely to form arches than angular crushed gravel because of its reduced inter-particle friction. Also, when the content of the aggregate is too high, arching is likely to occur around reinforcement. These blocking mechanisms can be seen in Figure 2.2.

To improve resistance to blocking, or passing ability, Bailey et al. (2005) recommend that the segregation be reduced using either VMAs or low water/cement ratios. Also to prevent arching, they propose that low coarse aggregate contents and smaller aggregate sizes should be considered in SCC mixes. In order to assess the passing ability of the mix; several tests have been developed including the L-box, J-ring, V-Funnel, and the Orimet with J-Ring. The general idea of these tests is to allow the concrete to flow under its own weight through reinforcing bars spaced at similar distances as the actual

reinforcement, and then measure the amount of concrete that passed through the bars relative to the amount that did not.

The third requirement for freshly mixed SCC is the resistance to segregation, i.e., separation of aggregates from paste. In order for the concrete to exhibit sufficient filling ability and passing ability, the shear stress in the paste must be reduced. However, when the shear stress in the paste is reduced too much severe segregation can occur and leave large pockets of aggregate that can jeopardize the integrity of the structure. During the casting of a structure, segregation can form around reinforcement, which is related to the passing ability of the concrete. Also, after the concrete has been poured, settlement of the aggregates can occur and cause weak surfaces and cracking in some elements (EFCA, 2005).

To improve segregation resistance, Bailey et al. (2005) suggests minimizing "bleeding due to free water" and reducing the segregation of solid particles. These can be accomplished by using VMAs and/or lowering the water/cement ratio of the mix. VMAs essentially reduce the viscosity of the paste and make the mix more stable. To assess the segregation resistances of the fresh concrete, tests such as the bleeding test, screen stability test, orimet test, and the visual stability index (VSI) have been developed. These tests aim to quantify the dynamic stability as well as the static stability of the concrete.

Researchers all over the world have been developing test methods to asses the filling ability, passing ability, and segregation resistance of fresh SCC. Some of the agencies that have been developing these tests are ASTM (USA), PCI (USA), EFNARC (Europe), Brite-Euram (Europe), JSCE (Japan), as well as universities around the world. A number of the current test methods and the properties measured can be seen in Table 2.1. A detailed explanation of these tests and their procedures can be found in the PCI document "Interim Guidelines for the Use of Self-Consolidating Concrete in Precast/Prestressed Member Plants" released in 2003 (PCI, 2003a). ASTM standards have recently been developed for slump flow (spread) of SCC (ASTM, 2009a) and the J-ring test (ASTM, 2009b).

The primary tests conducted in relation to fresh properties in this research included the spread test, L-Box, U-Box, and the Visual Stability Index (VSI) as described in more detail below.

Spread Test and Visual Stability Index (VSI): The slump spread test, or the "spread" test, is the most widely used test for the filling ability SCC. It is normally coupled with the Visual Stability Index (VSI) which is a method of visually examining the concrete paddy and giving it a stability grade from 0 to 3. This method quantifies the filling ability and lets the concrete producers examine the fresh concrete in an unconfined area. The equipment needed for the spread test is basically the same as that which is used for the conventional slump test. As shown in Figure 2.3, it consists of an Abrams slump cone, a square impervious plate at least 30 inches (762 mm) square, and a measuring tape. Also, like the conventional test, the spread test does not require or waste much fresh concrete and the results are very easy to interpret. The fresh concrete is poured in

either an upright or inverted slump cone. The cone is then lifted up at a rate of about 1 foot (305 mm) per second, and the concrete is allowed to spread as far as it can on an impervious level surface. The average of two perpendicular diameters is taken as the final spread reading.

The values for this test generally range from 20 - 30 inches (508 – 762 mm) with higher values indicating greater filling ability. For high performance SCC, the Federal Highway Administration requires the slump flow to be equal to or greater than 20 inches (508 mm) for FHWA HPC performance grade 1. Grade 2 requires slump flow of 20 - 24 inches (508 – 610 mm), and Grade 3 requires slump flow to be greater than 24 inches (610 mm) (FHWA, 2005). The "European Guidelines for Self-Compacting Concrete" (2005) suggest that for unreinforced concrete or small sections the lowest spread values should be in the range of 21.6 - 25.6 in. (550 - 650 mm). The recommended range for normal applications such as walls and columns is 26 - 29.5 in. (660 - 750 mm), and for structures with congested reinforcement such as large precast/prestressed bridge girders is 30 - 33.5 in. (760 - 850 mm). PCI proposes the use of "Mix Parameter Selection Tables" developed by J.A. Daczko (Badman et al., 2003) as shown in Table 2.2. The "Slump Flow Parameter Determination" table assists the user in determining the lowest slump flow value that is needed for certain structural characteristics such as reinforcement level, element shape intricacy, element depth, element length, coarse aggregate content, and placement energy. In these parameter tables the dark blocks represent potential problem areas. For instance if surface finish is of high importance, the table suggest that the concrete should have a spread greater than 26 inches (660 mm).

While performing the spread test, PCI (2003a) suggests that the T-50 time and the VSI are recorded also. The T-50 is another method to quantify the filling ability, but also gives an idea of the viscosity since it is related to flow rate of the fresh concrete. The T-50 test measures the time for the concrete spread paddy to reach the 20 in. (50 cm) mark on the spread board. Typical values range from 2 to 15 seconds for SCC mixes. Clearly a lower time indicates a higher flowability, but could also suggest segregation. The FHWA (2004) suggest that 2-5 seconds is adequate time for an acceptable SCC to reach a 20 in. (50 cm) spread. The European Guidelines quantify the T-50 times in three categories, i.e., < 3.5; 3.5 to 6; and > 6. These correspond to the three levels of spread values that they also recommend. PCI (2003a) indicated that 3-7 seconds is satisfactory for most civil engineering applications. It should be noted that considerable error can occur with this test due to the operator misjudging the timing. PCI suggests conducting this test with two or more operators so that one can lift the cone while the other reads the timing.

The Visual Stability Index (VSI) is an effective method for determining the stability of the mix in an unconfined space immediately after the spread test is performed. In this test the concrete is given a VSI according to the amount of bleeding, surface air bubbles that take place, and the existence of a mortar halo (ring of mortar around the concrete paddy). A concrete mix will be given a rating from 0 to 3 (0 most stable, 3 least stable) in increments of 0.5 according to PCI (2003a). Examples of SCC samples and their VSI ratings can be seen in Figures 2.4a through 2.4d.

L-box Test: To assess the passing ability and blocking resistance of SCC, researchers have developed the "L-box test". Figure 2.5 shows the L-box apparatus used at the University of South Carolina. This test uses an L-shaped box consisting of a vertical section and a horizontal section for the concrete to flow through. Vertical reinforcing bars are placed in the apparatus so that the concrete must pass through them as it flows from the vertical section to the horizontal section. These bars can be of different diameter and spacing depending on the application of the concrete and confinement of the member reinforcement. A sliding door separates the two sections so that the vertical section can be filled with concrete to a predetermined level before allowing flow. When the door is raised the concrete flows through the bars under its own weight to simulate the field placement of SCC. After the concrete stops, the height of the concrete is measured at a point before the reinforcing bars (H1) and at the opposite end of the L-box (H2). The "blocking ratio", H2/H1 can then be calculated and the passing ability of the mix quantified (PCI, 2003a).

The PCI Guidelines (2003a) suggest that the test must be performed within five minutes of the end of mixing and that a blocking ratio of 0.75 or higher represents a self-consolidating mix. However, they also present an "L-box Ratio Parameter Determination" table developed by J.A Daczko shown in Table 2.3. This table shows potential problems that may occur due to certain element characteristics such as element length, wall thickness, and reinforcement level. The EFNARC suggest that the blocking ratio should be 0.80 or higher for SCC to be accepted. A Brite-EuRam (2000) report on SCC also suggests that a blocking ratio of 0.80 should be used, but mentions that a blocking ratio of 0.60 has performed adequately without blocking in a real structure. This suggests that the criteria for this test should be reexamined.

U-box Test: The U-box test is another test method to determine the filling ability of the concrete. Unlike the spread test which finds the "unconfined" filling ability, the U-box determines the filling height of the concrete confined in a box while also forcing it to pass through reinforcing steel. Similar to the L-box, the size and spacing of the reinforcing bars should correlate to the application of the concrete. The apparatus used for this test is generally made of a non-absorbent material, and consists of two side-by-side compartments connected at the bottom by a U-shaped passageway. A sliding gate is placed behind the rebar so that one half of the apparatus can be filled completely to a predetermined level before release. About 0.67 ft^3 (0.019 m^3) of concrete is placed into one side of the apparatus, and the gate is pulled up. The height of concrete on the "filling" side is recorded. Theoretically if the mix were to flow like water, the final heights would be equal meaning a filling height of about 12 ¼ in. (311 mm).

PCI (2003a) suggests that a filling height of 11 ¾ in. (299 mm) will qualify the mix as an SCC. PCI also suggests the use of the "U-box Ranking Parameter Determination" table (Table 2.4) also developed by J.A. Daczko. This table ranks the self-consolidation of the mix as Ranks 1, 2, or 3. Rank 1 is a rising height of 12 in. (305 mm) through the most restricted obstacle [0.4 in. (10 mm) bars with 1.4 in. (36 mm) clear]. Rank 2 is a 12 in. (305 mm) rising height through a less restricted obstacle [0.5 in. (13 mm) bars with 1.4

in. (36 mm) or more clear], and Rank 3 is a 12 in. (305 mm) rising height through zero obstacles (PCI, 2003a). The FHWA (2004) suggest a minimum of 11.8 in. (300 mm) to qualify the mix as an SCC mix. The EFNARC does not specify any criteria for this test, but does suggest that the height in both chambers should be close to equilibrium (EFCA, 2005).

Hardened Properties

Engineers generally are more concerned with the hardened properties such as strength and durability than they are with the fresh behavior of the mix. Since SCC differs so much in fresh behavior and mix composition than normal concrete (NC) much of the research conducted on SCC has focused on the hardened properties. SCC and NC mixes usually differ in fine/coarse aggregate ratios, water/cementitious ratios, aggregate sizes, and amount of chemical admixtures. These differences can have major effects on the strength and durability of the mix. For instance, often self-consolidation is achieved by the use of super-plasticizers which allows for a reduced water/cementitious material ratio, and thus, higher strength. On the other hand, because of the increased fines in SCC mixes, it is suspected that higher drying shrinkage will occur in SCC than NC. The next few sections discuss the hardened properties and give some results from other programs. FHWA performance grade classifications for high performance concrete are shown in Table 2.5 for purposes of comparison and future reference.

Mechanical Properties: The mechanical properties of main interest are generally the compressive strength, f'_c, and the Young's modulus of elasticity, E_c. Other properties include tensile strength, shear strength, and bond strength, which are typically expressed in terms of the compressive strength (PCI, 1997). f'_c and E_c are the essential properties that are used in concrete design specifications such as ACI 318, IBC 2003, and the PCI specifications. ACI 318 (2005) offers a formula for predicting the compressive strength gain of concrete as well as formulas to predict Young's modulus based on f'_c. Equation 2.1 shows the compressive strength gain as a function of the 28-day strength, time, and constants α and β, which are related to the type of cement used and the curing procedures for the concrete. The values for these constants can be found in Table 2.6.

$$f'_c(t) = \frac{t}{\alpha + \beta} f'_c(28-\text{days}) \qquad \text{(eqn. 2.1)}$$

Experimentally, the compressive strength can be found by testing 4 x 8 in. (102 x 203 mm) cylinders or 6 x 12 in. (152 x 305 mm) cylinders following the procedures in ASTM C39 (2004). For precast applications, PCI recommends curing cylinders alongside the precast members or using a match-curing system to replicate the maturity of the member concrete (PCI 1997).

The compressive strength depends on many factors including water/cement ratio, type of cement, porosity, curing conditions, aggregate type, and admixtures used. Since SCC differs from NC in all these respects it is expected that the compressive strength should be affected. Attiogbe and Daczko (2003) conducted a study on the engineering properties

of SCC compared to those of conventional flowable concrete with a high slump [8 - 9 in. (203 – 229 mm)]. Both mixes were designed for compressive strength of 4,000 psi (27.6 MPa) at 24 hours. They found that the compressive strength for both mixes was very similar for the steam-cured specimens. For the air-cured specimens, the SCC had higher compressive strength than the conventional concrete at both 1 and 28 days (Attiogbe and Daczko, 2003). Naito et al. (2005) also conducted tests comparing SCC to High Early Strength Concrete (HESC). Since these mixes were going to be used in prestressed bridge girders they were designed to have a 6,000 psi (41.4 MPa) release strength and 8,000 psi (55.2 MPa) 28-day strength. The early strength allowed for early release of the prestressing strands which is an economical advantage to both the supplier and purchaser of the girders. Figure 2.6 shows the compressive strength gain from their tests. It can be seen that the SCC gained greater strength and faster than the HESC mix. Also, the HESC mix did not achieve the required design strength until about 80 days compared to about 7 days for the SCC mix.

Young's modulus can be predicted from the compressive strength or can be found experimentally. For concretes with f'_c up to 6,000 psi (41.4 MPa) PCI suggest the use of Equation 2.2 to predict the modulus of elasticity.

$$E_c(t) = 33(w_c)^{1.5}\sqrt{f'_c(t)} \qquad \text{(eqn. 2.2)}$$

where $E_c(t)$ is the modulus of elasticity at age t (days), w_c is the unit weight of the concrete (pcf), and $f'_c(t)$ is the compressive strength at age t (days). For higher strength concretes PCI (1997) suggests that Equation 2.2 tends to over-predict E_c and proposes the following formula;

$$E_c(t) = (40{,}000\sqrt{f'_c(t)} + 1{,}000{,}000)\left(\frac{w_c}{145}\right)^{1.5} \qquad \text{(eqn. 2.3)}$$

or for normal weight concrete:

$$E_c(t) = 40{,}000\sqrt{f'_c(t)} + 1{,}000{,}000 \qquad \text{(eqn. 2.4)}$$

Experimentally, Young's modulus is found by testing 6 x 12 in. (152 x 305 mm) cylinders following the procedures of ASTM C469-02.

Naito et al., (2005) measured the modulus of elasticity for an SCC mix and an HESC mix. These tests were derived from the above mentioned compressive test for which the concrete was designed to reach 8,000 psi (55.2 MPa) in 28 days. They performed the test on normal weight concrete at 79 days and the SCC at 98 days. By performing a linear regression of the data to 40 % of the compressive strength, the modulus of elasticity for the samples is found. Table 2.7 shows the comparison of Young's modulus calculated from Naito's testing. The modulus of the HESC was found to be about 12 % higher than the SCC. They suggest that this could be attributed to the higher coarse aggregate composition or the difference in the air void system of the two mixes. They also show

that the ACI equations over-predict the elastic modulus of the SCC while under-predicting that of the HESC.

Bailey et al., (2005) also conducted tests on a number of different concrete mixtures containing cement and fly ash. They report that regardless of the water-to-cement ratio, the fine-to-coarse aggregate ratio does not affect the strength development of the concrete. This can be seen in Figure 2.7a, where mixes 3, 4, and 5 which have fine-to-coarse aggregate ratios of 0.48, 0.44 and 0.40 respectfully. However, the normal concrete in their study outperformed the SCC in regards to compressive strength by 9 % at 56 days. Again, Figure 2.7a shows normal concrete, labeled as ODSC, as having a consistently higher compressive strength than SCC mixes with the same w/c ratio. The lower strength for the SCC mixtures is attributed to the higher replacement of fly ash which may prevent the reaction of some of the ash.

Bailey et al., (2005) also performed modulus of elasticity testing corresponding to the above mentioned compressive tests and the results can be found in Figure 2.7b. Again the SCC mixtures exhibited slightly lower values for the modulus than that of the normal concrete. They also compared their experimental results with the predicted modulus of elasticity values based on the equations of ACI 318-02 and the ACI 363 (1998). They determined that ACI 318-02 generally overestimates the modulus of elasticity for both types of concrete. Additionally, they found that as the compressive strength is increased, the ACI 318 model over-estimation worsened. In contrast, they found that the ACI 363 equation yields a more conservative prediction of the modulus based on the compressive strength. This is expected, they suggest, since the ACI 363 equation is valid for a wider range of concrete compressive strengths.

Durability Characteristics: Creep and shrinkage are two other significant material properties that can affect the performance of girders. ACI 209R-92, "Prediction of Creep, Shrinkage, and Temperature Effects in Concrete Structures," reviews methods for predicting these phenomena that affect the volume changes in concrete. Also, several research groups have studied the creep and shrinkage effects on SCC compared to those of normal concrete. However, these reports are not in agreement. For example, Raghaven et al., (2002) conclude that the creep and shrinkage strain of SCC is significantly lower than that of normal concrete. Conversely, Naito et. al (2005) determined that the creep and shrinkage strain for the SCC mix was higher than that of a similar high early strength concrete (HESC).

The ACI 209R-92 document presents prediction equations for creep and shrinkage that include a variety of correction factors to account for different concrete conditions. This document refers to creep in terms of the creep coefficient which is the ratio of creep strain to initial strain and is given by the equation:

$$\nu_t = \frac{t^{0.60}}{10 + t^{0.60}} \nu_u , \qquad \text{(eqn. 2.5)}$$

where t is the concrete age in days and v_u is the ultimate creep coefficient which is found by the equation:

$$v_u = 2.35\gamma_c, \qquad \text{(eqn. 2.6)}$$

where γ_c is the product of the applicable correction factors such as loading age, relative humidity, member size, temperature, and other correction factors for concrete composition. These factors can be found in detail in ACI-209R-92.

Shrinkage is dealt with in a similar fashion to creep regarding correction factors that are applied to a time related function such as:

$$(\varepsilon_{sh})_t = \frac{t}{55+t}(\varepsilon_{sh})_u, \qquad \text{(eqn. 2.7)}$$

where $(\varepsilon_{sh})_t$ is the total shrinkage at any time, t (days) after shrinkage is considered, and $(\varepsilon_{sh})_u$ is the ultimate shrinkage strain defined by:

$$(\varepsilon_{sh})_u = 780\gamma_{sh} \times 10^{-6} \qquad \text{(eqn. 2.8)}$$

where γ_{sh} is the product of applicable correction factors similar to those presented for the creep predicting equation. These factors may also be found in the ACI-209R-92 document.

Raghaven et al., (2002) tested creep and shrinkage of self-compacting concrete and compared the results with those of normal concrete. They used super plasticizers and viscosity-modifying admixture to achieve a stable and flowable SCC mixture. They also used increased paste by adding fly ash and increasing the sand volume. The control normal mix did not contain fly ash but contained more cement than the SCC mix. Mix proportions for these mixes can be seen in Table 2.8. The SCC mix exhibited adequate fresh properties such as a 26.4 in. (671 mm) slump flow and almost 13 in. (330 mm) in the U-Box (Raghaven, 2002).

The creep specimens were loaded to 30 % of their ultimate strength, and data was recorded for about 80 days (Figure 2.8a). Shrinkage data was collected corresponding to the testing schedule of the creep tests. Figure 2.8b shows the comparison of SCC and NC drying shrinkage. It can be seen that the SCC outperforms the NC in both cases. They conclude that even though the initial strain was greater in the SCC specimens, the final creep strain was less than that of NC. They also conclude that the rate of shrinkage of the SCC specimens was 25% lower than the shrinkage of NC (Raghaven, 2002). These results contradict with the general idea that increased fines in SCC would produce higher creep and shrinkage strains.

The research conducted by Naito et al. (2005) at Lehigh University, however, concludes that SCC is more susceptible to creep and shrinkage than an equivalent HESC as shown in Figures 2.9a and 2.9b. These figures also show a comparison of their data with the ACI 209 predictions. It can be seen that the ACI 209 equations largely under predicted the creep coefficient of the HESC. On the other hand, the shrinkage predictions from the ACI 209 equations over-predict the experimental results found in Naito et al. (2005).

2.3 Benefits of SCC versus Conventional Concrete

The increased workability of SCC is beneficial to both the precast concrete producer as well as the customer. Production times and quality control could potentially improve for the precast plant and both parties could see economical benefits by using SCC. There are many costs associated with the construction of precast structural elements including materials, production, placing, consolidation, and finishing. While the costs of materials could increase David Martin of Master Builders, Inc. suggests that SCC could provide total cost savings and increase profitability (Martin, 2003).

Placement and Finishing: The placement and finishing requirements of SCC are considerably less than that of normal concrete. For instance, since vibration is not required the workers that would normally be consolidating the concrete could be employed elsewhere at the plant, increasing the overall plant productivity, and saving labor cost. A case study by Martin (2003) revealed that for the production of 520 ft (159 m) long double-tee beam, approximately 10 man-hours were saved by utilizing SCC compared to NC. The conventional concrete beam required 13 workers and a total of 32.5 man-hours, while the SCC beam required only 11 workers and 22 total man-hours.

Other production benefits gained from the use of SCC include the decrease in maintenance and replacement of vibration tools and formwork. Without the use of vibration the steel formwork would receive considerably less wear and tear and require less frequent replacement.

Finally, SCC could drastically improve the work environment and safety at precast concrete plants. First of all, the dangers associated with walking on the top of formwork for vibration purposes are eliminated. Also the reduction in noise from the vibrators would improve the work conditions and reduce the need for hearing protection (Martin, 2003).

Economy: Typically the material costs for SCC will be higher than the costs for NC. However, the savings associated with the production, placement, and finishing can provide for a more economical product. The fresh properties of SCC require much closer control of the constituent materials than normal concrete. To achieve an adequate SCC mix, typically higher cement dosages are used to increase the fine content which increases the workability and adds stability to the mix. Therefore cement cost can increase an average of $3.00 - $6.00 per cubic yard (Martin, 2003).

The chemical admixtures also contribute to the material cost increase. Currently there are many high-range water reducing (HRWR) admixture manufacturers in the SCC market, and several different cost options. The more traditional HRWRS are not as effective, but cost less than the newer polymer based super-plasticizers, which are much more effective and more expensive. According to Martin, the HRWRs can add about $2.00 to the cost per cubic yard.

Other materials that impact the cost of the concrete include the use of fly ash and viscosity modifying admixtures (VMAs) which improve the plastic properties of the concrete. Fly ash is sometimes incorporated into the mix to improve workability and reduce the amount of cement used. Martin suggests that the use of fly ash in combination with HRWRs and VMAs can produce a cost-effective quality SCC mix to meet the material specifications.

2.4 Materials Considerations for SCLC

Fresh Properties of SCLC

As for normal weight SCC, self-compaction ability of SCLC depends entirely on its fresh properties; therefore, a successful SCLC mix must have high fluidity, deformability, good filling ability, and adequate resistance to segregation. Additionally, aggregate particles have to be uniformly distributed throughout the mix to avoid segregation at all times especially during transportation and placement. In general, SCLC with a slump flow less than 17 in. (432 mm) will not have self-compacting properties; on the other hand SCLC with a slump flow over 26 in. (660 mm) may experience severe segregation and bleeding.

Evaluation of the fresh properties for SCLC is essentially carried out in the same way as for SCC. Numerous investigations on the workability of SCC performed in North America and Europe have shown that L-box, U-box, J-rings, and the slump flow (spread) tests in conjunction with the visual stability index (VSI) are very effective to evaluate the workability of the mix on-site. However, current investigations on resistance to segregation of lightweight aggregate (LWAC) and volume stability of SCLC are still under development.

Visual Stability index (VSI), L-Box, U-Box and Slump flow (spread) test: A review of the literature pertaining to these testing procedures is discussed above.

V-funnel Test: This procedure evaluates the fluidity of the SCLC and the ability to change its path when passing through a constricted area. These parameters are examined using the total time (T_V) elapsed while flowing through the V-funnel apparatus (Fig. 2.10). EFNARC classifies the mix as SCC class 1 for $T_V \leq 8$ s and SCC class 2 for 9 s $\leq T_V \leq 25$ s.

Wet Sieve Segregation Test: This method was developed in France to quantify the resistance of SCLC to segregation. During the procedure, 10 liters of fresh SCLC are poured into a sealed container, after 15 min, 11 lbs. (5.0 kg) of the mix are taken out of

the recipient and poured onto a perforated metal sieve with 0.2 in (5 mm) of aperture (Fig. 2.11). The amount of SCLC mix that passes through the sieve within 2 min. is recorded. Finally, the segregation ratio (SR) is calculated as the mass percentage of the sample that has passed through the sieve. Smaller SR values represent higher resistance to segregation of the mix. According to EFNARC, the value of SR should be less than 15 % for SCC to have an appropriate resistance to segregation.

Surface Settlement Test: This test measures the volume stability of the mix using the settlement rate at the top of the SCLC mix in a plastic stage. The settlement rate (STR, relative settlement per hour) is defined as:

$$\mathrm{STR}\left(\frac{\%}{\mathrm{h}}\right) = \left\{\frac{\left[\ \mathrm{S_T}(\%) - \mathrm{S_{T-5}}(\%)\ \right] / 5(\mathrm{min})}{60(\mathrm{min})}\right\} \qquad \text{(eqn. 2.9)}$$

where,

S_T : Settlement value at given time t.
S_{T-5}: Settlement value at time T - 5 min.

A polyvinyl chloride pipe with diameter of 8 in and 28 in height is used for the test. A circular polypropylene colophony plate is placed over the mix to monitor the change in settlement. Hwang et al. (2006) found that settlement rate at 30 min should be less than 0.16% per hour and maximum settlement smaller than 0.5% for a good volume stability.

Column Segregation Test: Lightweight aggregate (LWA) used in SCLC has a tendency to float up producing segregation in the mix. Hence, providing adequate resistance to segregation is fundamental to guarantee workability of the mix and the quality of the concrete once it has set. This test is performed using a steel column formed by four short columns with diameter of 8 in. and 6.5 in. (203 mm and 165 mm) in height (Fig. 2.12). Fresh SCLC is poured into the column and after 30 min the short columns are removed one by one from the top. At the end, the mass ratio of coarse aggregate in each short column to the total mass of coarse aggregate are used to evaluate the uniformity of coarse aggregate distribution.

Mechanical Properties

Mechanical properties of the concrete dictate the structural efficiency and performance of the material once it is in its hardened state. Compressive strength, tensile strength, and modulus of elasticity for SCLC are discussed below.

Compressive Strength: For LC as well as SCLC, compressive strength of the mix is primarily controlled by the type of Lightweight Aggregate (LWA) present in the concrete matrix. Changes in the cement content, addition of silica fume and partial replacement of lightweight sand by natural sand produce smaller variations on the compressive strength. LC usually stops gaining strength at younger ages when compared to normal concrete, since improvement of strength in the concrete matrix will not result in further gains once

the LWA has reached its upper compressive limit (Zhang and Gjorv, 1991). Numerous investigations show that in general concrete becomes more brittle with an increase in strength; this trend is also accompanied by an increment in linearity within the ascending branch of the stress-strain curve and a much steeper descending path. Strain at ultimate compressive load is generally higher for LC when compared to normal concrete at the same strength level.

Tensile Strength: In concrete materials tensile strength is closely related to compressive strength. In general any increment in the compressive capacity of the mix will result in a higher tensile failure stress. However, the relationship between tensile and compressive strength varies considerably between types of concrete (normal, LW, SCC, SCLC). Usually, gains in tensile capacity are lower for lightweight concretes for similar increments in compressive strength (Lydon and Balendran, 1980) when compared to normal weight concrete.

Modulus of Elasticity: SCLC elastic modulus is usually around 80% of normal SCC (Lo et al., 2007), this value is also quite reasonable since LC values range from 50% to 75% that of normal weight concrete with similar strength (Chandra, 2002). This reduction in the Young's modulus value of lightweight concrete has been attributed to the effect produced by the elastic modulus of the lightweight aggregate and pore structure. Hence, increasing the cement content along with a reduction of aggregate volume may result in a higher elastic modulus for SCLC.

Previous Studies Related to SCLC Materials

Choi et al., 2006: This investigation was focused on the evaluation of high strength lightweight self-compacting concrete (HLSCC) manufactured by Nan-Su. Fresh properties and fluidity of the mix were analyzed as well as mechanical properties of the paste in its hardened state. Fluidity was studied according to the second class rating of JSCE divided in three categories of flowability, segregation resistance ability and filling capacity of fresh concrete. Mechanical properties monitored during the research included compressive strength with elapsed age, splitting tensile strength, elastic modulus and density, all after 28 days. HLSCC at its fresh state was rated with less than 50 % lightweight fine aggregate (LF) and 75% lightweight coarse aggregate (LC), hence satisfying the second class standard of JSCE. Compressive strength at 28 days resulted in values over 5,800 psi (40 MPa) for all mixes with the exception of LC 100 %. Also, structural efficiency (compressive strength vs. density) showed a proportional increment when the mixing ratio of LF increased. Mixture proportion of concrete was divided in four groups (A, B, C, and D) according to the use of LF and LC. Mixes within each group had a different percentage of mixing ratios for LC or LF or both. The authors presented the following conclusions:

- Flowability and resistance to segregation measured using the slump flow test and time required to reach 19.7 in. (500 mm) satisfied the expected levels in all HLSCC mixes. However, segregation resistance ability measured using the time required through the V-funnel only achieved expected levels in most of

the LC mixed concrete (Mix Nos. 2 - 4) and one of LF mixed concrete (Mix No. 6).

- Filling ability determined with the U-box test was satisfied for all mixes with LC (Mix Nos. 2 - 5) achieving the second class rating of JSCE while only the mix with LF 25 % (Mix No 6) reached the target level.

- LC mix ratios up to 75 % presented a 6 % average decrement compared to the control concrete while LC 100 % showed 31 % decrease. LF mixes up to 50 % presented a decrement around 6 % while higher percentage of LF mixes resulted in compressive strength increments between 8 % and 20 % compared to the control concrete.

- HLSCC's structural efficiency increased 7 % for the 75 % LC mix while the 100 % LC mix resulted in a 20 % reduction. Structural efficiency increased proportionally compared to the control concrete from 17 % to 33 % for LF mixes between 75 % LF and 100 % LF mix ratio.

- Linear regression analysis per mix ratio of lightweight aggregate was applied to the relationship between compressive and splitting tensile strength at 28 days. A correlation coefficient of 92 % obtained in the analysis indicates a close relationship between both capacities. The ACI 318/318R standard was used to evaluate the association between compressive strength and elastic modulus, the results were adequate and within the upper and lower curve range of ACI standard unit weight.

- Discrepancies between experimental and estimated values of compressive strength and structural efficiency were within a 10 % range.

Lo et al., 2007: This study presents a comparison between workability and mechanical properties of SCC and SCLC. A self-compacting lightweight mix with 31.2 - 37.4 lb/ft^3 (500 - 600 kg/m^3) binder content and a density of 103 lb/ft^3 (1,650 kg/m^3) was produced using less super plasticizer and viscosity agent along with a lower water/binder ratio than for normal SCC. Bulk density was reduced to 75 % of SCC obtaining a similar compressive capacity. Also, the elastic modulus for the SCLC mix was around 80 % of normal SCC. Results indicate that SCLC is excellent in workability, can attain high compressive strength with relatively small reductions in the elastic modulus while offering the advantages of a material with a lower density. Workability and mechanical properties of both concretes were evaluated using results from slump flow tests, L-box tests, compressive strength, modulus of elasticity and concrete density. The authors presented the following conclusions:

- SCLC with similar slump flow to that of normal SCC can be produced using less super-plasticizer and viscosity modifying agent along with a lower water/binder ratio to obtain a similar flowability to that of normal SCC with a binder content of 31.2 - 40.6 lb/ft^3 (500 - 650 kg/m^3).

- SCLC Compressive strengths were within the 5,800 - 8,400 psi (40 - 58 MPa) range, which are similar to the compressive capacity of a SCC concrete with 137 lb/ft^3 (2,200 kg/m^3) density.

- SCLC can attain a higher compressive strength than LC at the same water/binder ratio with a 25 % reduction in density.

- Elastic modulus for SCLC and SCC increase with the binder content. Elastic modulus for SCC resulted in values in the 4,280 - 4,570 ksi (29.5 - 31.5 GPa) range and within 3,290 - 3,950 ksi (22.7 - 27.2 GPa) which corresponds to a reduction of 20 % for SCLC.

Wu et al., 2009: This investigation deals with the workability of SCLC and its mix proportion design. Two mix proportions for SCLC according to the water absorption of Lightweight aggregate (LWA) were designed, both mixes had fixed fine and coarse aggregate contents using the overall calculation method. Slump flow test, V-funnel, L-box, U-box, wet sieve segregation, and surface settlement tests were applied to evaluate workability of the concrete in its fresh condition. Column segregation tests and cross section images were used to assess the uniformity distribution of LWAs throughout the specimens. Experimental results indicate that both types of fresh SCLC have adequate fluidity, deformability, filling ability, uniform aggregate distribution and minimum resistance to segregation. The authors presented the following conclusions:

- Water absorption of the LWA can be used effectively along with fixed aggregate contents and the overall calculation method to design mix proportions for SCLC.

- Both types of fresh SCLC presented good workability in all the tests applied.

- Column segregation tests and cross section images verified a uniform distribution of LWAs along the specimen.

- Increasing the binder content of the mix will increase the shear flow velocity but it will reduce resistance to segregation.

Hwang et al., 2005: This study evaluated the performance of self-compacting lightweight concrete using different water/cement ratios and different cement paste content. The slump and the slump-flow tests for the fresh SCLC were designed to be 9.0 - 10.6 in. (230 - 270 mm) and 21.6 - 25.6 in. (550 - 650 mm) respectively. Experimental results show that SCLC compressive strength at 91 days can reach values as high as 8,100 psi (56 MPa) with a cement and a water content of 24.1 lb/ft^3 (386 kg/m^3) and 9.36 lb/ft^3 (150 kg/m^3) in that order. Thirteen mixes were designed with the densified mixture design algorithm method (DMDA). The main goal of this method is to obtain high-strength along with a high flowing concrete. The approach taken during this investigation was to use fly ash to fill voids of aggregate instead of replacing part of the

cement as in traditional mix design methods. Thus, fly ash will physically fill the voids of aggregate densifying the mixture of aggregate acting chemically as a pozzolanic material strengthening the microstructure. The authors presented the following conclusions:

- SCLC can achieve high strength, flowability and durability using the densified mixture design algorithm method (DMDA).

- High water/cement ratio and low water content (low amount of paste) may reduce early compressive strength, nevertheless the strength efficiency of cement still can reach a higher value than LWC if DMDA is used.

- Due to physical packing of aggregate, reducing the water content as well as the cement content will result in better electrical resistance and lower permeability of SCLC.

2.5 Considerations for Girders Fabricated with SCLC

The preceding sections have addressed the materials properties of both SCC and SCLC. This project is focused on the incorporation of SCLC for bridge girder applications. Due to the substantial effort involved in full-scale testing fewer studies are available in the literature, and related to this lack of full-scale laboratory studies is a lack of wide-spread field implementation. Notable studies related to lightweight concrete and SCLC for field applications are summarized below.

Meyer and Kahn, 2002: This investigation was focused on the analytical maximum lengths attainable using simple-span pretensioned concrete composite girders fabricated with high strength lightweight concrete (HSLWC). Concrete strengths of 8, 10, and 12 ksi (55, 69, and 83 MPa) were used along with prestressing strands of 0.6 in (15.2 mm) diameter. The implementation of HSLWC allowed increments in span length up to 4 % when compared to girders made with high strength normal concrete (HSNWC). Considering the AASHTO I-girder and AASHTO-PCI bulb-tee sections analyzed in this research, lightweight girders offered additional advantages such as the elimination of requirements for special transportation "super load" permits. Modified AASHTO-PCI bulb-tees containing one extra row of strands in the bottom flange increased the girder's maximum span length by at least 10 ft. (3.1 m). Lightweight concrete beams experienced greater deflections than normal concrete girders, but deflections values were less than the L/800 ASSHTO limit in all cases. In general, the benefits of high strength lightweight concrete include lower girder weight, relief from special permit requirements, and longer span lengths. The authors presented the following conclusions:

- Utilization of HSLWC can increase the length of simple span AASHTO I-girders by up to 4 % for AASHTO-PCI bulb-tee girders.

- HSLWC will eliminate the need for super load permits for girders with a span between 125 and 155 ft. (38.1 and 47.2 m) since girders within this length range will take the total vehicle weight under the 150 kips (68,200 kg) mark.

- AASHTO type II and III sections did not obtain any appreciable benefit when fabricated with HSLWC.

- For concrete strengths of 8, 10 and 12 ksi (55, 69 and 83 MPa), the modified bulb-tee section can be extended by 10 ft. (3.1 m) when compared to a standard bulb-tee using either HSLWC or HSNWC.

- AASHTO-PCI bulb-tee standard and modified sections using HSLWC, provided longer spans at less weight than standard AASHTO I-girder sections for members with lengths over 105 ft. (32 m).

Khan and Lopez, 2005: This study investigated the time-dependent behavior and prestress losses in high strength precast bridge girders fabricated with high performance lightweight concrete (HPLC) using expanded lightweight aggregate. The mixes were divided into two strength groups (grade 2 and 3) of 8,000 and 10,000 psi (55 and 69 MPa) with air dry unit weights of 116 and 118 lb/ft3 (1,855 and 1,890 kg/m^3) respectively. Thirty-six concrete cylinders and four AASHTO type II girders were employed to monitor creep, shrinkage and other prestress losses. Overall, prestress losses obtained from the AASHTO type II girders were less than those predicted using AASHTO, PCI, and ACI 209 methods. Analysis of experimental data resulted in total prestress losses of 20 % and 15 % of the initial prestressing force in the 8,000 and 10,000 psi (55 and 69 MPa) specimens, in that order. The authors presented the following conclusions:

- Compression strengths at 56 days for the HPLC mixes were 9,350 psi (64.5 MPa) for grade 2 and 10,580 psi (73 MPa) for grade 3.

- Creep and shrinkage at 620 days for grade 2 HPLC were 0.51 με/psi (74 με/MPa) and 820 με. For grade 3 HPLC the corresponding values resulted in 0.37 με/psi (54 με/MPa) and 610 με. Creep values obtained from the experimental data during this investigation were considerably smaller than the ones reported by Pfeifer (1968).

- HPLC experienced considerably less creep than normal high performance concrete (HPC) with similar strength and cement content. HPLC showed 20 % greater shrinkage values than HPC of the same grade after one year. In other words, HPLC presented less creep but higher shrinkage than HPC with comparable strength.

- Final prestress loss calculations were performed using AASHTO refined, AASHTO lump sum, PCI, and ACI 209 procedures. All these methodologies resulted in overestimated values of the time-dependent losses for AASHTO

Type II prestressed girders fabricated with HPLC performance grade 3. AASHTO refined and ACI 209 also overrated losses for the HPLC grade 2 girders. Therefore, these methods are considered conservative for estimating time-dependent losses of expanded slate HPLC girders.

- Considering the experimental results obtained during this study, both AASHTO refined and ACI 209 can be used to predict prestress losses conservatively in beams fabricated with expanded slate high performance lightweight concrete.

Waldron et al., 2005: The main objective of this research was the construction and evaluation of a high performance lightweight concrete (HPLWC) bridge. The bridge analyzed in this study is located over the Chickahominy River near Richmond, VA, and incorporates 15 prestressed AASHTO Type IV girders. The HPLWC used in the beams had a density of 120 lb/ft3 (1,920 kg/m^3) and strength of 55 MPa (8,000 psi) at 28 days. The deck of the bridge was also fabricated using lightweight concrete with a density of 120 lb/ft^3 (1850 kg/m^3) and minimum required 28-day strength of 4,350 psi (30 MPa). This investigation was mainly focused on determining the effects that the implementation of lightweight concrete in prestressed girders will produce on transfer length, development length, flexural strength, girder live-load distribution factor, and dynamic load allowance. Transfer length was found to be 17 in. (432 mm) (around 33 d_b) at time of transfer without signs of cracking at the ends of the girders. Development length was determined to be 72 and 96 in. (1,830 and 2,440 mm). Flexural strength of the beams was 11 % to 30 % higher than the predicted AASHTO flexural capacity. Experimentally measured distribution factors and dynamic load allowance were also overestimated by the AASHTO standard as well as LRFD values. The authors presented the following conclusions:

- AASHTO standards and LRFD specifications produce conservative predictions when estimating transfer length, development length, and flexural strength of HPLWC girders.

- Transfer length was significantly shorter than the recommended values from AASHTO standard (50 d_b) and LRFD specifications (60 d_b). Additionally, transfer length values are inferior to data reported from similar studies such as Peterman et al., 1999 (43 d_b), and Kolzos, 2000 (71 d_b). These discrepancies have been attributed to differences in research parameters such as girder dimensions, initial prestress, and manufacturing variations in the strands.

- AASHTO specifications for development length of 75 in. (1,910 mm) might not be conservative in all cases since HPLWC type II girder's development length was found to be between 72 and 96 in. (1,830 mm and 2,440 mm). Nevertheless average value for the development length in the girders was determined to be around 72 in. (1,830 mm), from which additional flexural

resistance was achieved. Therefore, it was recommended to increase specification values for the development length of HPLWC by 18 %.

- AASHTO Type II HPLWC girders had a flexural strength between 11 % and 30 % greater than the unfactored flexural capacity from AASHTO specifications. HPLWC girders also showed higher ductility with similar strength to HPC normal weight concrete girders. Therefore, AASHTO specifications can be used conservatively for flexural design of HPLWC girders.

- Inferior stiffness of the HPLWC beams did not considerably change the live-load distribution factors or dynamic load allowance during live load testing of the Chickahominy River Bridge. Either standard or LRFD specifications can be safely used for determining the live-load distribution factors and dynamic load allowance for HPLWC bridge girders with a LWC deck.

Meyer et al., 2006: This document presents the development and material testing data obtained from high strength lightweight concrete (HSLC) mixture proportions for structural applications in precast, prestressed concrete highway girders. The main objective was to develop concrete mixture proportions using slate lightweight aggregate with the capacity to achieve design strengths of 8,000 and 10,000 psi (55.2 and 69 MPa) with a maximum unit weight of 120 pcf (1,922 kg/m^3). A systematic approach for proportioning mixture components was created and implemented to configure HSLC mixes. Field testing to verify mixture properties was carried out for implementation in a production environment. An extensive material testing program was applied to develop a database of material properties including strength, modulus of elasticity, modulus of rupture, coefficient of thermal expansion, and chloride permeability. The authors presented the following conclusions:

- Moisture content in the lightweight aggregate has a considerable influence in the final compressive strength of the mix.

- Design of a mix with a target compressive strength of 12,000 psi (82.7 MPa) could not be attained.

- ACI equation for high strength concrete produce elastic modulus values around 9% less than those determined experimentally for slate HSLC.
- Increasing the silica fume content along with a reduction in the water/cement ratio will decrease chloride permeability.

- High strength/high-performance concretes with a unit weight inferior to 122 pcf can be develop and constitute a competitive option for precast/prestressed bridge applications.

Table 2.1: Test methods for fresh SCC properties (PCI, 2003a)

Test Method	Measured Stability Characteristic
L-Box*	Passing ability/blocking resistance
U-Box*	Filling ability/blocking ability
J-Ring (ASTM C 1621)	Passing ability/blocking resistance
Slump Flow (Spread)* (ASTM C1611)	Filling ability, Stability
Visual Stability Index (VSI)*	Stability, Air migration
Screen Stability Test**	Static segregation resistance
Bleeding Test (French)**	Dynamic segregation resistance
Bleeding Test (ASTM C232)**	Propensity to bleeding
V-Funnel**	Passing ability/blocking resistance, viscosity
Orimet with J-Ring**	Dynamic segregation resistance, passing ability/blocking resistance

* Tests conducted in this research

**Tests for special situations

Table 2.2: Slump flow parameter determination (PCI, 2003a)

			Slump flow		
			<22"	22-26"	>26"
Member Characteristics	Reinforcement Level	Low			
		Medium			
		High			
	Element Shape Intricacy	Low			
		Medium			
		High			
	Element Depth	Low			
		Medium			
		High			
	Surface Finish Importance	Low			
		Medium			
		High			
	Element Length	Low			
		Medium			
		High			
	Wall Thickness	Low			
		Medium			
		High			
	Coarse Aggregate Content	Low			
		Medium			
		High			
	Placement Energy	Low			
		Medium			
		High			

Table 2.3: L-box ratio parameter determination (PCI, 2003a)

			L-Box		
			<75	75-90	>90
Member Characteristics	Reinforcement Level	Low			
		Medium			
		High			
	Element Shape Intricacy	Low			
		Medium			
		High			
	Element Depth	Low			
		Medium			
		High			
	Surface Finish Importance	Low			
		Medium			
		High			
	Element Length	Low			
		Medium			
		High			
	Wall Thickness	Low			
		Medium			
		High			
	Coarse Aggregate Content	Low			
		Medium			
		High			
	Placement Energy	Low			
		Medium			
		High			

Table 2.4: U-box ranking parameter determination (PCI, 2003a)

			U-Box		
			Rank 3	Rank 2	Rank 1
Member Characteristics	Reinforcement Level	Low			
		Medium			
		High			
	Element Shape Intricacy	Low			
		Medium			
		High			
	Element Depth	Low			
		Medium			
		High			
	Surface Finish Importance	Low			
		Medium			
		High			
	Element Length	Low			
		Medium			
		High			
	Wall Thickness	Low			
		Medium			
		High			
	Coarse Aggregate Content	Low			
		Medium			
		High			
	Placement Energy	Low			
		Medium			
		High			

Table 2.5: Performance grades for high performance structural concrete (FHWA, 2005)

Performance Characteristic	FHWA HPC Performance Grade				
	Test Method	1	2	3	4
Compressive Strength (ksi)	ASTM C39	$6 \leq f'_c < 8$	$8 \leq f'_c < 10$	$10 \leq f'_c < 14$	$14 \leq f'_c$
Modulus of Elasticity (ksi)	ASTM C469	$4{,}000 \leq E_c < 6{,}000$	$6{,}000 \leq E_c < 7{,}500$	$E_c \geq 7{,}500$	
Shrinkage (με)	ASTM C157	$800 > S \geq 600$	$600 > S \geq 400$	$S < 400$	
Normalized Creep (με /psi)	ASTM C512	$0.52 \geq C > 0.38$	$0.38 \geq C > 0.21$	$0.21 \geq C$	
Freeze-thaw durability	ASTM C666	$60\% \leq F/T < 80\%$	$80\% \leq F/T$		
Scaling resistance	ASTM C672	SR = 4,5	SR = 2,3	SR = 0,1	
Abrasion resistance (in.)	ASTM C944	$0.08 > AR > 0.04$	$0.04 > AR > 0.02$	$AR > 0.02$	$AR > 0.02$
Chloride Penetration (coulombs)	ASTM C1202	$3000 \geq CP > 2000$	$2000 \geq CP > 800$	$CP \leq 800$	

Table 2.6: Values from α and β constants for equation 2.1 (ACI 318-02)

Curing Procedure	Cement Type	α	β
Moist	I	4.00	0.85
Moist	III	2.30	0.92
Steam	I	1.00	0.95
Steam	III	0.70	0.98

Table 2.7: Modulus of elasticity comparison - SCC and HESC (Naito et. al., 2005)

Material	Age [days]	Compr. strength, f'_c (ksi)	E_c, Linear regression (ksi)	R-squared	E_c @40%f'c (ksi)
SCC	14	8,170	4,940	1	4,930
SCC	14	8,420	5,190	1	5,200
SCC	14	8,270	5,000	1	5,010
SCC	38	9,740	4,755	0.993	4,854
SCC	98	9,968	4,821	0.996	5,178
SCC	98	9,989	5,224	0.996	5,036
HESC	14	6,520	5,610	1	5,670
HESC	14	7,090	5,500	0.999	5,570
HESC	14	7,180	5,770	1	5,790
HESC	79	8,901	5,623	0.995	5,520
AVG SCC	14	8,287	5,043	-	5,047
AVG HESC	14	6,930	5,627	-	5,677
AVG SCC	ALL	9,093	4,988	-	5,035
AVG HESC	ALL	7,423	5,626	-	5,638

Table 2.8: Mix proportions from Raghaven et. al. (2002)

Mix Proportion Of Self-Compacting Concrete and Normal Concrete, lb/yd^3 (kg/m^3)		
	Mixture no. 1 - SCC	**Mixture no. 2 - NC**
Cement	238 (400)	268 (450)
Fly Ash	104 (175)	
Sand	494 (830)	425 (714)
Coarse Aggregate	437 (735)	638 (1072)
Water	47.5 (180)	47.5 (180)
Superplasticizer - polycarboxylate ether	0.6 (2.2)	
SNF		0.7 (3)
VMA	0.8 (3)	

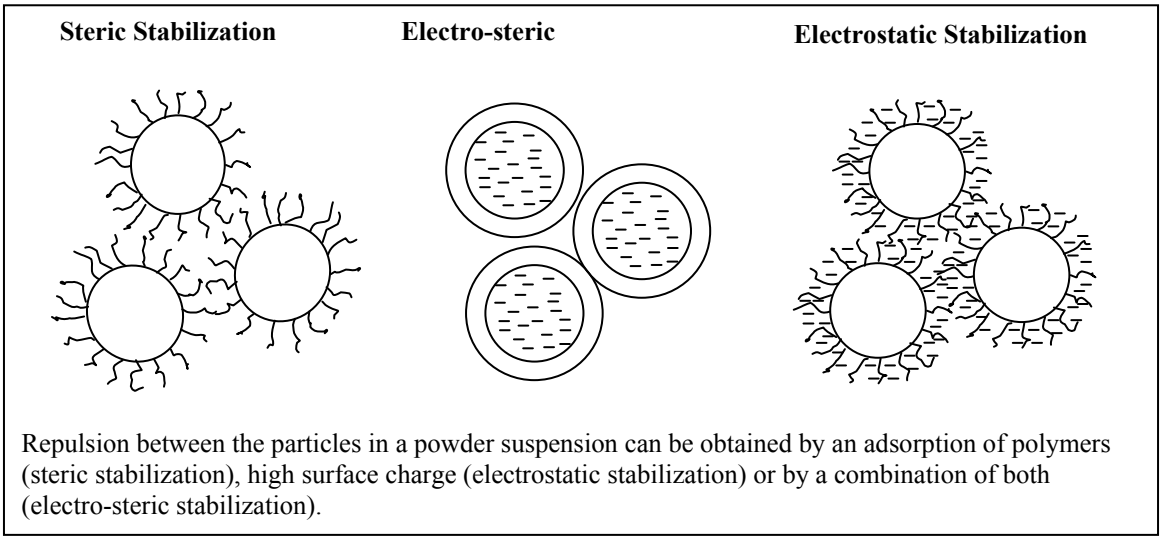

Figure 2.1: Surface Chemistry of Cement Particles and Super-plasticizers (SCI, 2003)

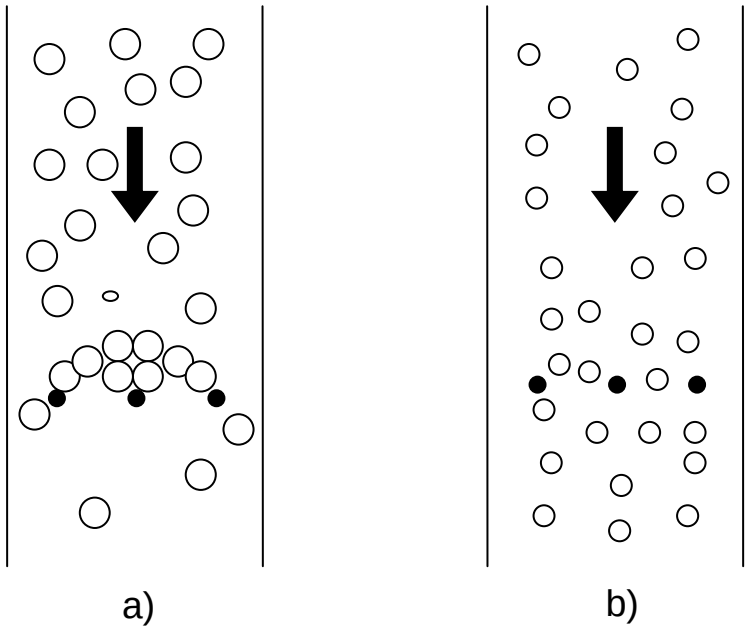

Figure 2.2: Blocking of concrete by aggregate arching; a) Larger aggregate and high content causing arching, and b) smaller aggregates showing good passing ability

Figure 2.3: Spread test and impervious surface

Figure 2.4a: VSI rating 0 (PCI, 2003a)

Figure 2.4b: VSI rating 1 (PCI, 2003a)

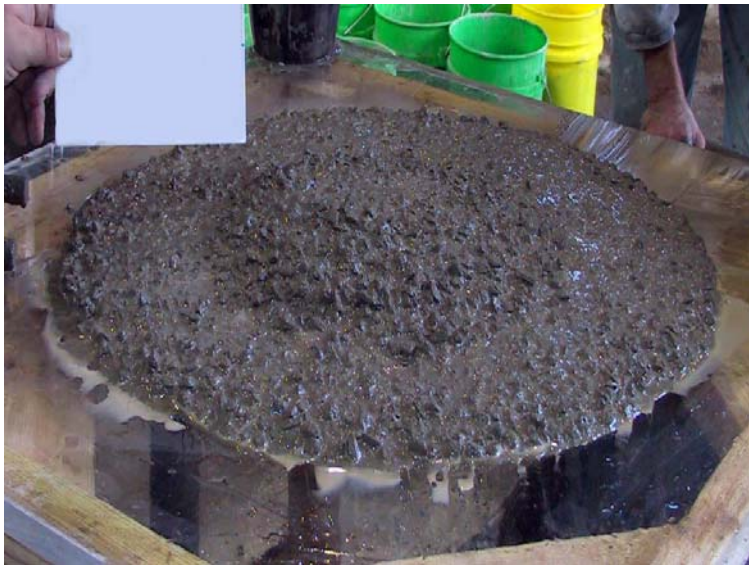

Figure 2.4c: VSI rating 2 (PCI, 2003a)

Figure 2.4d: VSI rating 3 (PCI, 2003a)

Figure 2.5: L-box testing apparatus

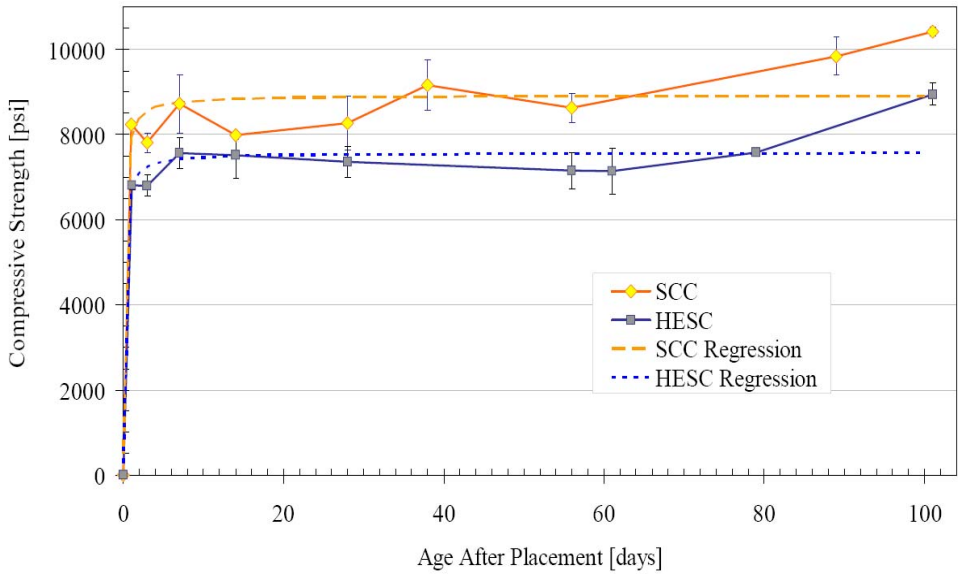

Figure 2.6: Compressive strength gain (Naito et. al., 2005)

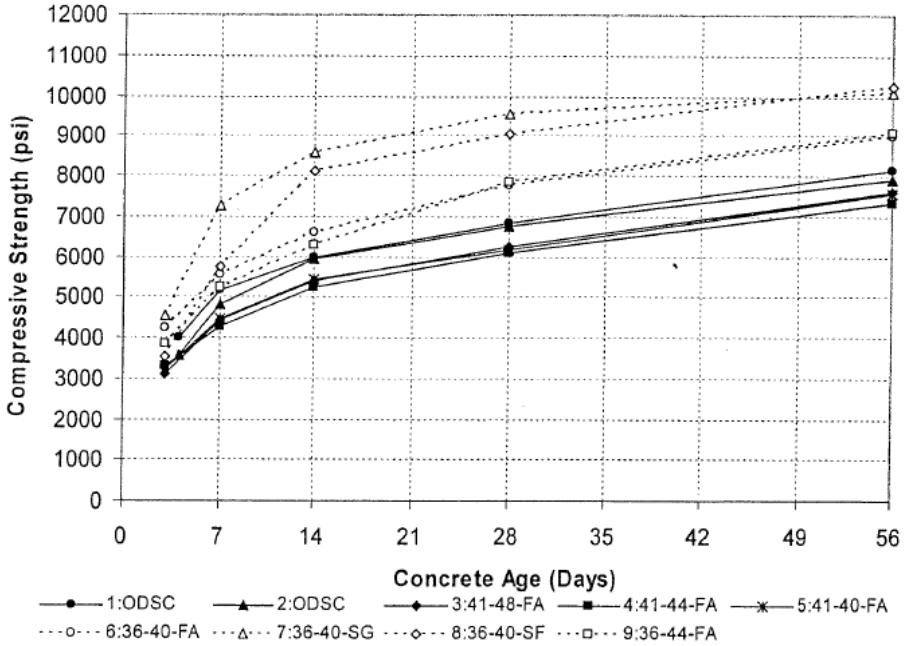

Figure 2.7a: Compressive strength versus concrete age (Bailey, 2005)

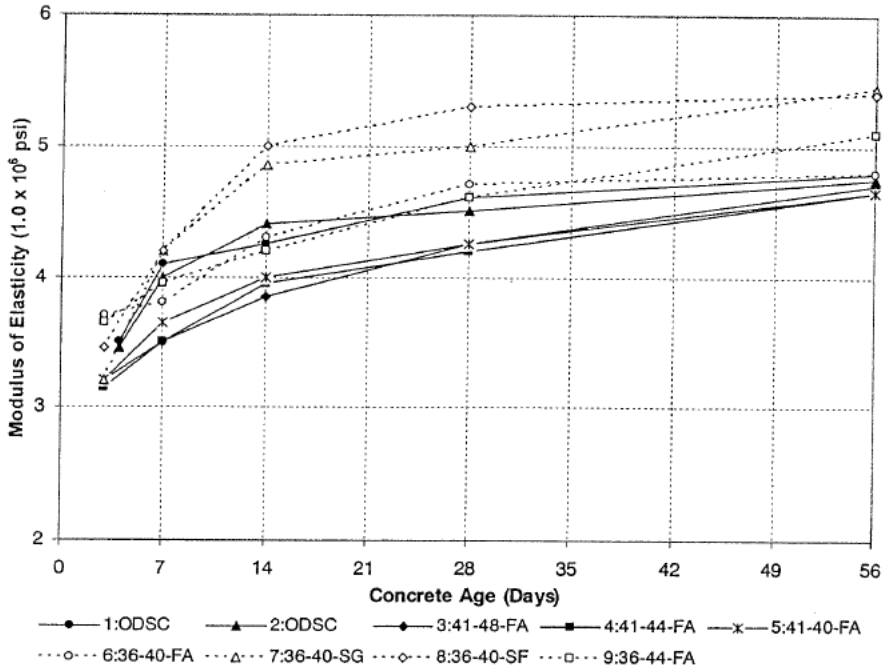

Figure 2.7b: Modulus of elasticity versus Concrete Age (Bailey, 2005)

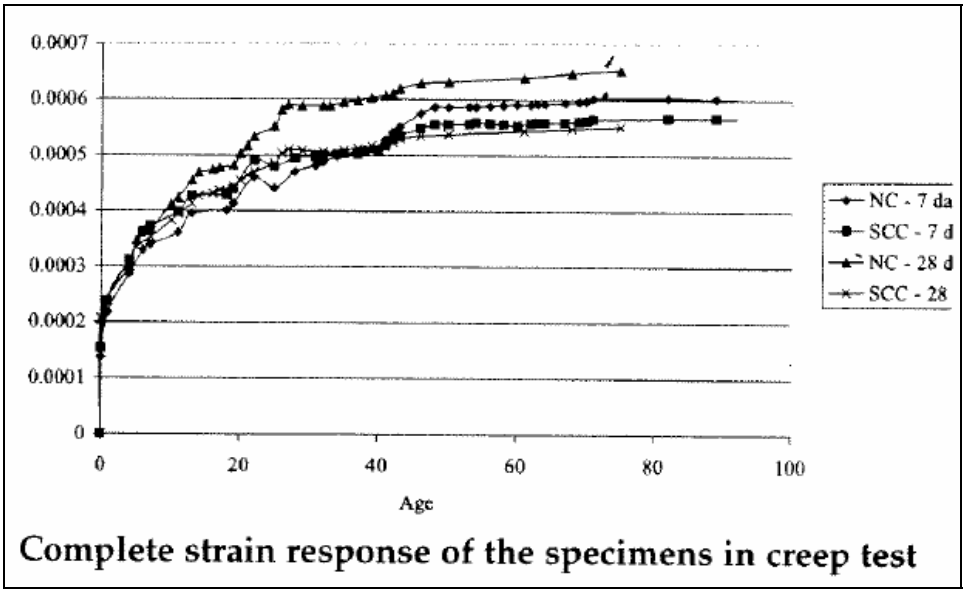

Figure 2.8a: Creep strain response (Raghaven, 2002)

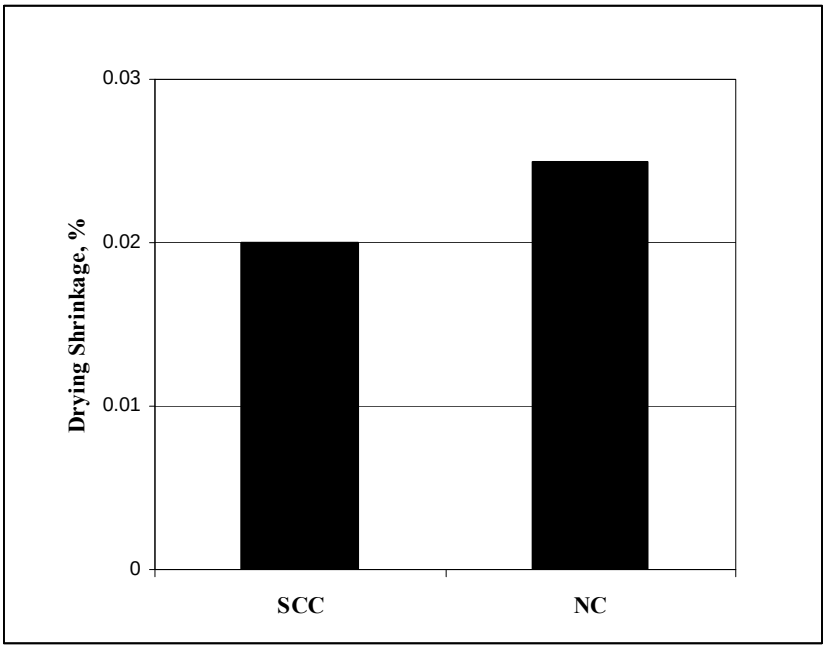

Figure 2.8b: Drying shrinkage at 28 days (Raghaven, 2002)

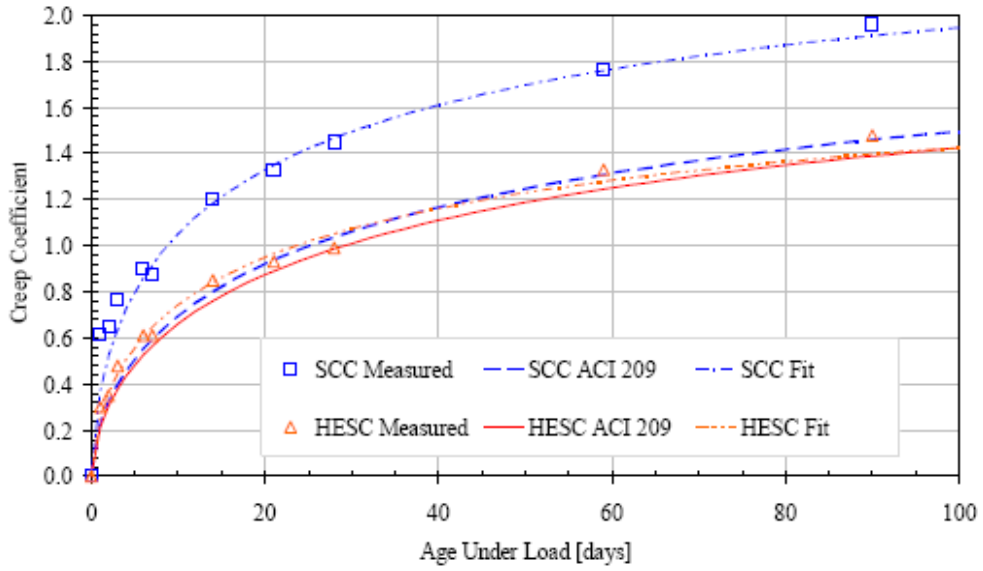

Figure 2.9a: Creep response from Naito et. al. (2005)

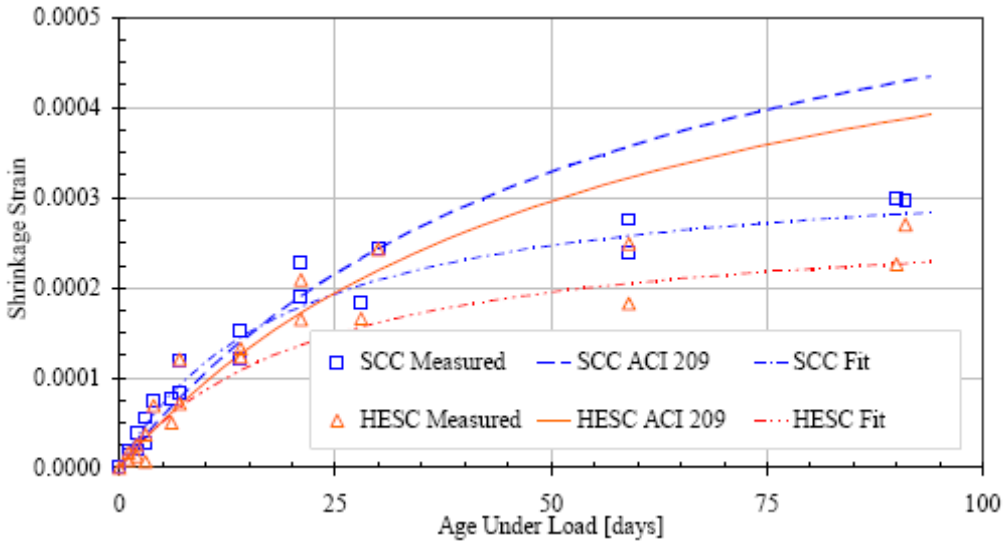

Figure 2.9b: Shrinkage response from Naito et. al. (2005)

Figure 2.10: V-funnel test

Figure 2.11: Wet sieve segregation test

Figure 2.12: Column segregation test

CHAPTER 3
DEVELOPMENT OF MIX DESIGNS

3.1 Introduction

Investigating the parameters that lead to consistent and beneficial concrete mixes exhibiting adequate performance in both the fresh and hardened states was the main goal of this portion of the research. The mixes were designed using materials readily available to concrete producers in the Carolinas and Georgia. The first objective was to become familiar with the constituent materials and also with the mixing techniques for SCC. Next, a number of trial mixes were tested for fresh properties such as slump flow, air content, and U-box (or L-box) performance.

The trial mixes that successfully passed these qualifying tests were further tested for their compressive strength. Finally, three mixes were chosen to be part of the material characterization program which will be discussed in later chapters. Additionally, Florence Concrete Products of Sumter, SC, supplied specimens for one Self Consolidating Lightweight Concrete (SCLC) mix and one High Early Strength Lightweight Concrete mix (HESLC) to be included in the material characterization. In total, five mixes were tested for fresh and hardened properties. The following sections discuss the constituent materials used in the SCC mixes, serve as an overview of the mix design studies conducted and, finally, outline the mixing and curing procedures employed.

The SCLC and HESLC mixes used for the girder test specimens were developed by Florence Concrete Products and the fresh and hardened properties of these mix designs were characterized by U.SC personnel.

3.2 Concrete Constituents

Concrete typically contains four main ingredients: coarse aggregate, fine aggregate, cement, and water. Additionally, mineral and chemical admixtures such as fly ash and super-plasticizers are used to modify the plastic and/or hardened state properties. As discussed previously, SCC mixes generally have a higher volume of fine aggregates and employ super-plasticizers and water-reducers to achieve their increased workability. The mixes developed in this study contained coarse and fine aggregates, cement, water, and chemical admixtures such as high-range water reducers, mid-range water reducers, and air-entrainers.

Aggregates: The coarse aggregate used in the laboratory portion of this study was crushed granite that was mined from the Vulcan Materials quarry in Columbia, SC. Therefore the material is very accessible to SC concrete producers. Both #67 and #789 stone were used in these mixes. The aggregate properties can be found in Table 3.1 courtesy of the South Carolina Department of Transportation. This table shows that the Vulcan Columbia Quarry aggregate has 24 % LA Abrasion Loss, absorption of 0.4 %, and Mohs Hardness of 6. It is very important to use a well-graded coarse aggregate

when specifying SCC materials so that inter-particle friction is reduced. Figures 3.1 and 3.2 show the gradation curves of the #67 and # 789 stones, respectively. It can be seen that the aggregate gradation is well within the specified upper and lower limits of the South Carolina specifications. The gradation of the aggregates was determined in accordance with ASTM C33, Standard Specification for Concrete Aggregates.

The sand used in this study was well-graded Glasscock sand from Sumter City Sand. The fine aggregate properties can be found in Table 3.2 courtesy of the South Carolina Department of Transportation. The gradation curve for this sand can be seen in Figure 3.3. It was determined that this sand was acceptable FA-10 sand and qualified for SCDOT usage. All aggregates were picked up by truck from the Ready-Mix Concrete Plant in Columbia, SC.

The aggregates were kept in a dry condition in large metal storage bins located in the U.SC lab where the temperature remained around 70° F (21° C). The storage conditions can be seen in Figures 3.4a and 3.4b. The moisture content was periodically checked so that the mix water could be adjusted to account for the extra water absorbed by the aggregates due to unavoidable humidity in the lab.

For the companion cylinders that were cast alongside the lightweight AASHTO Type III girder specimens, the coarse aggregates were supplied by North Carolina Stalite Corporation. Sumter County sand was used for these test specimens.

Cement Type: The cement used for the laboratory mixes was Type III Portland cement. The Type III cement was used because of its faster strength gain which is desirable in prestressed bridge girder applications. Holcim Cement Company of Holly Hill, SC supplied the cement in 80 lb. (36 kg) bags and also in large steel drums. The cement was also stored in the USC lab and kept sealed in the large steel drums to prevent any pre-hydration of the cement particles. Holcim performed chemical analysis on the cement as well as Blaine fineness tests to ensure that the cement was adequate. Holcim type T-1 cement was used for the companion cylinders that were cast alongside the lightweight AASHTO Type III test specimens.

Admixtures: The chemical admixtures for the laboratory mixes were supplied by Euclid Chemical Company and W.R. Grace Admixtures. Euclid products used included Eucon SPJ, Eucon SPC, Eucon Retarder 75, Plastol 5500, Eucon WR 91, Air Mix 250, Air 30, and Visctrol VMA. The Grace products used were Daravair 1000, WRDA WR, ADVA 100, AVA 370, V-MAR VMA and ADVACAST 530. The final mix designs chosen for further testing contained the Euclid products Eucon SPJ and WR 91. Eucon SPJ is a high efficiency polycarboxylate super-plasticizer and complies with ASTM C 494 as a Type F admixture. The WR 91 is an ASTM C 494 Type A water-reducing admixture. These two admixtures used together produced more consistent concrete batches than the others and problems with air content were not as frequent. For the companion cylinders that were cast alongside the lightweight AASHTO Type III test specimens, SIKA Plastiment, Viscocrete 2100, and AEA 14 were used.

A list of materials used can be found in Table 3.3a for the U.SC laboratory mixes and in Table 3.3b for the Florence Concrete Products mixes.

3.3 Laboratory Mix Design Studies

The mix design part of this study included researching SCC mixes with similar materials and adjusting those mixes until the desired characteristics were achieved. First, some design parameters had to be set in order to quantify and qualify the concrete. The first properties of concern were fresh state properties including flowability and air content. Next, if the mixes passed these qualifications, cylinders would be made, and the concrete compressive strength would be tested. If the concrete passed both the fresh and hardened state properties, then the mix would be considered for the full material characterization described later.

Design Parameters: In order for the fresh concrete to qualify as an adequate mix, the slump flow was limited to 26 ± 2 in. (660 ± 51 mm). Most of the mixes tested achieved this; however, many failed the other tests. The visual stability index (VSI) as described previously was used to rate the quality of the mix as it pertains to segregation resistance. By visually inspecting the fresh concrete paddy the concrete was rated in the range of 0 (best) to 3 (worst). A VSI of 1 or better would qualify as adequate. The other fresh state property tested during the trial mix phase was the air content. This proved to be a quick and effective way to disqualify mixes that would not have adequate strength. In order for a trial mix to be considered for further testing, the air content was limited to 6 % by volume.

If the concrete passed the three tests listed above, the U-box would then be used subsequently to characterize the flowability, and in particular the filling ability of the concrete. PCI (2005) recommends that the filling height through the U-box be 11 7/8 in. (300 mm) above the bottom of the 'U'. The U-box that was fabricated for this study varied slightly in dimensions from those of the U-box shown in the PCI document. For this reason the difference between h1 (distance from bottom of 'U' to top of fresh concrete on the side that is filled prior to conducting the test) and h2 (distance from bottom of 'U' to top of fresh concrete on the opposite side) was used for evaluation. Using the PCI U-box apparatus the h1 – h2 value corresponding to 11 7/8 in. (300 mm) height is approximately 1.5 in. (38 mm). The U-box test results were subject to variability and were used as a secondary indicator to the spread test for assessment of the mix designs.

If the fresh properties were achieved then larger batches would be mixed and cylinders cast for compressive strength testing. 4 x 8 in. (101 x 203 mm) cylinders were tested according to ASTM C 39 at 1 and 7 days. A compressive strength of 6,400 psi (44.1 MPa) was required in 7 days to qualify the mix for further testing.

Trial Mixes: The design quantities considered in the mix design proportions were:

- Total Cement, lb/yd^3 (kg/m^3)
- Fly Ash, lb/yd^3 (kg/m^3)
- Silica Fume, lb/yd^3 (kg/m^3)
- Coarse Aggregate - #67 SSD- lb/yd^3 (kg/m^3)
- Coarse Aggregate - #789 SSD- lb/yd^3 (kg/m^3)
- Water Cement (w/c) ratio
- Coarse/Fine Agg. Ratio
- Chemical admixtures oz/yd^3 (ml/m^3) (HRWR, WR, AE, VMA)

Sixteen trial mixes, shown in Tables 3.4a and 3.4b, were tested per the requirements of the preceding section and three were selected for further investigations. These included one mix with equal amounts of coarse and fine aggregates, one with more coarse than fine material, and one mix containing silica fume and fly ash. Related studies on SCC (girders cast at Standard Concrete Products, Savannah, GA) included mixes containing fly ash, and so it was decided that the U.SC mixes would focus primarily on aggregate ratio differences and the use of silica fume. Trial mixes 13, 14 and 16 were chosen for full material characterization. These mixes correspond with the final Batch names shown below:

- **"Batch 1"** = "Trial 13"
- **"Batch 2"** = "Trial 16"
- **"Batch 3"** = "Trial 14"

These three batches were chosen for several reasons. First, all three mixes had adequate slump flow ranging from 24 in. to 26.5 in. (609 – 673 mm). Second, all three mixes were made with the same admixtures. Therefore, since the materials were the same, the mix proportions would be the only parameter for comparison. All three mixes contained Euclid Eucon SPJ superplasticizer and Euclid WR 91 water-reducing admixture.

Another reason for choosing these mixes was the aggregate gradation differences. Trial 13 mix (Batch 1) contained two sizes of crushed granite giving a much more "well-graded" aggregate curve for the mix. This allows for more stable flow, and less segregation due to blocking as can be noticed in the U-box results in Table 3.4b. The #789 stone fills the gaps between the sand and the large #67 stone and separates the larger aggregates so that they do not get caught in congested rebar arrangements. Trial 14 (Batch 3) contained only #67 aggregate at a coarse to fine aggregate ratio of approximately 53/47. Trial 16 (Batch 2) contained both types of aggregates as well as other fine materials such as fly ash and silica fume. This mix showed excellent fresh properties with a slump flow of 26.5 in. (673 mm), and a filling height of 12.5 in. (318 mm). The air content of all three batches was around 3.5% air by volume.

The mix proportions for the companion cylinders cast alongside the HESLC and SCLC AASHTO Type III girders can be found in Table 3.4c. Table 3.5 is a summary of the mixes that were characterized beyond the fresh properties.

Laboratory Mixing Procedures: Mixing was conducted in a 2.5 cu. ft. (0.07 cu. m) mixer for the laboratory trial batches, and in a 6 cu. ft. (0.17 cu. m) mixer for the larger batches. The mixers can be seen in Figures 3.5 and 3.6. The first step is to ensure that the mixer is clean and free of leftover chemical admixtures that could affect the outcome of the mix. Once the mixer has been thoroughly cleaned, excess water must be removed so that only a small film of water exists inside the mixer. This ensures that the mixer will not absorb any of the intended mix water.

Another concern is the timing of the high-range water reducer addition. Some researchers have concluded that adding this before the cement addition is beneficial, while others indicate the opposite. It was decided that the HRWR would be added after the addition of the cement. This allows the concrete producer to assess the water demand of the cement and aggregates and adjust the HRWR dosage if needed. The mid-range water reducing admixtures, however, were added before any cementations materials. Since the WRs are not as effective, this keeps the water and cement from clumping before the addition of the extra water and HRWR. The measurement of the chemical admixtures is very important to the stability of the mix. In this project, measurement of the chemical admixtures was performed using a small and a large syringe as shown in Figures 3.7a and 3.7b, respectively.

The final mixing procedure was as follows:

1. 60 % of the mixing water was first added to the mixer.
2. The coarse and fine aggregates were added next to the mixer.
3. Mixing took place for 30 seconds.
4. The mid-range water reducing admixtures were added next.
5. Mixing took place for 30 seconds.
6. The cementitious materials were added next.
7. The super-plasticizers were added to the mixer.
8. Mixing took place for 1 minute.
9. If required, the rest of the mix water was added.
10. Mixing took place for an additional three minutes.
11. Slump flow readings were taken at this point.
12. Mixing was continued for two additional minutes.
13. A new slump flow reading was taken, and all other fresh state tests were conducted.
14. Specimens were cast for all hardened state property testing.

3.4 Curing Procedures

Proper curing is one of the most important steps in making quality specimens. Since the prestressed bridge girders would be cast in summer, the curing temperatures would be

very high. The curing temperature gets even higher inside large members such as the AASHTO Type III girders. To account for this increased temperature and to simulate the field-cast girders the cylinders were cured inside an increased heat room using small heaters and humidifiers. The temperature was kept around 90 - 95º F (32 – 35º C). All specimens were tightly sealed so that no extra moisture would be lost during the curing process. Increased temperature curing began within one hour after the specimens were made. Following the initial curing regimen the specimens were stored in a controlled environment. The temperature and humidity levels were monitored hourly after the initial concrete mixing. The temperature data can be found in Figure 3.8. Attempts were made to maintain the relative humidity level around 50 %. The relative humidity data can be found in Figure 3.9.

3.5 Mix Designs for Companion Specimens (AASHTO Type III Girders)

The SCLC mix used in the fabrication of the bridge girders for subsequent testing and evaluation registered a slump flow value of 22 in (560 mm) (Table 3.4c). According to EFNARC this value classifies the mix as SCC class 1 [slump flow between 21.6 – 26.0 in. (550 - 650 mm)] with excellent workability. A value of 1.3 in (33 mm) was measured in the U-box test. This measurement infers the SCLC mixture has good filling and passing ability confirming the result obtained from the slump flow test. The 28-day compressive strength did not attain the desired 8,000 psi (55.2 MPa).

Table 3.1: Approved coarse aggregate sources (SCDOT, 2007)

SUPPLIER (SOURCE NAME) LOCATION	SCDOT NO.	LAB NO.	LA ABRA LOSS %		ABSORPTION %	SPECIFIC GRAVITY			SOUNDNESS % LOSS at 5 CYCLES			SAND EQUIVALENT	MOHS HARDNESS	NOTES
			A	B		BLK. DRY	BLK. SSD	APPARENT	1 1\2 TO 3\4	3\4 TO 3\8	3\8 TO #4			
MARTIN MARIETTA AGGREGATES														
Appling, Ga.	SC120	N17882	41	46	0.8	2.61	2.63	2.66	0.0	0.0	0.2	72	6	1,C,Gr
Augusta, Ga.	SC134	N17881	22	19	1.1	2.59	2.62	2.67	0.1	0.3	0.7		7	1,4,C,Gr
Camak, Ga.	SC121	N12146	35	31	0.6	2.64	2.66	2.69	0.1	0.3	0.1	60	6	1,4,C,Gr
Cayce, SC	SC122	N18102	23	28	0.5	2.63	2.64	2.66	1.1	1.7	4.1	53	6	1,4,C,Gr
Charleston, SC (Kinder Morgan Terminal)	SC123	Transfer Stockpiles from Porcupine Mountain, Nova Scotia												
Charleston, SC (Montague Yard)	SC138	Transfer Stockpiles from Cayce Quarry and North Columbia Quarry												
Charlotte, NC (Mallard Creek)	SC124	N11996	16	17	0.5	2.84	2.85	2.88	0.1	0.2	1.5	58	7	1,C,Gr
Jefferson, SC (Chesterfield Q.)	SC130	N18924	37	39	0.6	2.59	2.61	2.63	7.7	0.7	3.3	--	5	C,Gr
Garner, NC	SC179	N17607	37	36	0.5	2.62	2.63	2.66	0.2	0.3	0.3	68	5	1,C,Gr
Hickory, NC	SC128	N12662	45	47	0.7	2.71	2.73	2.76	0.1	0.3	0.1	63	6	1,C,L
Kernersville, NC (Salem)	SC131	N12404	39	39	0.6	2.64	2.66	2.69	0.2	1.2	1.8	39	5	1,C,Gr
Kings Mountain, NC	SC132	N11719	29	26	0.6	2.71	2.72	2.75	0.0	0.1	0.1		6	1,C,L
Matthews, NC	SC135	N11797	13	12	0.6	2.79	2.80	2.84	0.1	0.1	0.2	53	6	1,C, Gr-Gn
Monroe, NC (Bakers)	SC136	N11795	18	18	0.7	2.72	2.74	2.78	0.2	0.2	0.2	61	7	1,C,Gr-Gn
Myrtle Beach, SC (Sales Yard)	SC137	Transfer Stockpiles from Lemon Springs Quarry												
Lemon Springs (information only) **		M87253	25	23	0.8	2.60	2.62	2.66	0.1	0.2	0.5	53	5	1,4,C,Gr
North Columbia, SC	SC139	N18599	35	37	0.4	2.65	2.66	2.68	0.2	0.2	0.3	74	5	1,C,Gr
Pineville, NC (Arrowood)	SC140	N11951	24	26	0.5	2.94	2.95	2.98	0.1	0.1	0.2	63	5	1,C,Gr
Porcupine Mountain, Nova Scotia	SC141	N18727	17	16	0.6	2.69	2.70	2.73	0.3	0.8	0.6		5	1,4,C,Gr
Rock Hill, SC	SC142	N11718	23	21	0.6	2.82	2.83	2.86	0.1	0.2	0.2	54	5	1,C,Gr
Savannah, Ga. (Marine Terminal)	SC177	Transfer Stockpiles from Porcupine Mountain, Nova Scotia and Bahamma Island												
Bahamma Islands (information only) **		N18726	40	37	5.3	2.22	2.34	2.52	3.0	1.0	1.6			1,4, C,ML
Savannah, Ga. (Sales Yard)	SC143	Transfer Stockpiles from Camak Quarry, Ga.												
Statesville, NC	SC144	N12664	39	38	0.6	2.80	2.82	2.85	0.4	0.6	0.8	60	5	1,C,Gr
Thomasville, NC	SC145	N12403	15	16	0.5	2.71	2.72	2.75	0.5	1.7	3.9	68	7	1,4,C,Gr
OCONEE COUNTY ROCK														
Oconee Cty Rock Quarry	SC186	N06780	57	62	0.6	2.60	2.61	2.64	0.5	0.2	0.5	71	4	C,Gr
RINKER MATERIALS														
Appling, Ga. (Dogwood)	SC146	N20314	40	42	0.6	2.61	2.63	2.65	0.1	1.7	0.1	72	6	1,C,Gr
Macon, Ga. (Hitchcock)	SC171	N12698	24	23	0.2	2.74	2.75	2.78	0.1	0.1	0.2	57	6	1,C,Gr
VULCAN MATERIALS COMPANY														
Anderson, SC	SC147	N07123	50	52	0.8	2.73	2.75	2.79	0.2	0.1	0.1		5	1,C,Gr
Blacksburg, SC	SC148	N20723	31	34	0.6	2.78	2.80	2.83	0.4	0.6	0.9	35	5	1,C,Sch
Blair, SC	SC149	N18412	42	47	0.7	2.60	2.62	2.65	0.2	0.4	0.6	69	5	1,C,Gr
Columbia, SC	SC151	N18089	23	24	0.5	2.62	2.64	2.66	0.3	0.7	0.9	50	6	1,4,C,Gr
Concord, NC (Cabarrus)	SC152	N11994	24	26	0.5	2.77	2.78	2.81	0.1	0.2	0.3	65	6	1,C,Gr
Charlotte, NC (Pineville)	SC150	N11950	23	27	0.4	2.95	2.96	2.99	0.3	0.3	0.3	62	6	1,C,Gr
Enka, NC	SC153	N18886	30	32	0.6	2.68	2.70	2.73	0.6	0.6	1.7	--	6	4,C,G,Sch

Table 3.2: Approved fine aggregate sources (SCDOT, 2007)

SUPPLIER	LOCATION NAME	SCDOT NO.	LOCATION	LAB NO.	FINE- NESS MODU- LUS	ABSORP- TION, %	SPECIFIC GRAVITY, BULK SSD	SOUND- NESS LOSS, %	NOTES
HANSON AGG.	Marlboro	SC106	BENNETTSVILLE, SC	N19422	2.80	0.1	2.66	0.1	1,6,D,N,P,S,W
HANSON AGG. EAST	Elliot	SC174	ERWIN, NC	M84370	2.40	0.5	2.63	1.1	1,6,P,S,W
HANSON AGG.	Harbersham	SC107	DEMOREST, GA	N10583	2.95	0.5	2.59	0.3	1,6,M,W
HANSON AGG.	Lithonia	SC188	LITHONIA, GA	N12381	2.88	0.4	2.63	1.9	1,M,P,W
HANSON AGG.	Brewer	SC529	PAGLAND, SC	N18743	2.42	0.6	2.61	3.1	1,P,S,W
HANSON AGG.	Sandy Flats	SC113	TAYLORS, SC	N20338	2.86	0.3	2.64	0.2	1,6,M,P,W
HANSON AGG.		SC114	TOCCOA, GA.	N10584	2.69	0.1	2.65	0.2	1,6,M,W
HEADRICK INDUST.	Piedmont Sand	SC541	PAGELAND, SC	N04366	2.28	0.4	2.62	0.2	1,6,N,P,S,W
KING ASPHALT	Theo Pit	SC571	WOODRUFF, SC	N14741	2.52	0.7	2.60	0.4	1,6,R
LAFARGE AGGREGATES	Lithonia	SC182	LITHONIA, GA	N12386	2.84	0.4	2.63	1.9	1,6,M,W,S
LANIER SAND & CONSTRUCTION	Glenn Rd. Pit	SC589	COLUMBIA, SC	N20069	2.17	0.3	2.65	1.3	1,6,N,B,P,W
LBM INDUSTRIES	Sapphire Mountain	SC119	SAPPHIRE, NC	N19524	2.75	0.3	2.70	0.4	1,6,M,P,W
L. C. CURTIS & SON	Oconee R.	SC534	WATKINSVILLE, GA	N20016	2.67	0.5	2.55	0.2	1,6,N,D,P,W,S
LOVELESS & LOVELESS	Screeming Eagle	SC537	PONTIAC, SC	N18085	2.05	0.3	2.70	1.1	1,6, N,P,W
MARTIN MARIETTA AGG	Orangeburg	SC126	EUTAWVILLE, SC	N06047	2.63	3.8	2.56	0.2	1,6, M,S,W
MARTIN MARIETTA AGG.	Garner	SC179	Garner, NC	N17608	2.72	0.6	2.64	1.0	1,M,P,S,W
MARTIN MARIETTA AGG.		Sc129	JAMESTOWN, SC	N18275	2.78	3.9	2.63	1.1	1,6,M,W
MARTIN MARIETTA AGG.		SC128	HICKORY, NC	N12663	2.55	0.3	2.75	1.9	7,6, M,P,W
MARTIN MARIETTA AGG.		SC137	MATTHEWS, NC	N11798	3.13	0.7	2.81	0.2	7,6,M,P,S,W
MARTIN MARIETTA AGG.	Augusta	SC134	AUGUSTA, GA.	N17880	2.47	0.6	2.62	1.3	1,6,M,W
MARTIN MARIETTA AGG.		SC142	ROCK HILL, SC	N11721	2.85	0.6	2.85	0.3	1,6,M,P,W
MARTIN MARIETTA AGG.		SC564	WOODLEAF, NC	N12666	2.88	0.3	2.66	1.1	1,6,M,W
MONTGOMERY SAND		SC557	MT. VERNON, GA.	N19299	2.79	0.2	2.70	1.7	1,6, N,D,P,W
MURRY MINES	Princpi Mine	SC593	RIDGEVILLE, SC	N18163	2.14	0.4	2.65	2.1	1,6, D,P,R,S
PALMETTO AGGREGATES	Saluda Pit	SC559	PIEDMONT, SC	N18630	2.65	0.8	2.63	1.6	1,6,R,D,W,S
PALMETTO SAND CO.	Pine Bluff Mine	SC601	RIDGEVILLE, SC	N16859	2.33	0.0	2.37	1.5	1, D,N,P,S,W
RINKER MATERIALS	Deerfield	SC544	RIDGELAND, SC	N18721	2.76	0.4	2.52	2.0	1,6,N,P,S
RINKER MATERIALS	Dogwood	SC 146	APPLING, GA	N20315	2.62	0.3	2.62	0.1	1,6,M,W,S
RINKER MATERIALS	Union Sand Mine	SC594	LUDOWICI, GA	N19301	2.33	0.1	2.65	2.4	1,6,N,P,W
SOUTHEASTERN SAND, LLC		SC543	OLANTA, SC	N19019	2.65	0.1	2.65	1.4	1,N,P,W,S
STANDARD SAND & SILICA	Saber	SC560	LYONS, GA.	N19300	2.74	0.2	2.57	2.2	1,N,D,P,S,W
STANDARD SAND & SILICA	Ivey	SC568	IVEY, GA.	N12151	2.61	0.5	2.63	0.1	1,6,N,B,W,S
SUMTER CTY. SAND	Glasscock	SC545	SUMTER, SC	N02353	2.80	0.3	2.66	0.5	1,6,N,P,S,W
SUPERIOR SAND, LLC		SC546	NICHOLS, SC	N18051	2.40	0.1	2.60	1.5	1,5,6,D,N,S,W
THE BURKE COMPANY	Burke mine	SC599	MAYESVILLE,SC	N20462	2.61	0.2	2.60	1.1	1,6,N,B,P,W,S
THOMAS SAND COM.		SC547	BLACKSBURG, SC	N15260	2.39	0.8	2.59	0.7	1,6,D,R,S,W
VULCAN MATERIALS CO.	Blair	SC149	BLAIR, SC	N18410	2.30	0.5	2.63	1.2	1,6,M,W
VULCAN MATERIALS CO.		SC147	ANDERSON, SC	N07122	2.65	0.2	2.77	4.5	1,6,M,W
VULCAN MATERIALS CO.	Cabarrus	SC152	CONCORD, NC	N11995	2.76	0.6	2.76	0.4	7,6,M,P,W
VULCAN MATERIALS CO.		SC151	COLUMBIA, SC	N18088	2.37	0.4	2.64	1.5	1,M,P,W

Table 3.3a: Source of materials for U.SC laboratory mixes

Type		Label	Product (Type)	Supplier	Specific Gravity	Absorption
Coarse Aggregate		CA1	#67 Granite	Martin Marietta	2.62	0.50%
		CA2	#789 Granite	Martin Marietta	2.62	0.50%
		CA3	#67 Granite	Vulcan	2.64	0.40%
Fine Aggregate		FA1	Washed Mortar Sand	Foster Dixianna	2.62	0.40%
		FA2	Concrete Sand	Glasscock	2.52	0.30%
Cementitious		C1	Type III	Holcim Cement Co.	3.15	
		C2	Class C	Boral	~2.6	
Chemical Admixtures	**Water Reducers**	A1	WRDA 35, (Water-reducer/Retarder - Type A/D)	W.R. Grace		
		A2	EUCON RETARDER 75 (Water-reducer/Retarder)	Euclid		
		A3	EUCON WR 91 (Water Reducer)	Euclid		
	High-range Water Reducers	A4	ADVA 100, (Polycarboxylate)	W.R. Grace		
		A5	ADVA 370, (Polycarboxylate)	W.R. Grace		
		A6	ADVACAST 530 (Polycarboxylate)	W.R. Grace		
		A7	PLASTOL 5500 (Polycarboxylate)	Euclid		
		A8	EUCON SPJ (Polycarboxylate)	Euclid		
		A9	EUCON SPC (Polycarboxylate)	Euclid		
	Viscocity Modifiers	A10	V-MAR 3, (VMA)	W.R. Grace		
		A11	VISCTROL, (VMA)	Euclid		
	Air Entrainers	A12	DARAVAIR 1000, (Air-entrainer)	W.R. Grace		
		A13	AIR MIX 250 (Air Entrainer)	Euclid		
		A14	AIR 30 (Air Entrainer)	Euclid		

Table 3.3b: Source of materials for fabricator mixes (Florence Concrete Products)

Type		Label	Product (Type)	Supplier	Specific Gravity	Absorption
Coarse Aggregate		CA1	NA	Stalite	1.53	0.50%
Fine Aggregate		FA1	NA	Sumter Co. Sand	2.64	0.00%
Cementitious		C1	Type T-1	Holcim Cement Co.	3.15	
Chemical Admixtures	**Water Reducers**	A1	Plastiment	Sika		
	High-range Water Reducers	A2	Viscocrete 2100, (Polycarboxylate)	Sika		
	Viscocity Modifiers	-	-	-		
	Air Entrainers	A3	AEA 14	Sika		

Table 3.4a: U.SC trial mixes – 1 of 2

Material Type	Mix Designation for USC Lab Trial SCC Mixes (1)							
	Trial 1	Trial 2	Trial 3	Trial 4	Trial 5	Trial 6	Trial 7	Trial 8
w/c Ratio	0.28	0.35	0.40	0.38	0.38	0.38	0.38	0.39
Cement, lb/yd^3 (kg/m^3)	700 (416)	620 (368)	650 (386)	650 (386)	650 (386)	650 (386)	650 (386)	810 (481)
Fly Ash, lb/yd^3 (kg/m^3)	250 (149)	105 (62)	115 (68)	115 (68)	115 (68)	115 (68)	115 (68)	0 0
Silica Fume, lb/yd^3 (kg/m^3)	0 0	0 0	0 0	0 0	0 0	0 0	0 0	0 0
# 67 Stone, lb/yd^3 (kg/m^3)	1200 (713)	1454 (864)	1455 (864)	1455 (864)	1455 (864)	1455 (864)	1455 (864)	998 (593)
# 789 Stone, lb/yd^3 (kg/m^3)	600 (356)	0 0	0 0	0 0	0 0	0 0	0 0	333 (198)
Fine Sand, lb/yd^3 (kg/m^3)	1100 (653)	1348 (800)	1325 (787)	1325 (787)	1325 (787)	1325 (787)	1325 (787)	1300 (772)
Total Water, lb/yd^3 (kg/m^3)	266 (158)	254 (151)	306 (182)	291 (173)	291 (173)	291 (173)	291 (173)	318 (189)
HRWR, oz/yd^3 (ml/m^3)	101.4 (3000)	49.6 (1467)	42.3 (1250)	48.8 (1442)	50.1 (1480)	39.0 (1153)	39.0 (1153)	81.0 (2396)
WR, oz/yd^3 (ml/m^3)	0.0 0.0	24.8 (733.4)	24.8 (733.4)	24.8 (733.4)	24.8 (733.4)	16.3 (480.6)	16.3 (480.6)	32.4 (958.2)
VMA, oz/yd^3 (ml/m^3)	0.0 0.0	0.0 0.0	0.0 0.0	0.0 0.0	0.9 (27.3)	0.9 (26.5)	0.9 (26.5)	0.9 (25.3)
AEA, oz/yd^3 (ml/m^3)	0.0 0.0	4.0 (118.3)	0.0 0.0	0.0 0.0	0.0 0.0	0.0 0.0	0.0 0.0	0.0 0.0
Coarse/Fine Ratio	1.64	1.08	1.10	1.10	1.10	1.10	1.10	1.02
HRWR Type	ADVA 370	ADVA 530	ADVA 531	ADVA 532	ADVA 533	Eucon SPJ	Plastol 5500	SPJ
Water Reducer	WRDA 35	WRDA 35	WRDA 35	WRDA 35	WRDA 35	Retarder 75	Retarder 75	Euclid WR 91
Slump Flow (in)	26.3	27.0	29.0	27.5	27.3	26.5	25.0	25.3
U-Box (h1-h2)	n.g.*	2.2	2.2	-	2.2	10.6	-	4.3
L-Box	n.g.	-	-	-	-	-	-	0.77
Air Content	2.20	18.00	6.80	9.00	4.90	2.80	9.50	3.00
7 day f'c, psi	n.t.	n.t.	4150	n.t.	5120	n.t.	n.t.	6572
14 day f'c, psi	n.t.	2092	n.t.	n.t.	6821	n.t.	n.t.	n.t.
56 day f'c, psi	8790	n.t.	n.t.	n.t.	n.t.	n.t.	n.t.	n.t.

*Shaded cells represent mix failure

Table 3.4b: U.SC trial mixes - 2 of 2

Material Type	Mix Designation for USC Lab Trial SCC Mixes (2)							
	Trial 9	Trial 10	Trial 11	Trial 12	Trial 13 *	Trial 14 **	Trial 15	Trial 16 ***
w/c Ratio	0.39	0.36	0.34	0.35	0.38	0.36	0.33	0.34
Cement, lb/yd^3 (kg/m^3)	567 (337)	810 (481)	567 (337)	648 (385)	810 (481)	810 (481)	800 (475)	800 (475)
Fly Ash, lb/yd^3 (kg/m^3)	243 (144)	0 0	243 (144)	162 (96)	0 0	0 0	100 (59)	100 (59)
Silica Fume, lb/yd^3 (kg/m^3)	0 0	0 0	0 0	0 0	0 0	0 0	48 (29)	48 (29)
# 67 Stone, lb/yd^3 (kg/m^3)	998 (593)	998 (593)	998 (593)	998 (593)	998 (593)	1463 (869)	1490 (885)	1266 (752)
# 789 Stone, lb/yd^3 (kg/m^3)	333 (198)	333 (198)	333 (198)	333 (198)	333 (198)	0 0	0 0	224 (133)
Fine Sand, lb/yd^3 (kg/m^3)	1300 (772)	1300 (772)	1300 (772)	1300 (772)	1330 (790)	1330 (790)	1215 (722)	1215 (722)
Total Water, lb/yd^3 (kg/m^3)	318 (189)	292 (173)	277 (165)	284 (168)	304 (180)	292 (173)	311 (185)	324 (193)
HRWR, oz/yd^3 (ml/m^3)	55.0 (1627)	81.0 (2396)	56.7 (1677)	64.8 (1916)	81.0 (2396)	81.0 (2396)	112.0 (3312)	74.70 (2209)
WR, oz/yd^3 (ml/m^3)	32.3 (955)	32.4 (958)	22.7 (671)	25.9 (767)	32.4 (958)	32.4 (952)	36.0 (1065)	36.00 (1065)
VMA, oz/yd^3 (ml/m^3)	0.9 (25.3)	0.9 (27.8)	0.9 (27.0)	0.9 (26.3)	0.0 0.0	0.0 0.0	0.0 0.0	0 0
AEA, oz/yd^3 (ml/m^3)	0.0 0.0	2.4 (71.9)	1.7 (50.3)	1.9 (57.5)	2.4 (71.9)	2.4 (71.9)	0.0 0.0	0.90 (26.62)
Coarse/Fine Ratio	1.02	1.02	1.02	1.02	1.00	1.10	1.23	1.23
HRWR Type	Euclid SPC	Euclid SPC	Euclid SPC	Euclid SPC	Euclid SPJ	Euclid SPJ	Euclid SPJ	Euclid SPJ
Water Reducer Type	Euclid WR 91	Euclid WR 91	Euclid WR 91	Euclid WR 91	Euclid WR 91	Euclid WR 91	Euclid WR 91	Euclid WR 91
Slump Flow, in	n.g.	27.8	27.0	26.3	25.0	24.0	27.3	26.5
U-Box (h1-h2)	n.g.	-	4.3	4.3	0.5	4.3	-	1.1
L-Box	n.g.	-	-	-	0.74	-	0.72	0.72
Air Content	n.g.	2.30	2.60	4.30	3.50	3.8	1.90	3.50
1 day f'c, psi	n.t.	5550	4062	n.t.	n.t.	4877	6224	4960
7 day f'c, psi	n.t.	7150	6090	4580	5127	6845	8046	n.t.
28 day f'c, psi	8790	8846	7543	n.t.	9226	n.t.	8821	n.t.

* Corresponds to final Batch 1 in Table 3.5
** Corresponds to final Batch 3 in Table 3.5
*** Corresponds to final Batch 2 in Table 3.5

Table 3.4c: Fabricator mix designs

Material Type	Mix Designation	
	HESLC	SCLC
w/c Ratio	0.36	0.36
Cement, lb/yd^3 (kg/m^3)	850 (504)	850 (504)
Fly Ash, lb/yd^3 (kg/m^3)	0	0
Silica Fume, lb/yd^3 (kg/m^3)	0	0
Stalite, lb/yd^3 (kg/m^3)	940 (558)	940 (558)
Fine Sand, lb/yd^3 (kg/m^3)	1082 (642)	1082 (642)
Total Water, lb/yd^3 (kg/m^3)	306 (182)	306 (182)
HRWR, oz/yd^3 (ml/m^3)	180 (5,332)	190 (5,618)
WR, oz/yd^3 (ml/m^3)	135 (3,992)	145 (4,287)
VMA, oz/yd^3 (ml/m^3)	0	0
AEA, oz/yd^3 (ml/m^3)	11.0 (325)	11.0 (325)
Coarse/Fine Ratio	0.87	0.87
HRWR Type	Sika Viscocrete	Sika Viscocrete
Water Reducer Type	Sika Plastiment	Sika Plastiment
Slump Flow, in	na	22
U-Box (h1-h2)	na	1.3
L-Box	na	0.77
Air Content	4.5%	4.5%
Unit weight, design (lbs/ft^3)	118	118
28 day f'c, psi	7,405	7,641
56 day f'c, psi	7,496	7,921

Table 3.5: Final mix matrix – laboratory and producer (FCP) mixes

Material Type	Batch 1	Batch 2	Batch 3	HESLC	SCLC
Location	USC-Lab	USC-Lab	USC-Lab	Florence Concrete Products	Florence Concrete Products
w/c Ratio	0.38	0.34	0.36	0.36	0.36
Cement, lb/yd^3 (kg/m^3)	810 (481)	800 (475)	810 (481)	850 (504)	850 (504)
Fly Ash, lb/yd^3 (kg/m^3) Boral Class C	---	100 (59)	---	---	---
Silica Fume, lb/yd^3 (kg/m^3) Grace Force 10000	---	48 (29)	---	---	---
# 67 Stone, lb/yd^3 (kg/m^3) Vulcan Quarry, Columbia, SC	998 (593)	1266 (752)	1463 (869)	na	na
# 789 Stone, lb/yd^3 (kg/m^3) Vulcan Quarry, Columbia, SC	333 (198)	224 (133)	---	na	na
Stalite, lb/yd^3 (kg/m^3)	na	na	na	940 (558)	940 (558)
Fine Sand, lb/yd^3 (kg/m^3) Sumter City Sand, Sumter, SC	1300 (772)	1215 (722)	1330 (790)	1082 (642)	1082 (642)
Total Water, lb/yd^3 (kg/m^3)	304 (180)	324 (193)	292 (173)	306 (182)	306 (182)
HRWR*, oz/yd^3 (ml/m^3)	81 (2,395)	74.7 (2,209)	81 (2,395)	180 (5,322)	190 (5,618)
WR**, oz/yd^3 (ml/m^3)	32.4 (958)	36 (1,065)	32.4 (958)	135 (3,992)	145 (4,287)
AEA***, oz/yd^3 (ml/m^3)	2.43 (72)	0.9 (27)	2.43 (72)	11.0 (325)	11.0 (325)
Coarse/Fine Ratio	1.02	1.23	1.10	0.87	0.87

* Euclid SPJ used in USC mixes, Sika Viscocrete used in FCP mixes.
** Euclid WR 91 used in USC mixes, Sika Plastiment used in FCP mixes.
*** Euclid AIR MIX used in USC mixes, Sika AEA 14 used in FCP mixes.

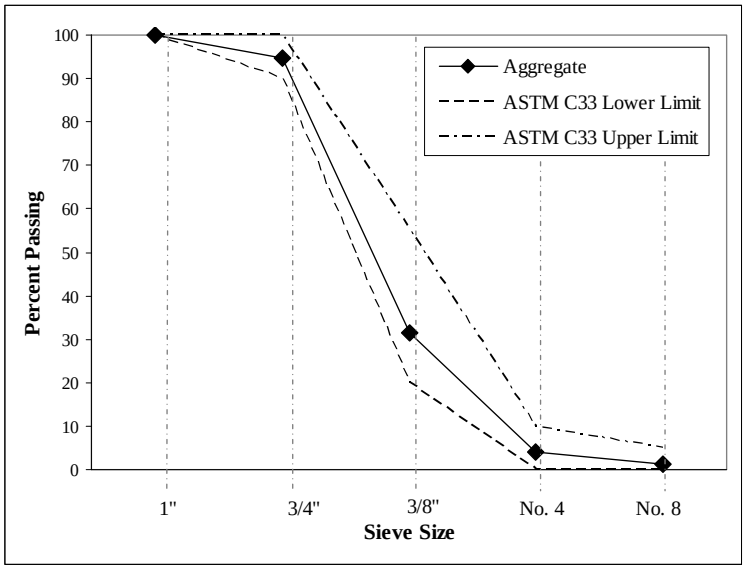

Figure 3.1: Sieve analysis of #67 coarse aggregate

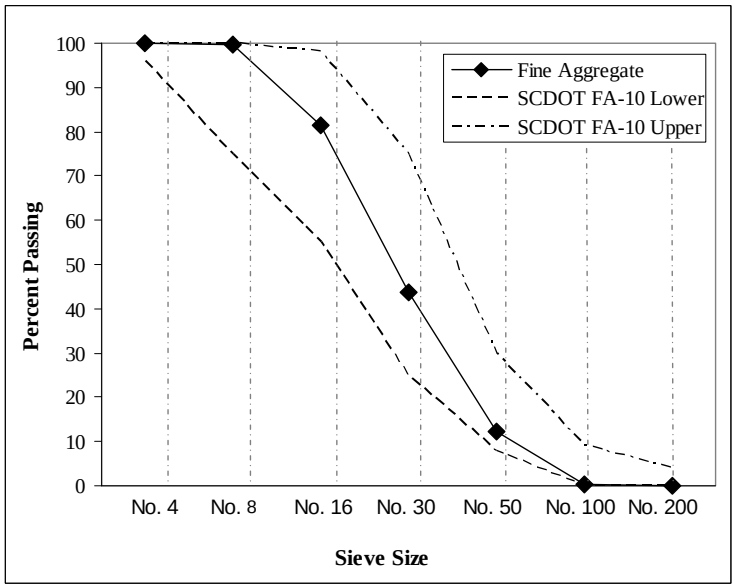

Figure 3.2: Sieve analysis of FA-10 fine aggregate

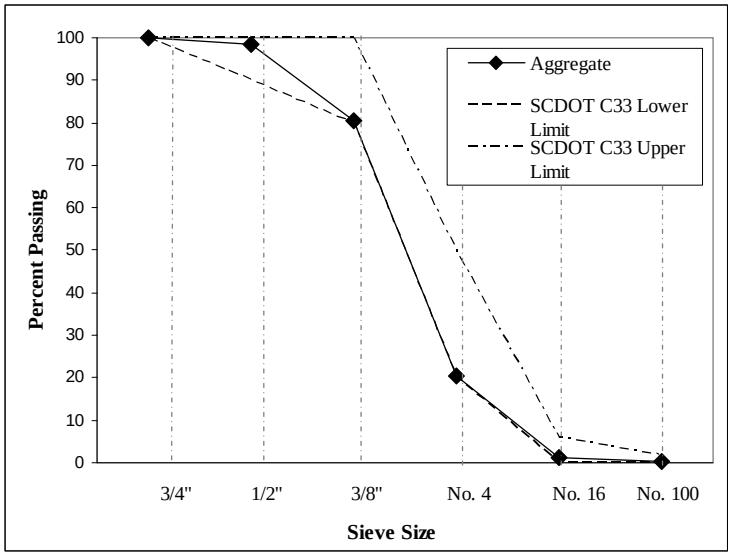

Figure 3.3: Sieve analysis of #789 coarse aggregate

Figure 3.4a: Coarse aggregate storage bin

Figure 3.4b: Fine aggregate Storage Bin

Figure 3.5: 2.5 cu. ft. mixer in U.SC Laboratory

Figure 3.6: 6 cu. ft. mixer in U.SC Laboratory

Figure 3.7a: Small syringe for admixture measurement

Figure 3.7b: Large syringe for admixture measurement

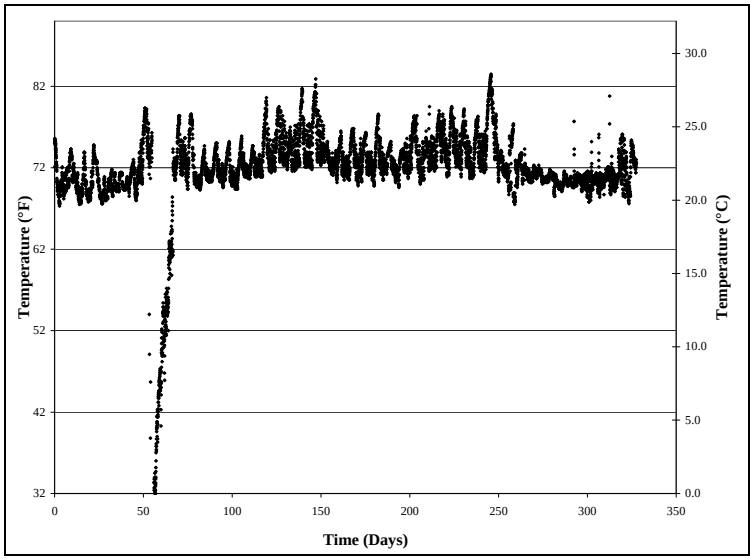

Figure 3.8: Long-term temperature curing data (inside creep/shrinkage room)

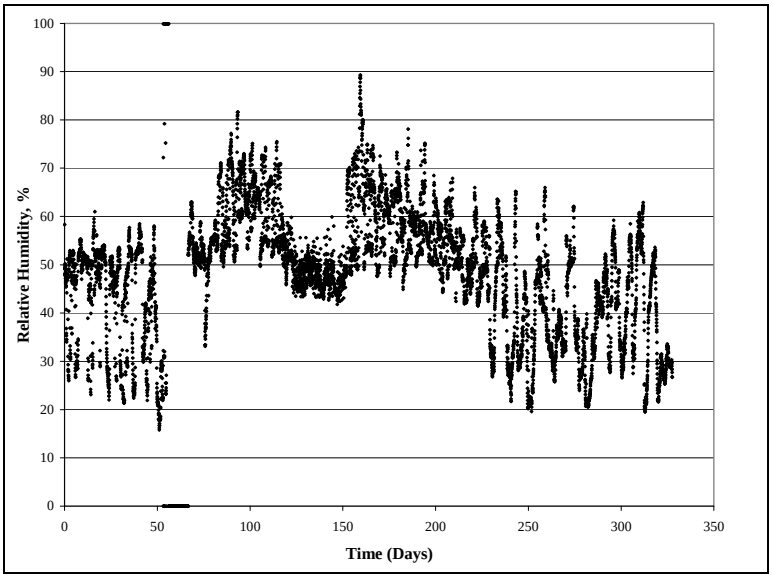

Figure 3.9: Long-term relative humidity curing data (inside creep/shrinkage room)

CHAPTER 4
MATERIAL CHARACTERIZATION PROCEDURES

4.1 Introduction

This chapter describes and illustrates the methods used to test the fresh and hardened properties of the SCC mixes. All testing was performed by University of South Carolina personnel with the exception of portions of the field testing at Florence Concrete Products in Sumter, SC. The fresh property test methodologies were obtained from the PCI document, "Interim Guidelines for the Use of Self-Consolidating Concrete in PCI Member Plants" (PCI, 2003a). The hardened property tests were in general conformance with ASTM procedures.

4.2 Fresh Properties

As discussed in preceding chapters the fresh properties of interest for self-consolidating concrete (SCC) are slump flow, filling ability, passing ability, segregation resistance (stability), and air content. ASTM committee C09 is currently developing and modifying standards for these properties. After reviewing current practices for SCC testing in the United Stated the U-Box, L-Box and the spread tests were chosen to evaluate the fresh performance of SCC. The standard practice to test the workability of normal concrete (NC) is the slump test described in ASTM C143, "Standard Test Method for Hydraulic Cement Concrete". Other tests conducted included air content, unit weight, and concrete temperature.

4.3 Hardened Properties

Hardened concrete properties were separated into two categories; mechanical properties and durability characteristics. Mechanical properties included strength, modulus of elasticity, creep and shrinkage. Durability characteristics included freeze-thaw resistance and chloride permeability.

Compressive Strength: ASTM C39-03, "Standard Test Method for Compressive Strength of Cylindrical Concrete Specimens," procedures were followed to determine the strength of the concrete. In this test, an axial force is applied to molded specimens at a pre-determined rate until failure. The apparatus used to test the cylinders is a manually controlled 500,000 lb. (2,220 kN) capacity compression testing machine made by ELE International. Both 4 x 8 and 6 x 12 in. (102 x 204 and 152 x 302 mm) cylinders were tested at loading rates of approximately 440 lbs/s (2.13 kN/s) and 990 lbs/s (4.4 kN/s), respectively. 4 x 8 (102 x 204 mm) cylinder results were used exclusively for strength. The cylinders were loaded to failure and then the strength was determined by dividing the load at failure by the cross-sectional area of the tested specimen. Figure 4.1 shows the compressive strength and modulus of elasticity testing arrangement.

Modulus of Elasticity: ASTM C469-94, "Standard Test Method for Static Modulus of Elasticity and Poisson's Ratio of Concrete in Compression," was used to determine

Young's modulus of the concrete. Under ASTM C469, 4 x 8 or 6 x 12 in. (102 x 204 and 152 x 302 mm) cylinders can be used. In this study the larger cylinders were tested because the larger specimens generally give more accurate results when following this method. The longitudinal concrete strain was measured while applying a uniform axial force over the cross-sectional area of the cylinder. Cylinders were tested for each batch at 7, 28, and 56 days after they were cast. At the time of testing, the cylinder was instrumented with a compressometer-extensometer which measures the longitudinal and transverse deformations or strains. This device consists of three rings that attach to the specimen by sharp steel pointed bolts. The bottom and top ring were connected by a linear variable displacement transducer (LVDT) which measures the deformation and inputs the data into a computer. Once the specimen was in place and instrumented with the compressometer jacket, as shown in Figure 4.1, the load was applied at a rate of approximately 990 lbs/sec (449 kg/sec).

Each specimen should be loaded at least twice. During the first loading, no data is recorded, and the displacement values from the LVRs should be examined to prevent error during the data acquisition load cycle. During the second cycle displacement and load data should be acquired and saved for calculations. At minimum, the applied load and longitudinal strain should be acquired at the point when the longitudinal strain is equal to 50×10^{-6} and when the applied load is 40 % of the ultimate load. Therefore, it is necessary to test each batch up to failure before attempting to test for the modulus of elasticity.

Once the data is acquired, the load and displacement values must be converted to their corresponding stress and strain values. At this point the chord modulus can be calculated as follows:

$$E = \frac{(S_2 - S_1)}{(\varepsilon_2 - 0.000050)} \qquad \text{(eqn. 4.1)}$$

where E is Young's Modulus of Elasticity (psi), S_2 is 40 % of the ultimate strength of the concrete (psi), S_1 is the stress in psi that corresponds to a strain of 50×10^{-6} ,and ε_2 is the strain produced by the stress S_2.

Creep: ASTM C512-87, "Standard Test Method for Creep of Concrete in Compression" was used to determine the effects of long term compressive loading of concrete specimens in terms of time-dependent strain. This is an effective method for determining the creep potential of different concretes. For each different batch of concrete, five 6 x 12 in. (152 x 305 mm) cylinders were cast. After curing the specimens in an increased temperature environment to simulate field conditions, the specimens were de-molded. Three of the specimens were loaded in the creep frames while the other two are used to determine the shrinkage strain so that the creep strain could be isolated.

The creep frames were designed and constructed in the University of South Carolina Structures laboratory. Four frames were built for this study so that four mix designs could be tested at the same time. The tools required for this test include the creep frames, a mechanical strain gage accurate to one ten-thousandth of an inch, gage studs to be

embedded in the specimens, a loading ram, and a load cell. Figure 4.2 shows a schematic of the creep frames. They are constructed entirely of steel, consisting of four Dywidag THREADBAR® bars, four 2-inch thick steel plates, five double-coil railcar springs, and twenty Dywidag nuts and washers. The frames were designed to hold three 6x12-inch cylindrical specimens each as well as two 6 x 6 in. (152 x 152 mm) cylindrical end caps cast from the same concrete.

The load was applied from the top of the frames by a hydraulic ram with a 100,000 lb. (445 kN) capacity. During loading, a load cell was used to monitor the load as well as the dial gage on the pump. Additionally, a ruler with 1/32 in. (0.8 mm) accuracy was affixed to the base plates of the frame to measure the displacement of the springs. The springs act as the load-maintaining element of the creep frames. Once the desired load is reached, the nuts on the Dywidag bars are tightened so that the load is locked into the frames.

For the load-maintaining element automotive, railcar, and "Belleville" disc springs were considered on the basis of spring rates, economy, and availability. Since the railcar springs were readily available, and provided adequate spring flexibility, they were chosen for the creep frames. Each frame consists of five double-coil railcar springs whose average spring constant, k, was found to be approximately 13,400 lb/inch as shown in Figure 4.3. Therefore, each set of springs provides 67,000 lbs. (298 kN) of force per inch (per 25.4 mm) of displacement. Since the maximum travel distance, S for each spring is just over 1.5 in. (38.1 mm), the maximum total loading capacity of the five spring set is:

$$P_{max}=5*k*S=100{,}500 \text{ lbs.} \qquad \text{(eqn. 4.2)}$$

It is also convenient to determine the maximum concrete strength that the frames are capable of testing. Since the frames are designed to load 6 in. (152 mm) diameter specimens to 30 % of the concrete strength, the maximum strength that can be tested is:

$$f'_c = \frac{P_{max}}{A_{specimen} * 0.30} = 11{,}850 \text{psi} \qquad \text{(eqn. 4.3)}$$

where f'_c is the maximum strength concrete that the frames can test (psi), P_{max} is the load capacity of the springs per frame (lbs.), and $A_{specimen}$ is the cross-sectional area of a 6 in. (152 mm) diameter cylinder.

A flexural bending analysis was performed on the plates, and it was determined that 2.0 in. (51 mm) thick plates would be adequate. Additionally, a finite element analysis on the plates proved the plate dimensions sufficient. The steel rods used were 1 in. (25.4 mm) diameter Dywidag THREADBAR® bars typically used in post-tensioning applications. If the frames were loaded to maximum capacity, and the force is assumed to be distributed evenly through the four bars, the stress in the rods would be approximately 32,000 psi (220 MPa). This is well below the yield strength of the Dywidag steel of about 130,000 psi (896 MPa).

For each batch of concrete three cylinders were tested for creep potential. After the specimens went through the 24-hour curing procedure, they were de-molded and ready to be tested. The following procedure was used for each batch of concrete;

- Sulfur capping compound was used to cap both ends of each specimen. Additionally, a fourth specimen was cut in half to make two 6 x 6 in. (152 x 152 mm) cylinders. Both ends of these were capped as well.

- Starting from the bottom, the cylinders were stacked in the creep frame as shown in Figure 4.2 making sure that the gage studs were accessible. Gage studs were spaced 8 in. (204 mm) apart at four locations around the cylinder. In between layers, a level was used to assure a horizontal surface for loading.

- The hydraulic loading ram and the load cell were placed between the upper and lower jacking plates. Before loading, the ram and load cell were securely tied to the frame, and a protective cage was placed around the frame to prevent the specimens from buckling outward if loaded eccentrically.

- Immediately before loading, the compressive strength of the concrete to be tested was determined. The specimens were loaded to 30 % of the ultimate strength. Once this load was reached the DYWIDAG nuts were firmly tightened down on top of the lower jacking plate to lock the load in the frame.

- Initial strain readings were taken immediately before and after the initial loading. Readings were then taken at least each six hours, daily for one week, weekly for three months, and then monthly for one year. This schedule varied slightly from the schedule suggested by ASTM C512, but was chosen to gather more data during the first half of the study.

Due to creep deformation of the specimens, the load in the springs relaxed marginally over time. Because of this load-relaxation the frames were adjusted periodically to keep the load within the designated "constant" range. The range for this study was 5% of the initial stress induced to the concrete. Whenever the stress was greater than ± 5% of the desired stress (0.30 f'_c) it was readjusted to be within range. Assuming that the initial load on the specimens is 60,000 lbs, the initial spring deflection would be:

$$\Delta_s = \frac{P_i}{k_{s,tot}} = 0.59 \text{ in.} = \frac{19}{32}\text{in.}(15\text{mm}) \qquad \text{(eqn. 4.4)}$$

where Δ_s is the deflection in each spring, P_i is the total initial load applied to the specimens, and $k_{s,\,tot}$ is the total spring constant for the system. Therefore, when the spring displacement gage drops below 9/16 in. (15 mm) the frame is reloaded.

All creep measurements were taken using a mechanical strain gage as shown in Figure 4.4. To ensure good averages of creep values, each cylinder was instrumented on four

evenly spaced locations around the perimeter of the specimen using a gage length of 8 inches. Two separate 6x12-inch cylinders were also instrumented so that the shrinkage strain could be determined. Every time the creep and shrinkage data is measured the creep strain is calculated as follows:

$$\varepsilon_c = \varepsilon_t - \varepsilon_{sh} \qquad \text{(eqn. 4.5)}$$

where ε_c is the creep strain (μs), ε_t is the total (creep + shrinkage) strain (μs), and ε_{sh} is the shrinkage strain (μs).

Shrinkage: ASTM C157/C157M-99, "Standard Test Method for Length Change of Hardened Hydraulic-Cement Mortar and Concrete," describes the procedure for determining the strain caused by drying shrinkage in concrete. In this procedure 3 x 3 x 11¼ in. (76 x 76 x 286 mm) concrete prisms are tested for length change using a digital comparator. ASTM C157 recommends standard conditions for curing, mixing, sampling, and storage which were not completely followed in this research program. Standard procedures require the specimens to be cured in lime-saturated water for a period of 28-days prior to the acquisition of shrinkage data (ASTM C157, 1999). Since the concrete in question is intended to simulate the concrete used in prestressed bridge girders, the data was recorded starting after 24 hours of curing. The specimens were cast using reusable steel molds that bolt together for easy disassembly. The molds hold small gage studs that are embedded into the specimen to use as the gage points for more accurate measurements. Figure 4.5 shows a typical shrinkage specimen along with the length comparator used in this study. To take a reading, the specimen is placed onto the bottom contact point of the length comparator first. Then the comparator lever arm is pressed down so that the top gage stud can fit into the device. The digital readout displays the comparator reading to the nearest thousandth of an inch.

The specimens were stored in a constant temperature, constant humidity room as described previously. After the initial readings measurements were taken at least once a day for one week, once a week for one month, and once a month for 6 months. The length change at any age after the initial comparator reading can be calculated as follows:

$$\Delta L_x = \frac{CRD - CRD_{initial}}{G} * 100 \qquad \text{(eqn. 4.6)}$$

where ΔL_x is the length change of a specimen at any age (%), CRD is the difference between the comparator reading of the specimen and the reference bar at any age (in.), and G is the gage length (in.).

Chloride Permeability: ASTM C1202-97, "Standard Test Method for the Electrical Indication of Concrete's Ability to Resist Chloride Ion Penetration," describes a relatively quick method to determine the chloride permeability of concrete. More commonly known as the Rapid Chloride Permeability Test (RCPT), this procedure is performed on 2 in. (51 mm) thick by 4 in. (102 mm) diameter concrete specimens. An electrical charge is maintained over the specimen for six hours and the passing current is

recorded. Figure 4.6 shows the permeability test specimen preparation table and Figure 4.7 shows the "Germann Proove-it" test control apparatus used during this research. As shown in Figure 4.7, the concrete specimen is sealed between two chambers filled with chemical solutions. The side with the positive terminal is filled with a 0.3N NaOH solution and the side with the negative terminal is filled with the 3.0% NaCl solution. As the chloride solution permeates through the specimen, the passing current increases, and therefore indicates the chloride permeation.

Before the specimens are tested they must go through a conditioning process. This process removes all air from the voids in the concrete using a vacuum and then fills the voids with deaerated water before they are tested. From 4 x 8 in. (102 x 204 mm) cylinders, the specimens are cut 2 inches from the top finished surface of the concrete. Any rough edges on the specimens are sanded down with a belt sander. After the specimen is dry, a two-part epoxy is lightly applied around the perimeter of the specimen. The epoxy should completely coat the sides of the specimens so that no air or liquid can escape. After the epoxy is no longer sticky to the touch, the specimens should be put into the vacuum desicator. The open ends of the specimens should be exposed completely. The vacuum should then be turned on and allowed to run for 3 hours with the pressure below 0.04 in. (1 mm) Hg. With the vacuum still running, the de-aerated water should be allowed to flow into the desicator, without allowing air to enter the chamber. Once the water is covering the specimen, the water valve should be closed and the pump should run for an additional hour. Next, the vacuum valve should be closed and air should be allowed to enter the chamber. The specimens should then be soaked for 18 ± 2h in the same water before they are transferred to the loading cells. This concludes the conditioning part of the procedure.

After removing the specimens from the desicator, the excess water is blotted off. The specimens are then placed in the testing cells with 4 in. (102 mm) diameter rubber O-rings to seal them in. Once both sides of the cell containing the top surface of the cell is filled with the 5 % NaCl solution, and the other side is filled with 0.3N NaOH solution. Next, the lead wires are connected to the banana posts.

Once the specimen is in place and the wires are connected, the power source should be turned to 60.0 ± 0.1 V, and an initial current reading should be recorded. In this study the "Proove-it" system by Germann Instruments was used. After setting the power supply to 60.0 V, the test is started, and all data is automatically recorded to a laptop computer. The test will conclude after six hours and the results should be saved. If at any time during the test the solution gets above 190° F (88° C), the system will automatically shut down to avoid damaging the cells.

Freeze-Thaw Resistance: Freeze-thaw durability was tested in accordance with ASTM C666-97, "Standard Test Method for Resistance of Concrete to Rapid Freezing and Thawing – Procedure A, Rapid Freezing in Water." In this method 3 x 4 x 14 in. (76 x 102 x 356 mm) long concrete prisms are subjected to extreme temperatures and the fundamental frequency is measured which is related to the dynamic modulus of the material. Therefore, as the concrete continues to weaken due to the freeze-thaw cycles,

the reduction in stiffness can be measured along with the specimen geometric properties such as the cross-sectional dimensions.

Since the purpose of these material tests was to simulate the field development of the prestressed girders, the F-T specimens were tested after about 56 days of curing. After the specimens were cast, they were cured in the increased temperature environment for 24 hours in which the surrounding air was about 95 to 100° F (35 to 38° C). After the initial curing period, the specimens were demolded and placed on the drying rack in the controlled environment room along with other specimens to be tested.

After the specimens have cured for at least 56 days, they are ready for F-T testing. Per ASTM C666-97, the target freeze temperature is 0° ± 3° F and the target thaw temperature is 40° ± 3° F. The test begins with the specimens in a thawed state. The initial starting temperature should be between 30° and 44° F. Once the specimens are in the specified thawed state, they should be tested for weight, fundamental frequency, and optionally the geometric properties. The time that the specimens are out of the F-T chamber should be minimized. After all specimens have been tested for their initial properties, the chamber should be energized and the freezing cycle begun. A typical cycle consists of the internal temperature of the specimen going from 40° F to 0° F and back to 40° F. This cycle should take between 2 and 5 hours. After 36 cycles, the specimens should be retested for the fundamental frequency and weight, again in a thawed condition. The testing is complete when either 300 cycles have been completed or 60 % of the initial dynamic modulus has been reached.

The test chamber used in this study, shown in Figure 4.8, completed a full cycle in approximately 3.85 hours. This meant that specimen testing should have been conducted every 5.75 days. ASTM C215-97, "Standard Test Method for Fundamental Transverse, Longitudinal, and Torsional Resonant Frequencies of Concrete Specimens" was followed to find the transverse frequency of the specimens. This test method offers two alternate procedures to determine the frequencies, including the forced resonance method and the impact resonance method. For a given series of tests on a specimen type or certain mix, only one of the two methods should be used. The method used for this research was the impact resonance method. In this method, a supported specimen is impacted with a predefined mass and the vibration response is measured with a lightweight accelerometer. The signal from the accelerometer is amplified and the vibration response is displayed on a nearby data acquiring computer.

The impact resonance apparatus requires the following equipment: (1) Impactor – steel ball bearing weighing approximately 0.24 ± 0.04 lbs. (0.11 ± 0.02 kg); (2) Sensor – piezoelectric accelerometer weighing less than 0.06 lbs. (27 g), (3) Frequency Analyzer – signal conditioner into computer, and (4) Specimen Support – supports specimen as a simply supported beam, so that is may vibrate freely in the transverse mode. Once the geometric properties and weight of the specimens have been recorded, the specimen is placed on the supports. Since the specimens were usually wet after being removed from the F-T chamber, a spot was typically dried off where the accelerometer was placed so that the wax would adhere to the specimen. With the accelerometer in place and the

specimen supported correctly, the impactor was used to strike the specimen approximately 2 in. (51 mm) away from the accelerometer. The data was then read out from the nondestructive evaluation software for analysis.

Figure 4.1: Compressive loading apparatus

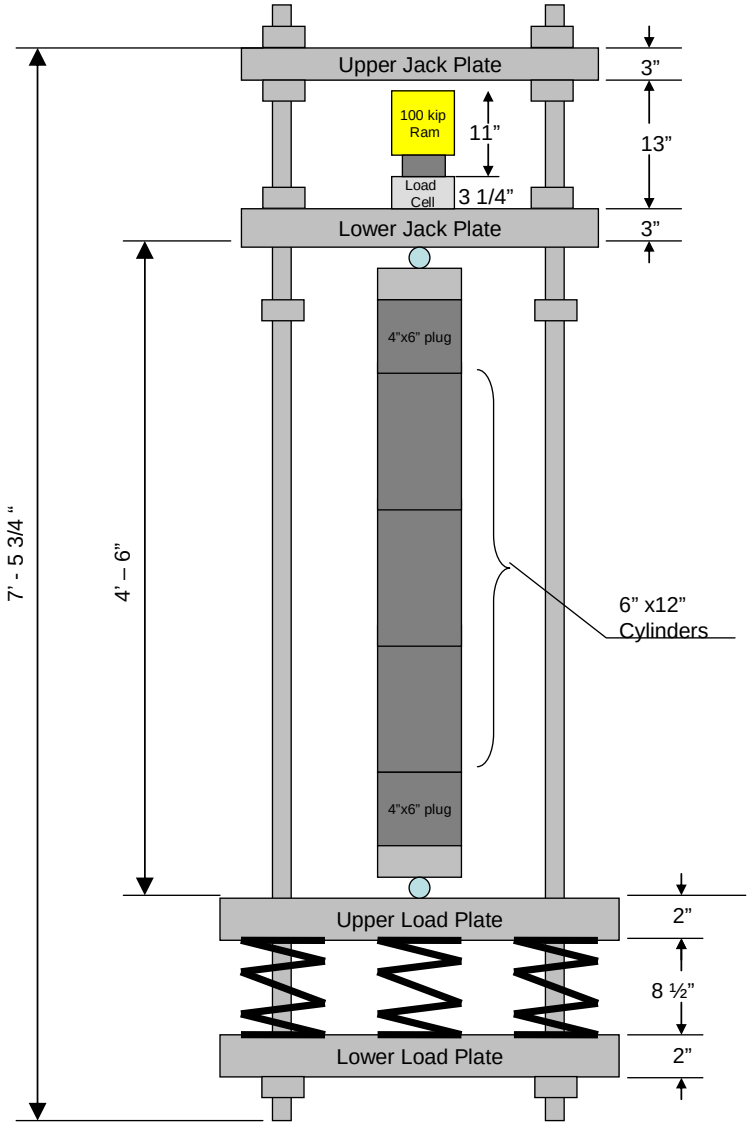

Side View

Figure 4.2: Schematic of creep frames

Figure 4.3: Railcar springs at base of creep frame

Figure 4.4: Mechanical strain gage and creep specimen

Figure 4.5: Digital length comparator test setup

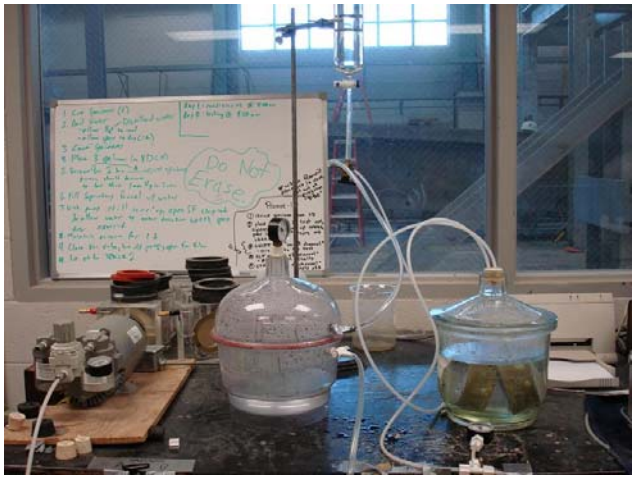

Figure 4.6: Permeability sample preparation

Figure 4.7: Rapid chloride permeability test setup

Figure 4.8: Freeze-thaw chamber

CHAPTER 5
GIRDER FABRICATION AND INSTRUMENTATION

5.1 Introduction

In July of 2007, personnel from the University of South Carolina (U.SC) traveled to Sumter, SC for the fabrication and instrumentation of three prestressed lightweight concrete bridge girders. The bridge girders were 59 ft. 2 in. (18.0 m) long Type III as designated by the American Association of State Highway and Transportation Officials (AASHTO). The properties and dimensions of an AASHTO Type III girder can be seen in Figure 5.1.

The testing and fabrication of the girders was completed at Florence Concrete Products (SCP). The instrumentation, casting and initial readings took place over a three day period. Tests conducted on-site included transfer length measurements, endslip, midspan deflection (camber), midspan strain, and temperature history. The three girders were shipped to the structures laboratory at U. South Carolina approximately 2 months after casting.

5.2 Fabrication of Girders

Description of Prestressing Strand: All three AASHTO girders were cast in a line on the same prestressing bed. Seven-wire uncoated prestressing strand ran straight through all three girders, with no draping pattern. The strand was ½ in. (12.7 mm) diameter, grade 270, LO-LAX (low relaxation). Each strand had an applied prestress force of 31,000 lbs. (138 kN). All reinforcing steel within the girder was grade 706. Before release of the prestressing strand could take place, the girder concrete was required to have a minimum strength of 6,400 psi (44.1 MPa). Concrete strength was monitored by conducting compressive tests on sample cylinders from the same mix as the girders. The pattern for both the prestressing strand layout and the reinforcing steel can be seen in Figures 5.2 and 5.3.

Description of Instrumentation: The prestressing strand was pre-tensioned and the reinforcing bar was in place prior to arrival (Figure 5.4). Internal instrumentation was placed within the girders the first day. After the concrete was placed and allowed to cure for 24 hours, external instrumentation was applied to the girders. In some instances photos from a parallel research project related to normal weight SCC (having the same type of girders with identical span length and reinforcing pattern) are used. The content of the information is unchanged.

Internal Instrumentation

Midspan Strain: Geokon vibrating-wire strain gages (VSG), model 4200 series, were installed to monitor the long-term strain and other variables within the girders. The VSG measured and displayed strain (micro-strain), temperature (°C), period (micro-seconds), and frequency (Hz). Figure 5.5 shows how the VSG were attached within the girders.

Strain is measured with VSG gages in the following way:

> *"Strains are measured using the vibrating-wire principle: a length of steel wire is tensioned between two end blocks that are firmly in contact with the mass of concrete. Deformations in the concrete will cause the two end blocks to move relative to one another, altering the tension in the steel wire. This change in tension is measured as a change in the resonant frequency of vibration of the wire. Electromagnetic coils that are located close to the wire accomplish excitation and readout of the gage frequency." (Quotation from GEOKON VSG Manual)*

To measure strain during installation and testing at the precast plant, a VSG readout box was used. The strain gages were measured numerous times during the visit.

In addition to the vibrating wire strain gages, sister bars (SB) with electrical resistance weldable strain gages, designation CEA-XX-W250A-120, were also installed. The sister bars were ½ in. (12.7 mm) diameter reinforcing bar, 5 ft. (1.53 m) long that were tied in with the girder reinforcement. Weldable strain gages were tack-welded to the sister bars and covered with epoxy to protect them from the concrete during casting. The strain gages have wiring that can be read to record strain during loading of the girder. See Figure 5.6 for a picture of the sister bar strain gages.

Temperature History: Along with the VSG and SB gages, ACR Smartbutton temperature gages were also placed inside each girder. The gages were placed in small PVC pipes and tied to the reinforcing bar within the girder. The temperature gages were pre-programmed before installation and took continuous measurements of the temperature history. The rate for readings was once every 10 minutes. See Figures 5.7 and 5.8 for a photo of the temperature gage and how the gage was installed within the girder. Figure 5.9 shows the internal instrumentation within the girders.

External Instrumentation

Transfer Length: For assessing transfer length, the concrete surface strains along the zone of transfer were measured. At both ends of the girder, metallic points (Demec points) spaced four in. (102 mm) apart were adhered to the concrete surface after the concrete had cured for 24 hours and prior to the de-tensioning of the prestressing strands. The Demec points, spaced 4 in. (102 mm) apart, stretched a distance of approximately 6 ft. (1.83 m) from the end of the girder. The first Demec points were placed 2 in. (50.8 mm) from each end of the girder.

A Humboldt strain measuring device, with an 8 in. (203 mm) gage length, was used to measure the distance between the Demec points before de-tensioning of the prestressing strands. This value was the zero strain value on the concrete surface. A second measurement was taken after de-tensioning the prestressing strands to record the strain values of the concrete surface after prestressing. The difference between the first and

second Humboldt readings divided by the gage length gave the strain values within the concrete surface due to the prestressing forces. Figure 5.10 demonstrates how transfer length was measured and Figures 5.11 and 5.12 are additional photos related to the Demec points.

Endslip: The method used to measure the endslip of the ½ in. (12.7mm) diameter prestressing strand was as recommended by the FHWA. This method can be found in the FHWA document "*Implementation Program on High Performance Concrete - Guidelines for Instrumentation of Bridges*" (FHWA, 1996). A U-shaped metal channel was attached to the prestressing strand, outside the end form, by hose clamps. The metal channel had a hole through which a depth gage passed to measure the slippage to the nearest 0.0254mm (0.001 in.). Measurements were taken before and after release of the prestressing strands. Figure 5.13 shows a schematic of the endslip measurement method. Figure 5.14 is a photograph of the endslip measurement method.

Midspan Deflection: The method used to measure camber (midspan deflection of the girder) was the taut wire method described in the FHWA document "*Implementation Program on High Performance Concrete - Guidelines for Instrumentation of Bridges*" (FHWA, 1996). This method consisted of stretching a taut wire between the two ends of the girder. The deflections were measured by marking the initial location of the wire at midspan, then marking the new wire position during subsequent weeks, and then measuring the distance between the initial mark and the new mark. Anchor bolts were used to stretch the wire along the length of the girder. One end of the wire was fixed while the other end was attached to a 90 lb. (0.40 kN) weight and run over a pulley at the other anchor bolt. This provided consistent tension in the wire to account for any sag that may have occurred.

Once the prestressing strands were de-tensioned, the distance between the bottom of the girder and the top of the prestressing bed was measured and recorded as the initial camber. See Figure 5.15 for the camber measurement technique used. See Figure 5.16 for a diagram of the piano wire attachment and Figure 5.17 for a diagram of the typical girder end and anchor bolt placement. Figure 5.18 shows a photograph of the weight used for the camber measurements and Figure 5.19 is a photograph of the anchor bolt holding the looped end of the wire. Camber can also be measured by the vibrating wire strain gages that were installed in the top and bottom flanges of the girders. This method is described more fully in later chapters.

Casting of Girders

Three AASHTO Type III girders were cast at the precast plant. Two of the girders were cast with an SCLC mix and the third girder was cast with a high-early strength lightweight concrete (HESLC) mix.

The three girders were identified as SCLC girder No. 1, SCLC girder No. 2, and HESLC girder. The three girders were all in a single line (single bed) with the prestressing strands running through all of them and hydraulically tensioned at the live end.

For both of the SCLC girders, some areas were vibrated slightly with a stinger and were given vibration in intermittent 10-second bursts. This was necessary because the flow was judged insufficient to adequately consolidate the concrete, particularly at the ends of the girders.

As the girders were being cast, extra concrete from the two mixes was used to prepare specimen molds to assess hardened properties. Fresh properties of the two mixes were also being measured during this time. The fresh properties measured for the SCLC mix were spread, filling ability, passing ability, and air content. The companion specimens were set with the girders and all were covered with plastic and allowed to cure alongside them.

De-tensioning Process: The strands were flame-cut one at a time. A schematic of the de-tensioning process can be seen in Figure 5.20. Pictures of cut prestressing strands can be seen in Figures 5.21 and 5.22.

5.3 Fresh Property Tests Conducted

For a complete description of the procedure for all fresh property tests conducted refer to previous chapters and PCI, 2003a. Prior to fresh property tests being conducted the temperature was recorded for each mix.

HESLC Slump Flow: This test method was used to determine the slump of the plastic hydraulic-cement concrete. The concrete mix was placed and compacted within a slump cone. The mold was then raised vertically, and the concrete was allowed to settle. The vertical distance between the original and displaced location of the top of the concrete was measured. See Figure 5.23 for a photo of the slump cone.

SCLC Spread Test: This test method was used to examine the horizontal flow of the SCLC mix. The method used was based upon the test method used for the slump test of conventional concrete. The flowability of the SCLC mix was determined by measuring the diameter of the concrete circle at the completion of the test. See Figure 5.24 and 5.25 for photos of a spread test prior to testing and subsequent to testing.

U-Box Test: This test method was used to measure the filling ability of the SCC mix. Between the two sections of the U was a sliding gate fitted reinforcing bars. See Figure 5.26 for a photo of the U-Box test apparatus.

L-Box Test: Along with the U-Box test this test method was used to measure the flow of the SCLC mix. This test also assessed the passing and filling ability of the SCC mix. Between the two sections was a partition with fitted reinforcing bars. See Figure 5.27 for a photo of the L-Box test apparatus.

Air Content – Pressure Method: This test was used to determine the air content of the plastic concrete mix by observing the change in volume that occurred due to a change in applied pressure. See Figure 5.28 for a photo of the air content test apparatus.

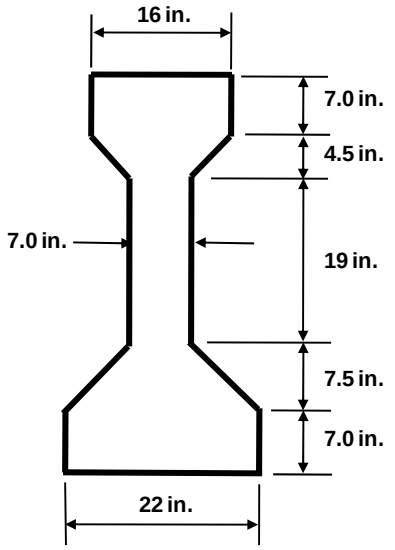

Area ($in.^2$)	Y_{bottom} (in.)	Inertia ($in.^4$)
560	20.27	125,390

Figure 5.1: Dimensions of AASHTO type III girder

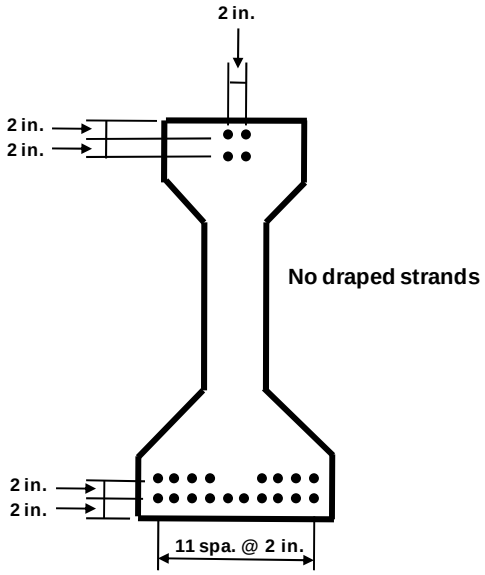

STRANDS @ ENDS and ℄

- = (22) ½" Regular LO LAX Strands @ 31,000 lbs. each

Figure 5.2: Prestressing strand layout

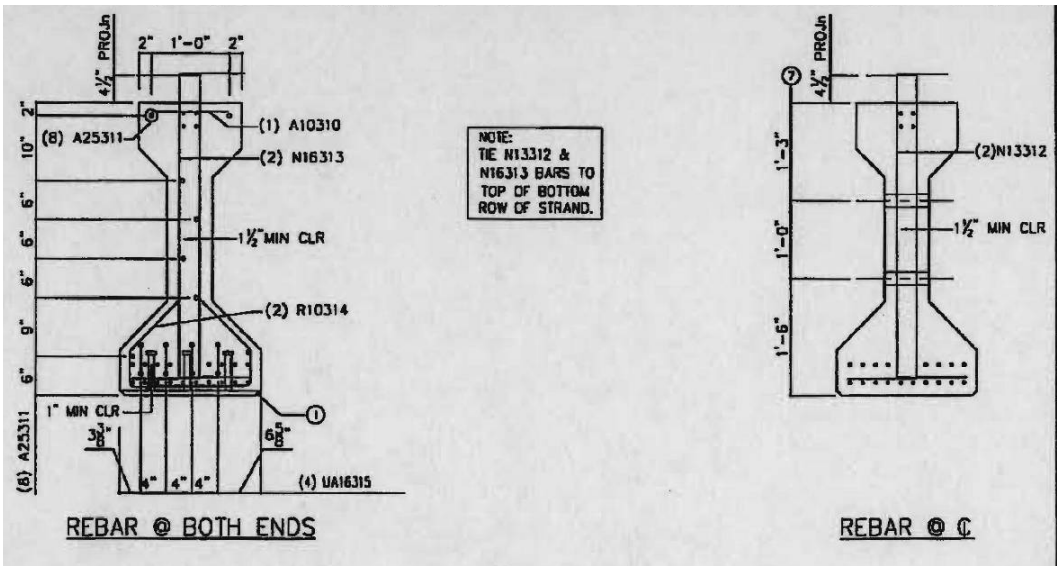

Figure 5.3: Reinforcement pattern

Figure 5.4: Reinforcing bar and girder appearance upon arrival

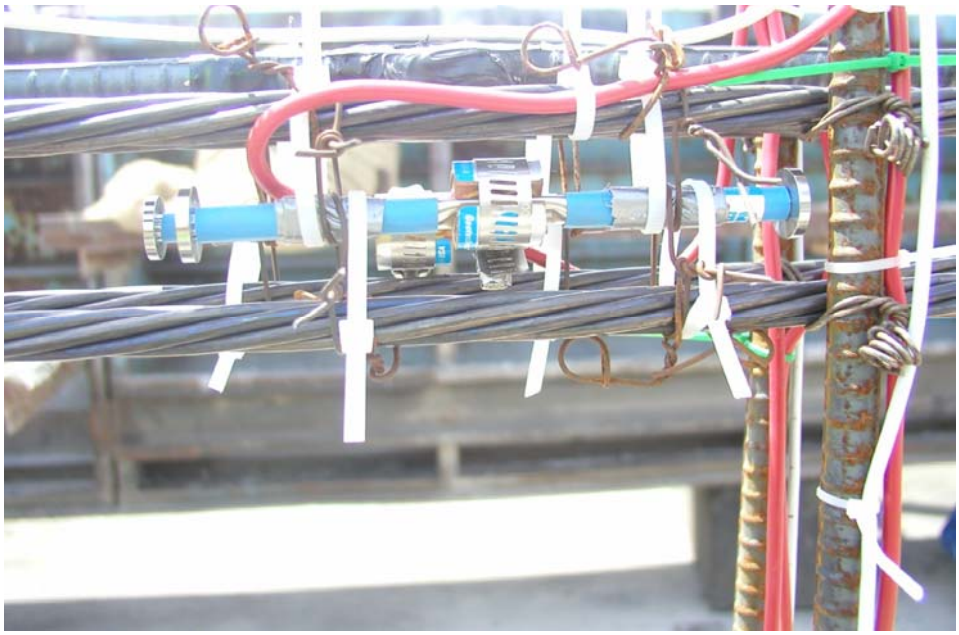

Figure 5.5: Vibrating-wire strain gage inside girder

Figure 5.6: Sister bar strain gage

Figure 5.7: Temperature gage (SmartButton)

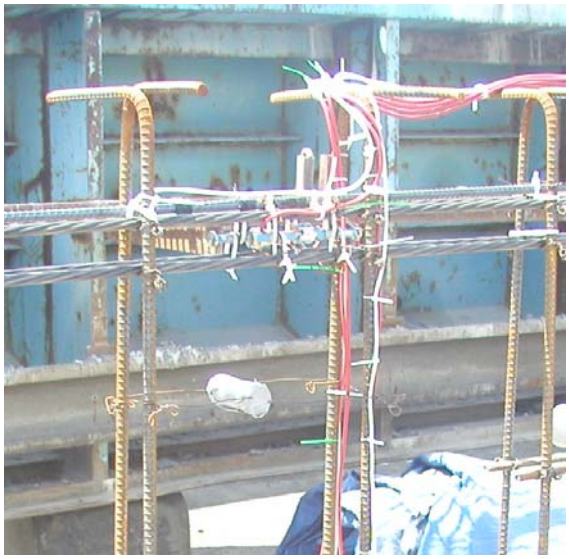

Figure 5.8: Temperature gage installation layout

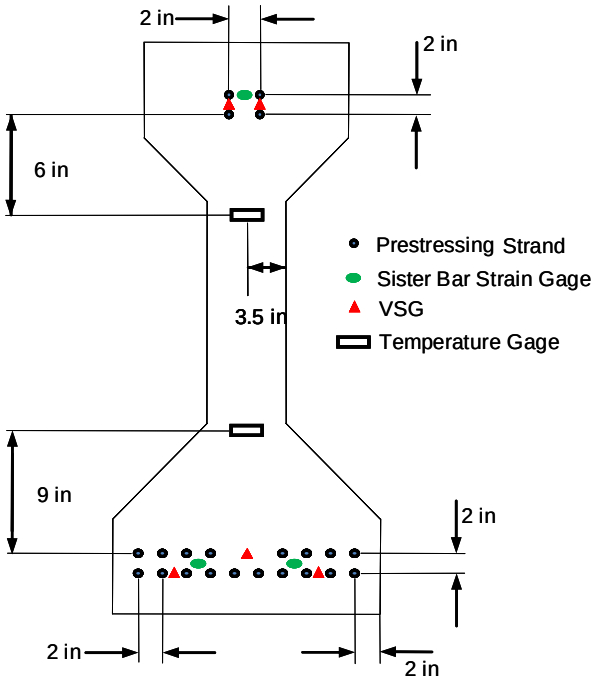

Figure 5.9: Internal instrumentation layout

Figure 5.10: Transfer length measurement

Figure 5.11: Demec point layout

Figure 5.12: Demec points for transfer length calculations

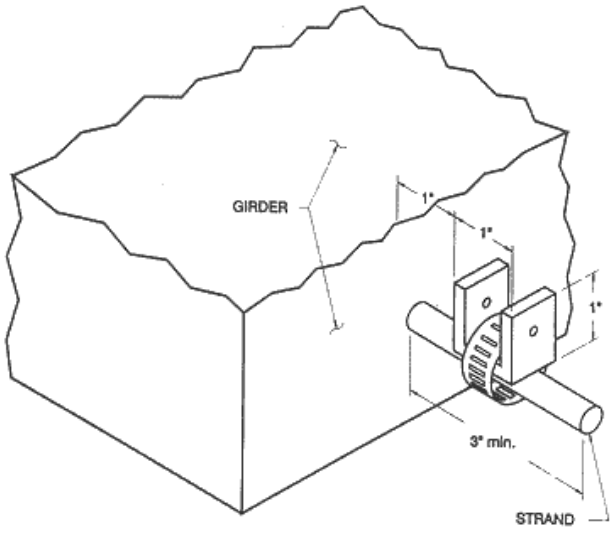

Figure 5.13: Endslip measurement (from *FHWA SA-96-075*)

Figure 5.14: Endslip measurement

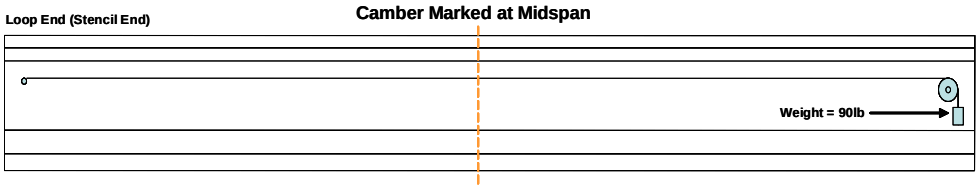

Figure 5.15: Camber measurement technique

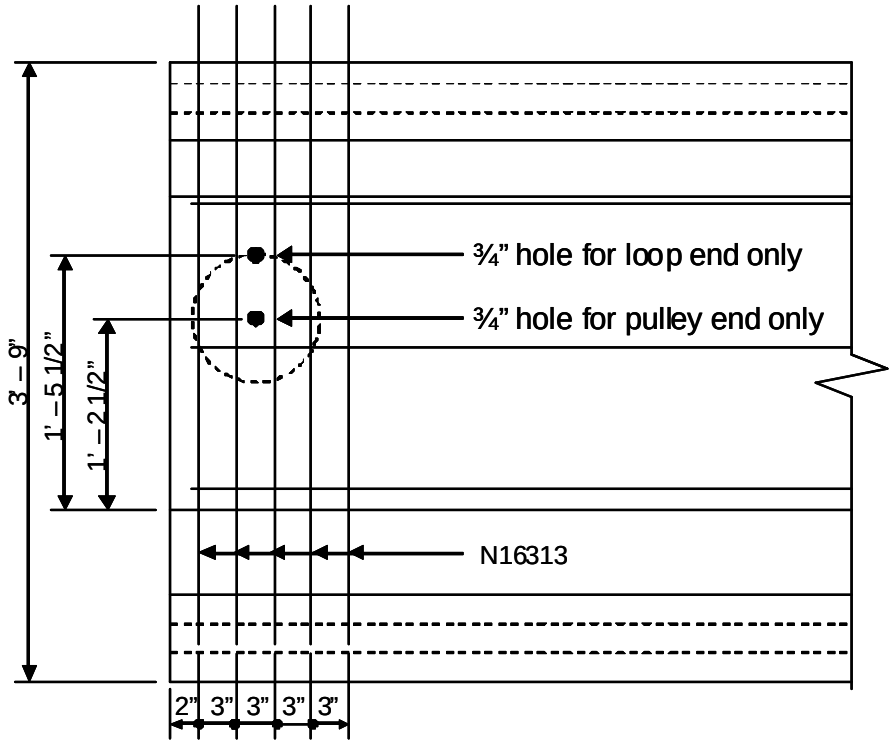

Figure 5.16: Piano wire attachment

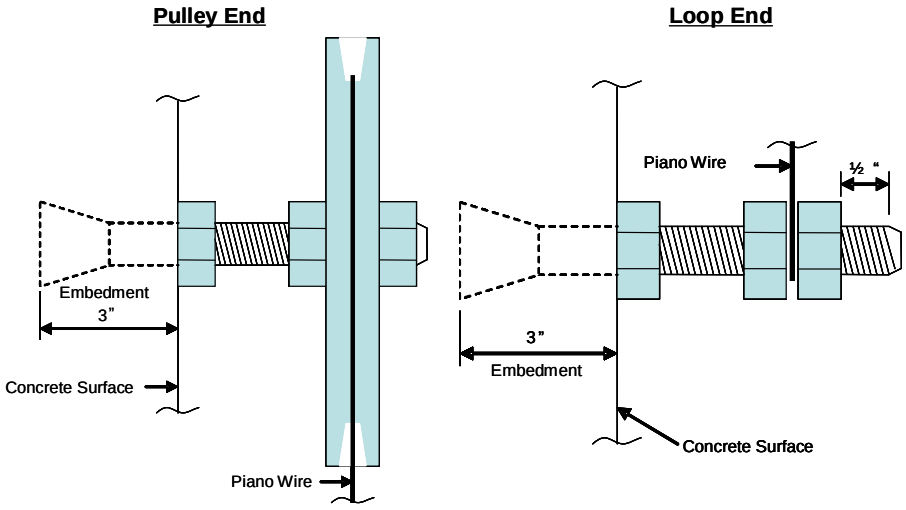

Figure 5.17: Typical girder end and anchor bolt placement

Figure 5.18: Weight for camber measurement

Figure 5.19: Anchor bolt for camber measurement

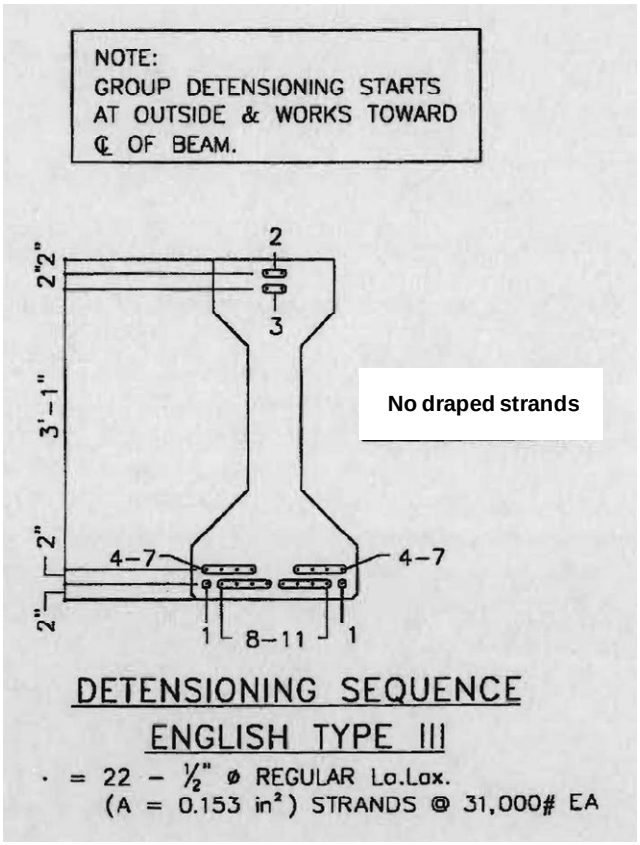

Figure 5.20: De-tensioning sequence

Figure 5.21: Cut prestressing strands (top flange)

Figure 5.22: Cut prestressing strands (bottom flange)

Figure 5.23: Slump cone

Figure 5.24: Spread test (prior)

Figure 5.25: Spread test (subsequent)

Figure 5.26: U-box apparatus

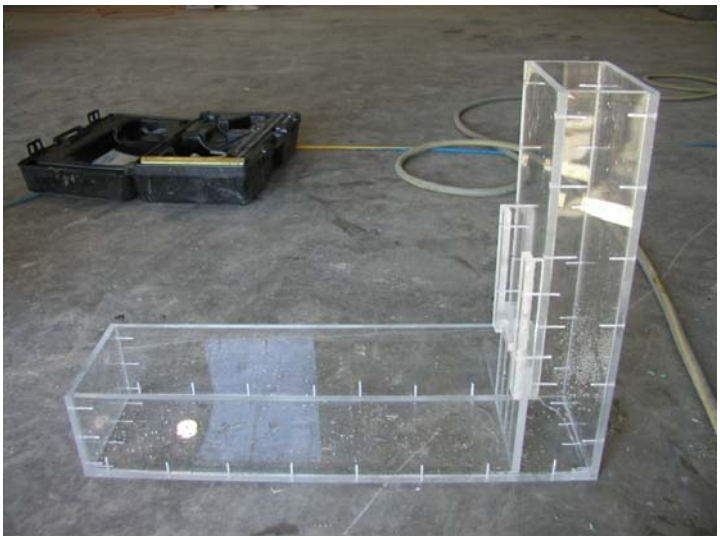

Figure 5.27: L-box apparatus

Figure 5.28: Air content apparatus

CHAPTER 6
LOADING OF GIRDERS

6.1 Introduction

The first stage of the experimental program for the full-scale girders consisted of ultimate strength tests conducted on two of the three specimens. The two girders had identical geometry and prestressing strand layout. The single variable in the two girders was the type of concrete used in fabrication. The first girder tested was fabricated with a lightweight self-consolidating concrete (SCLC) – SCLC girder No. 1. The second was fabricated with a high-early strength lightweight concrete (HESLC) mix – HESLC girder. A third girder was fabricated with an SCLC mix - SCLC girder No. 2. This third girder was subjected to cyclic loading and then taken to ultimate.

Prior to the testing of each girder a conventional concrete deck was added. The geometric properties, prestressing strands, reinforcing steel, and fabrication for these girder specimens are described previously.

6.2 Specimen Details

All three girders were AASHTO Type III. Each girder had a length of 59 ft. 2 in. (18.0 m) and a depth of 45 in. (1,143 mm). A 4,000 psi (27.6 MPa) concrete deck was cast in the laboratory on top of each girder prior to testing. The deck was thicker and less wide than would ordinarily be found on actual bridges. This was done to approximate the behavior of actual bridge girders in the laboratory while still allowing for the testing program to be completed within the time and cost constraints. The reinforcing steel that projected from the top of the girder extended 4.5 in. (115 mm) into the deck. Figure 6.1 is a schematic of the girder and deck dimensions from a parallel testing program related to normal weight SCC and HESC girders. Figure 6.2 is a schematic of the deck design used for the testing program described here.

6.3 Test Setup

The girders were placed on two concrete end supports (reaction stands) having a height of 2 ft. 6.5 in. (0.76 m). This height allowed the girder to achieve full deflection at ultimate. Acting as a simply-supported connection between the concrete end support and the girder was a combination of steel and neoprene plates sandwiched around a steel roller. Embedded within the bottom of the girder was a ½ in. (12.7 mm) thick steel sole plate. See Figure 6.3 for a photograph of the roller connection.

A steel frame was assembled around the specimen that housed the lateral supports as well as the load-applying device. The columns of the frame were bolted to the strong floor of the structural lab. A photograph of the framing and test setup can be seen in Figure 6.4. In this photograph one girder from a parallel testing program is placed alongside the girder from the current testing program. Figure 6.5 shows a similar view with two girders from this testing program side by side. Steel plates were bolted to the columns at

midspan for lateral support. The girders were stable and the steel plates did not actually contact the sides of the deck, rather a small [approximately 0.5 in. (12 mm)] gap was allowed between the lateral support plates and the sides of the deck (Figure 6.6).

To provide for longitudinal support during the test tie-down straps were used. The straps allowed free movement but offered support for safety in the event that a girder was to move in the longitudinal direction. Significant movement (shifting) in the longitudinal direction was not observed during any of the tests.

The static load was applied to the specimen by two hydraulic rams, spaced two feet on center, attached to a manual control pump. Each of the two hydraulic rams had a capacity of 300 kips (1,335 kN) and a cross-sectional area of 30.7 in.^{2} (19,813 mm^2). During the loading process each ram applied the same force. Between the concrete deck and the head of the rams was a combination of steel plates and neoprene pads. This was done to protect the surface of the deck during loading. A photograph of this setup can be seen in Figure 6.7 (photograph from a parallel testing program).

An electric pump with a manual control device (Figure 6.8) allowed the load to be applied incrementally and at varying rates when necessary. The display on the manual control device gave the total pressure that was being applied to the test specimen by way of a digital pressure transducer. A load cell was also used. The transducer was wired to a data acquisition system so that load measurements could be recorded during testing.

A hydraulic actuator was used to apply a cyclic load to the girder tested in fatigue (SCLC girder No. 2). The footprint of the actuator was 1 ft. (305 mm) off the center line of the girder. A 1 in. (25 mm) thick piece of neoprene was placed between the deck surface and the actuator footprint to avoid damage to the deck from the actuator.

6.4 Instrumentation

Strain gauges at mid-span were mounted for continuous strain monitoring during loading. Additionally, displacement wire transducers (DWTs) were mounted at the bottom of the beam to record mid-span deflection. Load was applied though a set of hydraulic rams and monitored throughout the test with the use of a load cell. Descriptions of internal and external instrumentation are below.

Internal Instrumentation: During fabrication of the girders, instrumentation was placed internally at midspan to measure concrete strains and temperature history. To monitor concrete strains, vibrating-wire strain gages (VSG) and sister bar (SB) strain gages were placed in both the upper and lower flanges of the girder. To record the temperature history of the girder, two temperature gages were placed within the web of the girder. The sister bars, vibrating-wire strain gages, and temperature gages are shown schematically in Figure 6.9.

External Instrumentation: Instrumentation was outfitted externally on both the girder and deck to measure and record displacement and concrete strain data. To measure

displacement multiple devices were used. Four draw-wire transducers (DWT) were used to measure larger deflections of the girder (maximum stroke of 15 in. (381 mm), in the vertical direction. Two were placed at midspan. To measure smaller deflections [maximum stroke of 1.5 in. (38 mm)] two LVRs were used.

To measure concrete strains, two strain gages were adhered to the top of the deck. The strain gages were fastened in the longitudinal direction in relation to the deck and girder, and were situated at the midpoint of the two hydraulic rams.

See Figures 6.10 and 6.11 for diagrams of the external instrumentation used during testing. Wiring from all instrumentation was connected to computers so data could be monitored during all testing and recorded for data analysis as well. Additionally, cracks were marked on the girders with permanent markers as they developed (Figure 6.12).

6.5 Load Testing Procedure

The first two girders were loaded first in general conformance with the Cyclic Load Test (CLT) method, then the 24 hour Load Test (24h LT) method, and then taken to failure. The third girder was initially subjected to cyclic loading for two million cycles, then loaded in general conformance with the CLT and 24h LT methods, and finally taken to failure. A brief description of these methods is given below.

24 hour Load Test (24h LT) Method

The requirements of Chapter 20 of the ACI 318 Building Code (ACI 318 2005) provide guidelines to perform the widely used 24h LT on reinforced (RC) and prestressed concrete (PC). This method involves the gradual loading of the structure to a specific maximum level, sustaining it for a 24 hour period, followed by a subsequent unloading stage of 24 hours. Measurements are taken before and after the loading period and at the end of the unloading stage. Many authors consider the 24h LT test to be less than ideal (Galati et al. 2008; Ziehl et al.2008; Ridge 2006) due to the following:

- It was developed for simply supported, passively reinforced members and is based on a working stress design approach (ACI 437, 2007).
- The duration of the test impedes the use of the structure for 48 hours.
- Modern principles of design and construction techniques are not explicitly considered in the test.
- Implementation of new materials suggests a more detailed evaluation than that provided with the 24h LT.
- Application of a uniformly distributed load can be laborious and inconvenient.

With these considerations in mind, researchers and engineers have developed alternative load testing and nondestructive evaluation procedures that minimize these drawbacks and hence can provide better insight into the behavior of a structural system. The alternative load test used in this investigation is referred to as the Cyclic Load Test (CLT) method

(Gold and Nanni 1998; Nanni and Gold 1998a, b; Mettemeyer and Nanni 1999; Galati et al. 2004; Casadei et al. 2005; ACI 437, 2007; Ziehl et al. 2008).

Cyclic Load Test (CLT) Method

In this approach, performance of the system is evaluated through three criteria termed *permanency, repeatability,* and *deviation from linearity.* The structure is loaded with hydraulic rams that permit the use of a cyclic load pattern designed according to the characteristics of the specific system. This load pattern is executed in a stepped fashion and grouped in loadsets. Each loadset consists of two identical load cycles for the evaluation of permanency and repeatability (Figure 6.13).

Load Intensity: When the failure of the member (or structure) is governed by flexural tension the ACI 437.1R-07 (2007) document recommends the maximum load to be applied during the test as the largest of the following expressions:

$$TLM = 1.2\ (D_w + D_s) \qquad \text{(eqn. 6.1)}$$

or,

$$TLM = 1.0D_w + 1.1D_s + 1.4L + 0.4\ (L_r \text{ or } S \text{ or } R) \qquad \text{(eqn. 6.2)}$$

or,

$$TLM = 1.0D_w + 1.1D_s + 1.4\ (L_r \text{ or } S \text{ or } R) + 0.9L \qquad \text{(eqn. 6.3)}$$

where;

D_w = dead load due to self weight
D_s = dead load due to superimposed loads
L = live loads not including construction or environmental loads
L_r = live loads during maintenance due to workers and equipment
R = rain load
S = snow load

The first loadset level should be less than the service load or 50 % of the maximum load level. There should be a minimum of three loadsets but additional sets can be performed depending upon the grade of detail desired in the experiment. A minimum load level of at least 10% of the total load should be maintained at the bottom of each of the unloading stages to keep the equipment engaged. There are three criteria associated with the CLT method.

Repeatability evaluates the uniformity of the response of the structure when subjected to two identical loading cycles (one loadset). It is defined as the ratio of the difference between the maximum and the residual value of any structural parameter within a loadset.

Usually values between 95 % and 105 % for the repeatability index are considered adequate (Mettemeyer, 1999).

Permanency assesses the total permanent change in any structural parameter (strain, displacement, rotation, etc.) within the second loading cycle of a single loadstep. The permanency index should be less than 10 % (Mettemeyer, 1999) for the structure to meet the criterion.

Deviation from Linearity assesses the nonlinear behavior and is often a clear sign of damage in civil structures (steel yielding and cracking in concrete). Thus, the deviation of a structure from linear response constitutes a good indicator of the amount of damage suffered by the system when subjected to external demands. Linearity is computed as the ratio between the slopes of the secant line at any point to the secant line at the reference point (peak load at the first load cycle) on the load-deflection envelope. Linearity is therefore expressed in terms of displacement. The index for deviation from linearity at any point is computed as the compliment of the linearity at that point.

Values less than 25 % are generally considered acceptable (Mettemeyer 1999). This criterion may be of limited use in structures that are expected to behave in a nonlinear fashion, in such cases more importance should be given to permanency and repeatability criteria as they will be better indicators of the presence of damage in the structure.

CLT has been applied with relative success in various investigations (Gold and Nanni 1998; Nanni and Gold 1998a, b; Mettemeyer and Nanni 1999; Galati et al. 2004; Casadei et al. 2005); nonetheless this load procedure also has limitations:

- Due to its novelty and recent introduction there are limited case studies and practical applications.
- Validations of the method when applied to complex structural geometries and boundary conditions are limited.
- Comparative studies between the CLT and the 24 h LT methods are rare and they are restricted to a few construction materials and methods.

Fatigue Loading (SCLC girder No. 2)

The fatigue (cyclic) load was applied in a continuous manner at a rate of 0.5 Hz. The load applied was determined from SCDOT regulations, girder dimensions, material properties, an uncracked section, and stresses calculated at midspan. The SCDOT guidelines are based on the concrete stresses at midspan in the extreme bottom fiber of the girder. The SCDOT Bridge Design Manual (2006), Section 15.5.3.1, states the following:

"Tensile stress limits for fully prestressed concrete members shall conform to the requirements for "Other Than Segmentally Constructed Bridges" in LRFD Article 5.9.4, except that the tensile stress at the Service Limit State, after losses, shall be limited as follows: For components with bonded prestressing tendons or reinforcement, the tensile

stress in the pre-compressed tensile zone shall be limited to a maximum of 0.0948 $\sqrt{f'_c}$ (ksi). This limit applies to all projects, regardless of the site location."

An SCDOT design memo (SCDOT, 2008) was later issued that made reference to distinctions between moderate and severe corrosive conditions.

To determine the allowable test load the existing stresses in the concrete fibers in the bottom of the girder were determined. The existing stresses were a combination of stresses due to initial prestressing, stresses due to self-weight of the girder, stresses after release of strands at the prestressing site, stresses due to the weight of the deck added to the girder and prestress losses over time. A comparison was made between theoretical values and measured values. The comparison resulted in values that were comparable with one another. The target value of strain in the bottom fibers was approximately 230 microstrain ($\mu\varepsilon$) and a corresponding load was applied to achieve this level of strain.

The natural frequency was also calculated and measured experimentally and the values were comparable. This was done to ensure the frequency used during testing would be safe in relation to the frequency of the specimen so that the specimen would not go into resonance. The calculated value of the natural frequency was 7.8 Hz. The measured experimental natural frequency was 10 Hz. The measured experimental natural frequency was found by manually exciting the girder. A piece of neoprene was placed on top of the girder and a sledge hammer was used to strike the girder. One accelerometer was used during the natural frequency testing. The specimen was struck several times and digital signal processing algorithms were used to view the signals and thus the natural frequency. The difference in the values may be attributable to the condition of the girder when the manual excitation took place. Some shoring was still in place to brace the girder and deck during the 28-day curing of the deck concrete. The shoring was located at the end of the girder on either side of the deck. Therefore, one shore was at each of the four corners of the deck.

Actual Applied Loading Patterns

SCLC girder No. 1 and HESLC girder: The CLT load profile applied to the girders is shown in Figure 6.14. This load contour was developed according to the expected ultimate capacity of the previous SCC girders and their deck geometry, resulting in a total test load of 160 kips (712 kN). This load level was determined to be around 72 % of the experimental ultimate capacity. For the SCLC members the load profile was not modified, resulting in a relative reduction of the maximum load to around 60 % of the expected ultimate capacity. After completion of the CLT profile a 24h LT was performed on the girders for purposes of comparison between both methodologies. The beams were then loaded monotonically to failure.

SCLC girder No. 2 (after fatigue loading): The CLT load profile applied to this girder is shown in Figure 6.15. This load contour was modified from that of the previous girders (SCLC girder No. 1 and the HESLC girder) to increase the total test load. After completion of the CLT profile a 24h LT was performed on the girder for purposes of

comparison between the load testing procedures. The girder was then loaded monotonically to failure.

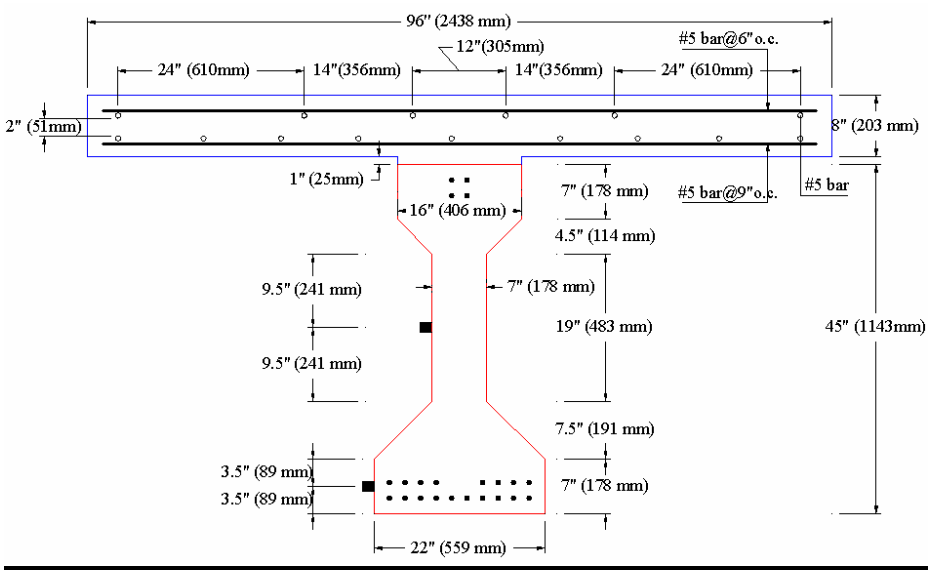

Figure 6.1: Girder and deck dimensions for parallel test program

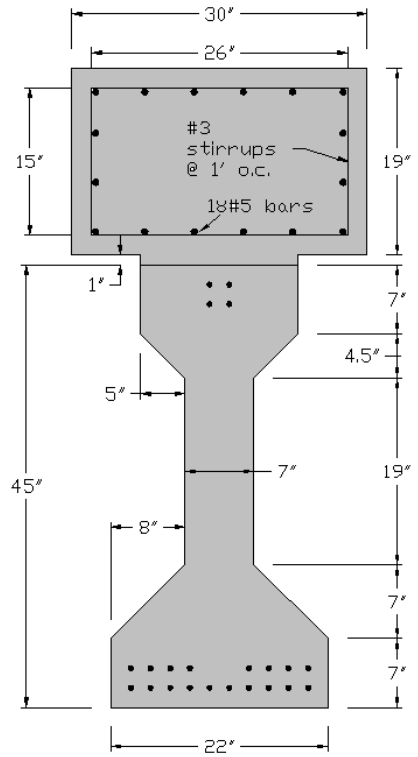

Figure 6.2: Deck dimensions for current test program

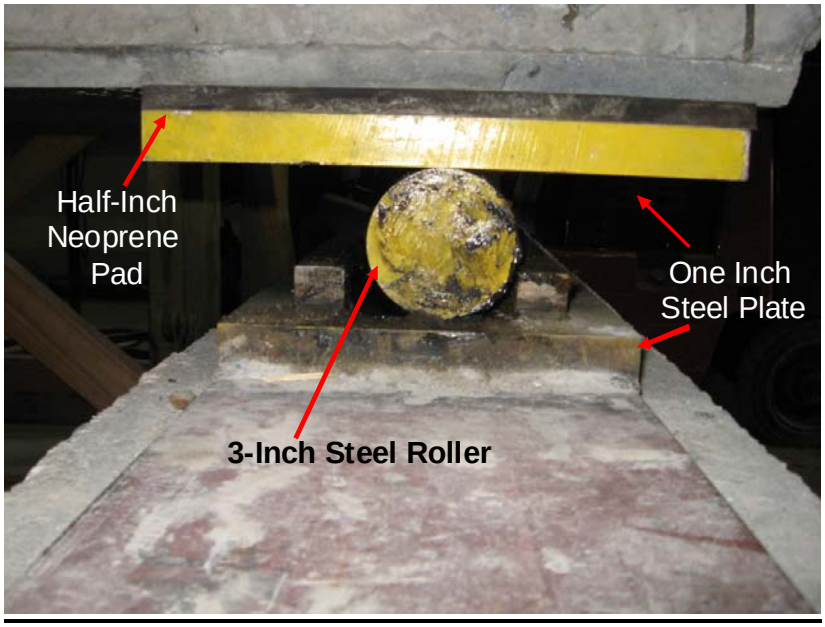

Figure 6.3: Roller connection (simply supported)

Figure 6.4: Test setup in laboratory
(lightweight girder left, normal weight girder right)

Figure 6.5: Test setup in laboratory (both girders lightweight)

Figure 6.6: Static loading apparatus

Figure 6.7: Hydraulic rams and plates

Figure 6.8: Electric pump

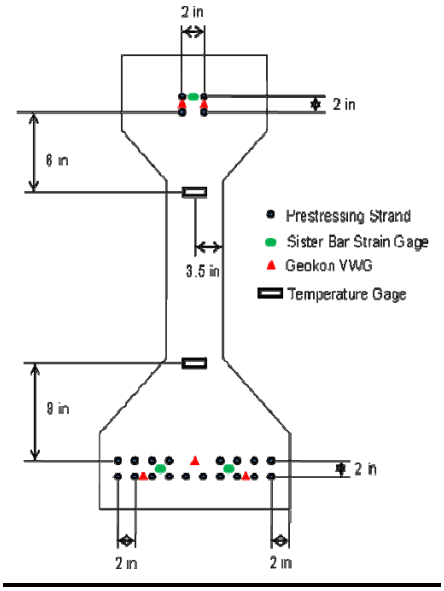

Figure 6.9: Girder internal instrumentation

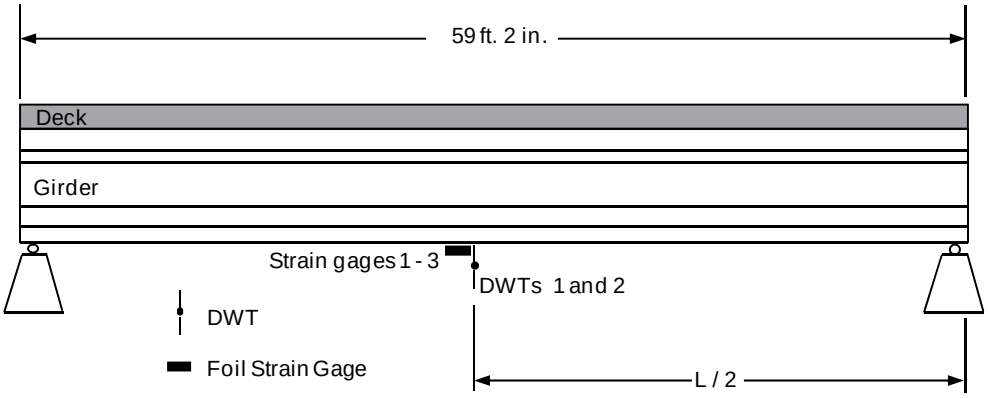

Figure 6.10: External instrumentation (elevation view)

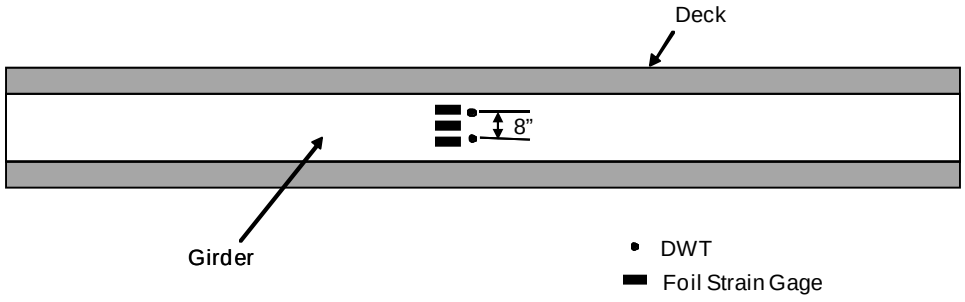

Figure 6.11: External instrumentation (viewed from below)

Figure 6.12: Cracks marked during load holds

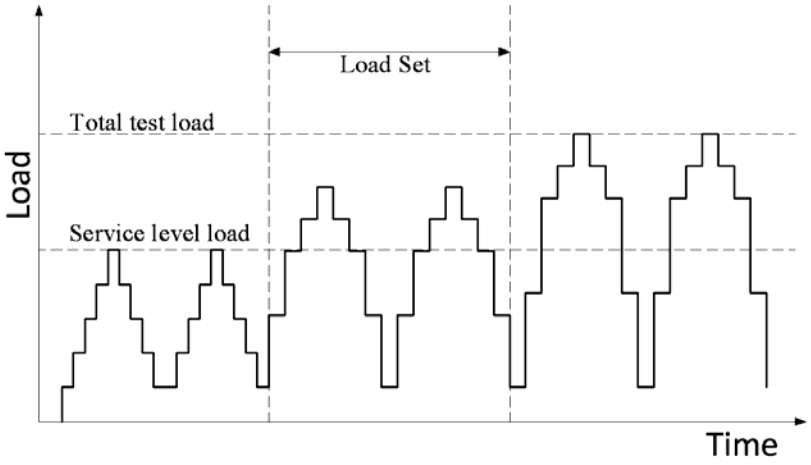

Figure 6.13: Loading profile for CLT method

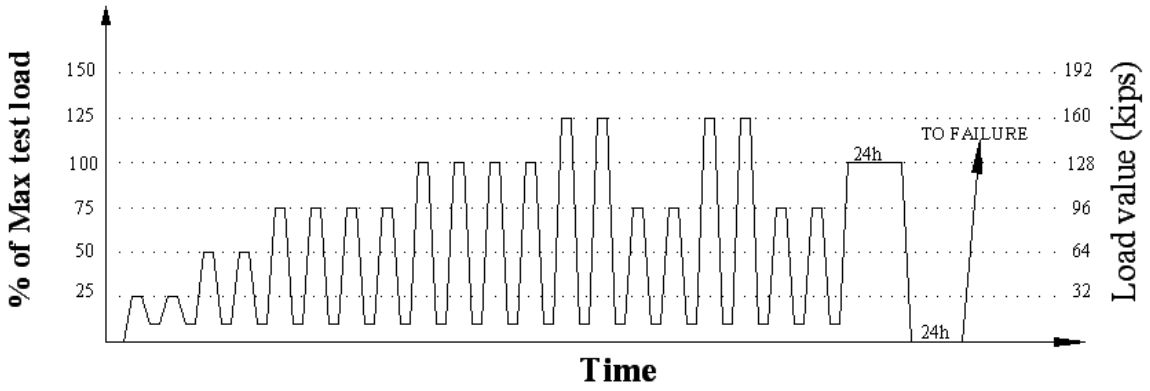

Figure 6.14: Load profile for SCLC girder No. 1 and HESLC girder

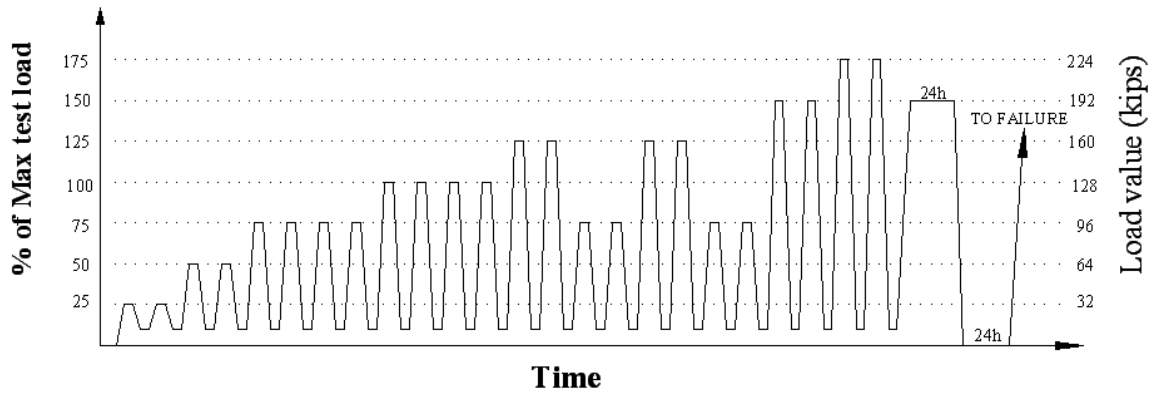

Figure 6.15: Load profile for SCLC girder No. 2 (after fatigue loading)

CHAPTER 7
RESULTS AND PERFORMANCE

7.1 Introduction

Batch Nos. 1 - 3 and the companion cylinders cast at Florence Concrete Products were tested for fresh and hardened properties following the procedures described in previous chapters. The results of the material characterization and girder performance are discussed below. The behavior is compared to available predictive methods including but not limited to the AASHTO LRFD, 4th Edition (2007). Calibration of testing devices is performed on a regular basis (not exceeding once each two years) by third parties and calibration is checked routinely (approximately three times per year) with a reference load cell/data acquisition system.

7.2 Material Performance

Compressive Strength: Compressive strength data is presented in Tables 7.1 to 7.3 for Batch Nos. 1 - 3 and for the companion cylinders cast alongside the AASHTO Type III lightweight girder specimens in Tables 7.4 and 7.5. A graphical representation of the compressive strength gain with time is shown in Figure 7.1. In general, the compressive strength of the concrete increases with time, but eventually becomes almost constant. For most laboratory mixes, this occurred prior 28 days. The two lightweight mixes continued to gain in strength from 28 to 56 days.

All laboratory batches reached the design compressive strength of 8,000 psi (55.2 MPa) in less than 28 days with the exception of Batch No. 2. Batch No. 2 contained fly ash while Batch Nos. 1 and 3 did not. Therefore, the slow strength gain may be due to the presence of fly ash. However, it is also possible that the strength of Batch No. 2 may have been adversely affected by the presence of other chemicals in the mixer. This is mentioned because it was discovered after mixing of Batch No. 2 (and prior to mixing of Batch No. 3) that lower strength concrete was mixed in the same mixer for an unrelated research project. The mixer was thoroughly cleaned after this discovery was made. Due to the sequencing, the unwanted chemicals did not adversely affect the results for Batch Nos. 1 or 3. To investigate the possibility that the low early strengths may have been due entirely to the use of fly ash in this mix, cylinders from Batch No. 2 were tested just prior to the writing of this report (approximately 1,300 days after casting). The results indicated that the compressive strength for this Batch still had not reached 8,000 psi (55.2 MPa), but was approaching this value at 7,639 psi (52.7 MPa).

The 7-day compressive strengths for Batch Nos. 1 and 3 were above 8,000 psi (55.2 MPa). The mix with the highest strength at 7 days was Batch No. 3. Batch Nos. 1 and 3 had the same cement content, but Batch No. 1 had a slightly higher water/cement ratio and more fine aggregate. The 1-day compressive strength for Batch No. 1 was about 16 % higher than Batch No. 3, with 1-day strength of 7,429 psi (51.2 MPa). This difference in initial strength gain is attributed to the different water/cement ratio and the coarse-to-fine aggregate ratio.

For the companion specimens that were cast alongside the AASHTO Type III girder test specimens, compression strength tests were performed at 28 and 56 days. Values from both mixes (HESLC and SCLC) were comparable at 28 and 56 days. Even though the experimental strength data were somewhat lower than the designed strength [f'_c = 8,000 psi (55.2 MPa)] for both mixes, the SCLC specimens had a slightly higher compressive strength than did the HESLC samples.

With the correct air content and mix designs, SCC can gain adequate strength in the time required for prestressed applications with consideration of early strand releases. In the case of the lightweight concretes (SCLC and HESLC) release of the strands was delayed because the compressive strength was less then intended. However, the compressive strength was still adequate to be classified as FHWA HPC performance grade 1. Due to the low strength results at both 28 and 56 days an alternate design that is intended to overcome this issue was prepared by the producer. The suggested mix design is shown in Table 7.6. The most significant differences in the suggested mix design are related to cement content (950 lb/yd^3 for the suggested design compared to 850 lb/yd^3) and the incorporation of intermediate aggregate (normal weight) to replace a portion of the lightweight aggregate. This leads to increased predicted unit weight (127 pcf for the suggested lightweight concrete compared to 118 pcf).

FHWA performance grade: Batch Nos. 1 and 3 met the criteria for FHWA HPC performance grade 2 with respect to compressive strength, while Batch No. 2 and the two lightweight concretes (SCLC and HESLC) met the criteria for FHWA HPC grade 1 concrete.

Unit weight: The measured unit weights of Batch Nos. 1 – 3 and the SCLC and HESLC lightweight mixes were as follows:

Batch No. 1:	148 pcf
Batch No. 2:	145 pcf
Batch No. 3:	144 pcf
SCLC:	116 pcf
HESLC:	115 pcf

Modulus of Elasticity: The modulus of elasticity (E_c) for Batch Nos. 1 and 3 was measured at 7, 28, and 56 days after the cylinders were cast and for Batch No. 2 at 7 days. The results from these tests can be found in Tables 7.1 to 7.3. It can be seen that for Batch No. 3 the measured modulus of elasticity slightly reduces from 7 to 56 days. This effect is most likely related to the normal variability of the test specimens and procedure. For the companion specimens that were cast alongside the lightweight AASHTO Type III girder test specimens, the modulus of elasticity was measured at 28 and 56 days and the results are shown in Tables 7.4 and 7.5. The predicted E_c values according to the AASHTO equation are also shown in Tables 7.1 to 7.5.

Several predictive equations are available for the modulus of elasticity of concrete, including AASHTO, ACI 318, ACI 363, NCHRP report 496, and NCHRP report 595. NCHRP reports 496 and 595 both deal with high strength concrete. The ACI 363 report likewise addresses higher strength concretes. For design all of the predictive equations in these documents are given in terms of unit weight. The NCHRP 496 equation is slightly different from the others because it predicts unit weight based on strength and incorporates the predicted unit weight into the equation. It should be noted that the use of unit weight in these equations is primarily for convenience. It has been shown that the modulus of concrete is strongly related to the stiffness and quantity of coarse aggregate (Meyers and Carasquillo, 1999).

A summary of the predictive equations for modulus is given below. The ACI 318 and AASHTO equations are very similar and therefore only the AASHTO equation is shown. The NCHRP 496 equation is also very similar to the AASHTO equation when the values of K1 and K2 are taken as unity.

AASHTO LRFD, 4th Edition:

$$E_c = 33{,}000K1(w_c)^{1.5}\sqrt{f'_c} \qquad \text{[kcf and ksi]} \qquad \text{(eqn. 7.1)}$$

NCHRP Report 595:

$$E_c = 310{,}000K1(w_c)^{2.5}(f'_c)^{0.33} \qquad \text{[kcf and ksi]} \qquad \text{(eqn. 7.2)}$$

ACI committee 363:

$$E_c = \left(\frac{w_c}{0.145}\right)^{1.5}\left[1{,}000 + 1{,}265\sqrt{f'_c}\right] \qquad \text{[kcf and ksi]} \qquad \text{(eqn. 7.3)}$$

NCHRP 496:

$$E_c = 33{,}000K1K2\left[0.140 + \frac{f'_c}{1{,}000}\right]^{1.5}\sqrt{f'_c} \qquad \text{[kcf and ksi]} \qquad \text{(eqn. 7.4)}$$

In these equations the values of K1 and K2 are related to specific information that is generally not available during the design phase. Therefore, the default value of unity is used when comparing the results.

The predictive equations for modulus typically make use of design as opposed to measured values of concrete strength (f'_c). This cannot be avoided during design because the measured strength is unavailable. For purposes of comparison between equations the use of design strength can be misleading. This effect is amplified for concrete that either significantly exceeds or falls short of the design value. Therefore, plots were produced using measured values of concrete strength and unit weight at both 28 and 56 days as

shown in Figures 7.2 and 7.3. In the plot for 28 days the modulus data from a parallel research program related to normal weight concrete is included (labeled as HESC and SCC in the figures). This additional data is not included for comparison in the 56-day plot because the modulus data in that case was based on a single cylinder.

For the normal weight concrete mixes the modulus is over-predicted by all of the equations at 28 and 56 days regardless of concrete types (SCC or conventional). It is generally understood that the AASHTO/ACI equation tends to over-predict the modulus of concrete for strengths in excess of 6,000 psi (41.4 MPa) and therefore the results shown in the figures are not surprising for these equations. Likewise, the NCHRP 496 equation is very similar to the AASHTO/ACI equations unless specific values for K1 and K2 are included. For the normal weight concretes the ACI 363 method provides a relatively good fit to the measured data. At 28 days the measured HESC and SCC modulus from the parallel research project are essentially the same and the laboratory SCC mixes (Batch Nos. 1 and 3) show higher modulus when compared to the HESC mix.

For the lightweight concrete mixes the modulus is relatively well predicted by all but the NCHRP 496 method at both 28 and 56 days. When comparing the SCLC to the HESLC specimen the measured values of modulus are very similar at both 28 and 56 days with the SCLC mix indicating slightly higher modulus at 56 days.

FHWA performance grade: All normal weight laboratory batches and the SCC mix from the parallel project had modulus values between 4,000 and 5,000 ksi (27.6 and 34.5 GPa). Therefore, these batches qualify as FHWA HPC performance grade 1. The lightweight concrete mixes (SCLC and HESLC) were both less than 4,000 ksi and therefore do not meet the FHWA HPC performance criteria for modulus.

Tensile Strength: For the companion specimens that were cast alongside the AASHTO Type III girder test specimens split tension testing was performed (ASTM C 496). Results in the split tension test were in general higher for the SCLC than for HESLC samples, but both concrete types were within the same range. The results for tensile strength are shown in Tables 7.7 and 7.8.

The AASHTO LRFD equation for prediction of splitting tensile strength is based on compressive strength as follows:

$$f_{ct} = 0.23\sqrt{f'_c} \qquad \text{[ksi]} \qquad \text{(eqn. 7.5)}$$

For sand-lightweight concrete it is recommended that a 15 % reduction factor be applied to this value ($\sqrt{f'_c}$ replaced with $0.85\sqrt{f'_c}$) unless a value for f_{ct} is specified.

The FHWA synthesis report related to lightweight concrete (FHWA, 2007: FHWA-HRT-07-053) indicates that Slate, 1987 has recommended that equation 7.5 be modified as follows:

$$f_{ct} = 0.16\sqrt{f'_c} \quad \text{[ksi]} \quad \text{(eqn. 7.6)}$$

The resulting predictive values are shown in Tables 7.7 and 7.8. The AASHTO equation tends to over-predict the split tensile strength while the modified equation provides a closer fit to the measured data and generally under predicted the tensile strength.

Shrinkage: The shrinkage measurements were recorded from 3 in. x 3 in. x 11.25 in. prisms using a digital length comparator as recommended by ASTM C157. The shrinkage data for Batch Nos. 1 – 3 is shown in Figures 7.4 – 7.6. The shrinkage data from a parallel research program related to normal weight SCC and HESC prisms that were cast alongside full-scale specimens is shown in Figures 7.7 and 7.8. In these figures the predictive AASHTO LRFD equation, 4th Edition, is plotted as a solid line:

$$\varepsilon_{sh} = k_s\, k_{hs}\, k_f\, k_{td}\, 0.48 \times 10^{-3} \quad \text{(eqn. 7.7)}$$

where:

k_s = size factor for volume to surface ratio = $1.45 - 0.13(V/S) \geq 1.0$
k_{hs} = humidity factor for shrinkage = $(2.00 - 0.014H)$
k_f = factor for the effect of concrete strength = $5 / (1 + f'_c)$
k_{td} = time-development factor = $t / (61 - 4f'_{ci} + t)$

For predictions the measured properties of the concrete mixes were used. From the figures it can be seen that the AASHTO predictions tend to marginally under-predict the shrinkage strain at 300 days, however, the estimate of the shrinkage strain is reasonable in all cases.

The shrinkage strain was between 400 – 600 $\mu\varepsilon$ for all of the SCC mixes and therefore all of the SCC mixes qualify as FHWA HPC performance grade 3. The shrinkage for Batch Nos. 1 – 3 were close to qualifying as performance grade 4. The HESC companion specimen from the parallel research project also qualified as FHWA HPC performance grade 3.

Creep: Two of the laboratory mixes, Batch Nos. 1 and 2, were tested for creep. In addition to the laboratory mixes, creep was also measured for companion specimens (both SCC and HESC) that were cast alongside the full-scale specimens for a parallel research project related to normal weight SCC girders.

The measured creep behavior for Batch Nos. 1 and 2 and the specimens from the parallel research project are shown in Figures 7.9 - 7.12 along with the AASHTO LRFD (4th Edition) predictions for creep. For the predictive equations measured properties were used. The creep coefficient is calculated as follows:

$$\Psi(t, t_i) = 1.9\, k_s\, k_{hc}\, k_f\, k_{td}\, t_i^{-0.118} \quad \text{(eqn. 7.8)}$$

where:

k_s = size factor for volume to surface ratio = $1.45 - 0.13(V/S) \geq 1.0$
k_{hc} = humidity factor for creep = $1.56 - 0.008H$
k_f = factor for the effect of concrete strength = $5 / (1 + f'_c)$
k_{td} = time-development factor = $t / (61 - 4f'_{ci} + t)$

For prediction of creep an effective modulus approach is used:

$$E'_c = E_c / (1 + \psi) \quad \text{(eqn. 7.9)}$$

Therefore, total concrete strain under long term conditions is calculated as follows:

$$\varepsilon_1 = f_c/E'_c + \varepsilon_{sh} \quad \text{(eqn. 7.10)}$$

Creep strain is by necessity an indirect measurement and was extracted from the overall strain so that it could be compared to the predictions as follows:

$$\varepsilon_{cr} = \varepsilon_{tot} - \varepsilon_e - \varepsilon_{sh} \quad \text{(eqn. 7.11)}$$

where ε_{cr} = creep strain, ε_{tot} = total strain, ε_e = elastic strain, and ε_{sh} = shrinkage strain. The total strain is the measured strain value at time t (days) from loading. The elastic strain is simply the measured strain at the time of loading, and the shrinkage strain is the average shrinkage of like-sized cylinders at time t. The shrinkage strain in the like-sized companion shrinkage cylinders was measured with an analog gage (Demec gage) in an identical manner to that used for the creep specimens.

It can be seen for Batch Nos. 1 and 2 and for the SCC specimen (plant mix) that the AASHTO equations under-predict the creep. This is most significant for Batch No. 1 and the SCC plant mix. When all three specimens are averaged the amount of under-prediction can be quantified as approximately 40 percent. The HESC specimen (plant mix) had lower creep values than predicted with the AASHTO equation.

FHWA performance grade: The creep performance was within the FHWA HPC performance criteria. The creep criterion specified by FHWA for purposes of classifying HPC is the 'normalized creep', defined as the 300 day creep (in micro-strain) divided by the applied stress (in psi). Batch No. 1, Batch No. 2 and the SCC specimen (plant mix) had normalized creep values of 0.40, 0.38, and 0.45, respectively. The HESC specimen (plant mix) had significantly lower normalized creep of 0.19. Therefore, all of the SCC mixes qualified as HPC performance grade 1 and the HESC mix qualified as HPC performance grade 3.

Freeze-Thaw Resistance: Freeze-thaw testing was conducted on Batch Nos. 1 - 3 as described in previous chapters and in general conformance with ASTM C666-97, "Resistance of Concrete to Rapid Freezing and Thawing". The reduction in the relative

dynamic modulus for Batch Nos. 1 and 3 can be found in Figures 7.13 and 7.14. The relative dynamic modulus data for Batch No. 2 was inconclusive and is not included in the discussion of results (for Batch No. 2 change in weight data was used for evaluation as described below). For Batch Nos. 1 and 3, the dynamic modulus reduced to below 60% of its original value in less than 125 cycles. The FHWA HPC criteria require that this value remain above 60 % after 300 full freezing and thawing cycles. Therefore, Batch Nos. 1 and 3 do not meet the FHWA performance criteria for HPC grade mixes.

The decrease in weight of the specimens is shown as an average for each Batch in Figure 7.15. Batch No. 1 outperformed Batch No. 3, but only by about 5%. The decrease in specimen weight was minimal compared to the high loss in relative dynamic modulus. Although this weight loss was minimal, a visual inspection of the specimens confirmed that the concrete was not very resistant to cyclic strains due to freezing and thawing. Large cracks are seen on the top faces of the concrete as shown in Figure 7.16. The air content of Batches 1 and 3 was approximately 3.5 % by volume for both mixes. While the air content is one important aspect for freeze-thaw durability, the content alone may not be as important as the air void distribution.

Results of freeze-thaw durability testing of specimens from the parallel research program related to normal weight SCC and HESC are included in the Appendix. These specimens also failed to meet the ASTM criteria.

FHWA performance grade: The test results indicate that the SCC specimens did not meet the FHWA HPC performance criteria. However, it should be noted that the HESC specimens from the parallel project also failed to meet the FHWA HPC performance criteria.

Chloride Permeability: Rapid Chloride Permeability testing was conducted on Batch Nos. 1 - 3. Testing was conducted on all specimens after 56 days of curing. The results from these tests can be found in Table 7.9. When tested according to ASTM C1202, Batches 1 and 3 had moderate chloride permeation ranging from 2,000-4,000 coulombs passed, while Batch No. 2 had high chloride permeation at 4,323 coulombs.

The rapid chloride permeability results for the lightweight concrete specimens (SCLC and HESLC) are also shown in Table 7.9. Both showed high chloride permeation of greater than 4,000 coulombs. A sample of the 'Proove-It' output is shown in Figure 7.17.

FHWA performance grade: The test results indicate that Batch No. 3 can be rated as FHWA performance grade 1. However, Batch Nos. 2 and 3 and both of the lightweight mixes (SCLC and HESLC) did not meet the FHWA HPC performance criteria.

7.3 Girder Performance

CLT load profile and failure tests have been completed all three girder specimens; SCLC girder No. 1; HESLC girder; and SCLC girder No. 2 (fatigue specimen). The results of

the girder testing program, including measurements made during the girder fabrication procedure, are summarized below.

Fresh Properties: The fresh properties were assessed on site at Florence Concrete Products in Sumter, South Carolina during casting of the girders. The SCLC mix used in the fabrication of the bridge girders registered a slump flow value of 22 in. (559 mm). According to EFNARC this value classifies the mix as SCC class 1 (slump flow between 21.7 – 25.6 in [550 - 650 mm]) with excellent workability. The slump of the HESLC mix was measured at 7 in. (178 mm).

A value of 1.3 in (33 mm) difference between h1 and h2 was measured in the U-box test. This measurement indicates the SCLC mixture had good filling and passing ability confirming the result obtained from the slump flow test. For the L-box test, values of 3.5 in (89 mm) and 2.7 (69 mm) were measured in this test for h1 and h2 respectively. These values obtained an h2 to h1 ratio of 0.77, which is very close to the recommended value of 0.8 and further supports the good workability of the mix. The measured air content of the SCLC and HESLC mixes were 3 % and 3.5 %, respectively.

Temperature history: Temperature values recorded for the SCLC mix from casting up to day 14 are presented in Figure 7.18a and b. The graphs show a comparison with data recorded from a normal weight SCC mixture with the same design strength used in a parallel project at U.SC. Temperature values reached higher levels for the SCLC mixes in both locations (TG-1 and TG-2) with a relatively high value of approximately 80 deg. C. The normal weight SCC mixtures experienced a faster curing process since the peak of exothermal reactions observed in the temperature profile occurred at earlier times after casting of the beams.

End-Slip: End-slip data were collected using small metallic u-shaped channels tied to the end of the strands; the difference in the channel location before and after release represents the slip of the strand during transfer. Measurements of end-slip were taken at both ends of six cables in each beam (Figures 7.19a, b and c). The end-slip values were smaller in the SCLC girders (SCLC girder No. 1 and SCLC girder No. 2) compared to the HESLC girder. It should be noted that end-slip data is generally subject to scatter owing to a number of factors including variations in the elastic modulus of the concrete and defects in bonding at the strand to concrete interface.

Transfer Length: Demec points were installed on the concrete surface of the girders in order to measure transfer length. The points were located 2 in (50.8 mm) from the end of the beams and were spaced 4 in (102 mm) apart, measurements were taken before and after releasing of the strands using both digital and analog strain measuring devices. The results of the analog device were more consistent and these results are shown in Figures 7.20a, b and c.

Transfer length values were calculated according to the procedure described in Cousins and Nassar (2003). With this method a 95 % average maximum strain line is calculated and the intersection of this line with the sloping strain profile is taken as the transfer

length. Results indicated values of transfer length between 14 in and 18 in (356 and 457 mm) for the HESLC girder and 16 in and 22 in (406 and 560 mm) for the SCLC girders. In terms of average values, the SCLC girders had transfer length values approximately 15 % greater than those recorded for the HESLC girder. The maximum value registered in all girders in terms of the strand diameter was $44d_b$ which is less than the $60d_b$ value recommended by the AASHTO LRFD, 4th Edition. Based on these limited results, the AASHTO LRFD appears to provide a conservative estimate of transfer length for SCLC and HESLC prestressed bridge girders.

Camber: Camber values for each girder were calculated using measured strain values obtained from the vibrating wire strain gauges installed within the beams. Once strain readings were recorded and temperature corrected, camber values can be determined from the curvature of the members (ϕ) and mechanics of materials relationships. The camber values are separated into two components, one produced by the prestressing force and the other due to the self-weight of the girder. Curvature induced by the self-weight load is calculated and extracted from the value obtained using the strain readings. Once curvature values have been separated, individual camber components can be computed. This procedure minimizes the human error and bias implicit in the reading process when camber measurements are taken through the taut wire method.

$$\delta = \frac{\theta(\ell)^2}{8} \quad \text{(camber at midspan due to prestress)} \qquad \text{(eqn. 7.12)}$$

$$\delta' = \frac{5\varphi(\ell)^2}{48} \quad \text{(deflection at midspan due to self-weight)} \qquad \text{(eqn. 7.13)}$$

where:

$$\phi = \theta + \varphi = \frac{\Delta\varepsilon}{h} \quad \text{(curvature at midspan based on readings)} \qquad \text{(eqn. 7.14)}$$

$$\theta = \phi - \varphi \quad \text{(curvature at midspan due to prestress)} \qquad \text{(eqn. 7.15)}$$

$$\varphi = \frac{M_{sw}}{EI_{initial}} \quad \text{(curvature at midspan due to self-weight)} \qquad \text{(eqn. 7.16)}$$

and ℓ = girder span; M_{sw} = moment due to self-weight at midspan; $EI_{initial}$ = product of E_c and gross moment of inertia at release; $\Delta\varepsilon$ = difference between top and bottom measured strain values; and h = distance between top and bottom strain gages.

Midspan strain data on all girders was recorded immediately after releasing and continuously monitored upon arrival of the specimens at the University of South Carolina structures laboratory (Figure 7.21). Continuous camber increment is generally related to time-dependent prestress losses due to creep and shrinkage since the area subjected to the

highest compression stresses will also incur larger deformations. Relaxation of the strands usually generates smaller losses than other long-term phenomena.

From Figure 7.21 it can be seen that the HESLC girder experienced slightly less initial camber than the two SCLC girders. However, as time progressed the camber values were very similar for all girders. The PCI multiplier method (PCI, 2003b) was applied to the measured initial camber data for predictions at 30 days (erection) and 5 years (final). This method produces different results for the HESLC and SCLC girders due to the difference in initial camber. For Figure 7.21 the lower and upper bound values for 30 days and 5 years are shown for the SCLC girders. The HESLC girder approached the prediction for 5 year camber at 300 days but did not exceed the value. The SCLC girders did not exceed the 30 day prediction and did not approach the 5 year prediction at 300 days. In general the greatest camber growth was measured from the time of initial readings just after release and delivery to the structures laboratory with limited camber growth thereafter.

Prestress Losses: Prestress losses were evaluated using strain readings obtained from the vibrating wire strain gauges installed within the beams and located at the same level of the prestressing strands (bottom flange of girder). The strain data was then converted to stress values. Measured prestress losses are plotted for all beams in Figure 7.22 along with theoretical predictions from ACI-ASCE, AASHTO-LRFD and NCHRP-496 methods. Total prestress losses converged to an approximate value of 30 ksi at 300 days for all the specimens; however, predicted losses from every method were over-predicted with NCHRP-496 giving the closest match with 34 ksi at 300 days.

Load versus Displacement Behavior (Cyclic Load Test)

Load versus displacement behavior during the entire CLT load profile for all girders is shown in Figure 7.23. The results presented show that all specimens displayed very similar behavior during the application of the CLT loading protocol. The third specimen tested (SCLC girder No. 2 – fatigue girder) was loaded to a higher percentage of ultimate capacity than the previous two specimens (SCLC girder No. 1 and the HESLC girder). Results from the application of the CLT evaluation criteria to the girders are presented in Figures 7.24a - c, 7.25a - c, and 7.26a - c as well as in Tables 7.10, 7.11 and 7.12.

According to the CLT criteria, the first two specimens (SCLC girder No. 1 and the HESLC girder) did not experience significant structural damage below 125 % [160 kips (712 kN)] of the theoretical maximum test load and even at this load level the girders failed only one of three criteria (deviation from linearity). As a consequence, two additional loadsets at 150% [192 kips (854 kN)] and 175 % [224 kips (996 kN)] of the theoretical maximum load test were included in the CLT loading profile for SCLC girder No. 2. In addition, a fatigue test consisting of 2,000,000 cycles at approximately 0.5 Hz was performed on SCLC girder No. 2 prior to applying the CLT method. Subsequent observation of the structural performance of SCLC girder No. 2 (during CLT as well as failure) suggests no evidence of considerable stiffness degradation in the mechanical behavior of the specimen caused by the fatigue cycles. This conclusion is also supported

by load versus displacement and load versus strain data (Figure 7.27a and b) gathered from several static load tests which were carried out at different stages during the fatigue loading.

24 Hour Load Test Results

A 24 hour load test (24h LT) based on ACI 318 (2005) was performed on each of the girders following the cyclic load test (CLT), Figures 7.28 and 7.29. The results show that after 24h of load hold at 100 % of maximum test load, the first two specimens (SCLC girder No. 1 and the HESLC girder) retained a small percentage of residual deflection (less than 8 % of Δ_{max}) when compared to the maximum residual deflection value of 25 % of Δ_{max} specified in the evaluation criteria for this method.

Following the same approach taken for SCLC girder No. 2 regarding the CLT method, the maximum load level for the 24h load test was increased to 150 % of the maximum test load. Despite the considerable increase in the applied load and the significant amount of cracking present in SCLC girder No. 2 the girder still passed the evaluation criteria with less than 5 % of Δ_{max} for residual deflection.

Load versus Displacement during Failure Testing

Load versus displacement behavior from loading to failure for all girders is shown in Figure 7.30. The data presented indicates that all specimens had a similar initial stiffness and ultimate capacity (around 10 % maximum difference). Also, all girders (especially both SCLC girders) behaved similarly during reloading stages on the load versus deflection curves.

The calculated nominal capacity of the girder specimens is not dependent on the type of concrete used in the girder. This is because the compressive stress block resides entirely within the conventional concrete deck. The nominal moment capacity as calculated in general conformance with the AASHTO LRFD, 4th Edition was found to be approximately 51,400 kip-in (5,800 kN-m). This corresponds to a total load value of approximately 290 kips (1,290 kN) applied through the midpoint of the two loading rams. This value is slightly higher than the ultimate capacity that was achieved during loading in most cases, with the girder having the lowest measured capacity (HESLC girder) being within approximately 10 % of the calculated nominal capacity. The SCLC girders were within approximately 5 % of the calculated nominal capacity. As described below, tensile failure of the prestressing strands was not observed in the tests. Rather the failure was governed by splitting along the strands. This failure mode may have contributed to the observed behavior in regard to ultimate moment capacity.

All specimens attained a significant amount of deflection [Δ > 10.0 in. (250 mm)] prior to collapse. Consequently, it appears that the girders did not sustain enough damage during the CLT and posterior 24h load test (including fatigue for SCLC girder No. 2) to significantly compromise the deformation and ultimate capacity of the girders.

Description of Failure Modes

SCLC Girder No. 1: Failure of this girder started with yielding of the strands and with the continuous propagation of nearly vertical cracks at midspan. Once the cracks reached the deck, significant crushing of the concrete deck appeared simultaneously with horizontal cracks close to the bottom of the girder and traveling parallel to it. Further loading of the girder resulted in the horizontal cracks producing a splitting failure of the bottom flange which propagated further up diagonally and finally meeting diagonal cracks traveling down from the concrete deck and producing the catastrophic collapse of the specimen. Twisting and breaking of the deck reinforcing steel was present along with substantial disintegration of the web displaying visible diagonal cracks as far as eight feet from midspan (Figures 7.31a and b).

HESLC girder: Yielding occurred prior to significant cracking of the concrete deck. Next, a significant nearly vertical crack developed as the top of the deck crushed at midspan (Figure 7.32a). As load was increased, the concrete on the bottom of the deck spalled as crushing occurred on the top and the reinforcing bars buckled within the deck. As the displacement continued the nearly vertical crack continued along the strand in the bottom flange resulting in a splitting failure of the bottom flange (Figure 7.32b). The girder deflection was increased until the girder had deflected at least 19 in. (482 mm). At this point loading was ceased and the girder was shored.

The final failure mode was longitudinal splitting along the bottom flange combined with crushing of the concrete deck. Loud popping as is normally associated with reinforcing bar breakage was heard on one occasion late in the loading process and it is believed to have been associated with breakage of one of the vertical stirrups near midspan.

SCLC girder No. 2 (fatigue girder): This girder failed in a very similar manner to that of the previous two girders. Yielding of the strands occurred first, leading to a good deal of deflection with noticeable nearly vertical cracking at midspan (Figure 7.33a). Beyond this level, the concrete deck crushing and the extension of longitudinal splitting cracks occurred at similar times. Audible popping was noticed on at least one occasion and during demolition it was found that one vertical stirrup had ruptured near the top bulb to web interface region. The strands were inspected and none were found to be ruptured. Photographs of the longitudinal splitting cracks and deck crushing can be seen in Figures 7.33b through 7.33e. It appears that the longitudinal splitting may be due to the detail of the stirrups at the bottom of the girder where a double 90-degree hook is used to anchor the stirrups (Figures 7.33f and 7.33g).

Table 7.1: Compressive strength and E_c data, Batch No. 1

Spec.	Age, Days	f'c psi (MPa)	Avg. f'c, psi (MPa)	E_c ksi (GPa)	Avg. E_c ksi (GPa)	Pred. E_c (AASHTO) ksi (GPa)
1	1	6,159 (42.5)	6,170 (42.5)	-	-	-
2		6,180 (42.6)		-		
1	3	7,416 (51.1)	7,378 (50.9)	-	-	-
2		7,340 (50.6)		-		
1	7	8,885 (61.3)	8,563 (59.0)	5,047 (34.8)	4,967 (34.2)	5,498 (37.9)
2		8,240 (56.8)		4,886 (33.7)		
1	14	8,240 (56.8)	8,547 (58.9)	-	-	-
2		8,854 (61.0)		-		
1	28	9,893 (68.2)	9,495 (65.6)	4,726 (32.6)	4,721 (32.6)	5,790 (39.9)
2		9,096 (62.7)		4,716 (32.5)		
1	56	9,548 (65.8)	9,548 (65.8)	4,960 (34.2)	4,992 (33.9)	5,806 (40.0)
2		8,568 (59.1)‡		4,884 (33.7)		
1	90	9,616 (66.3)	9,616 (66.3)	-	-	-
-		-		-		

‡ = low value not used

Table 7.2: Compressive strength and E_c data, Batch No. 2

Spec.	Age, Days	f'c psi (MPa)	Avg. f'c, psi (MPa)	MOE ksi (GPa)	Avg. MOE ksi (GPa)	Pred. MOE (AASHTO) ksi (GPa)
1	1	4,776 (32.9)	4,960 (34.2)	-	-	-
2		5,143 (35.5)		-		
1	3	-	-	-	-	-
2		-		-		
1	7	6,364 (43.9)	6,385 (44.0)	4,416 (30.4)	4,151 (28.6)	4,604 (31.7)
2		6,406 (44.2)		3,885 (26.8)		
1	14	6,783 (46.8)	6,782 (46.8)	-	-	-
2		6,781 (46.8)		-		
1	1,300	7,388 (50.9)	7,639 (52.7)	-	-	-
2		7,797 (53.8)		-		
3		7,732 (53.3)		-		

Table 7.3: Compressive strength and E_c data, Batch No. 3

Spec.	Age, Days	f'c psi (MPa)	Avg. f'c, psi (MPa)	E_c ksi (GPa)	Avg. E_c ksi (GPa)	Pred. E_c (AASHTO) ksi (GPa)
1	1	7,186 (49.5)	7,307 (50.4)	-	-	-
2		7,429 (51.2)		-		
1	3	8,105 (55.9)	8,199 (56.5)	-	-	-
2		8,292 (57.2)		-		
1	7	8,926 (61.5)	8,916 (61.5)	4,726 (32.6)	4,741 (32.7)	5,384 (37.1)
2		8,905 (61.4)		4,755 (32.8)		
1	14	9,500 (65.6)	9,498 (65.5)	-	-	-
2		9,495 (65.5)		-		
1	28	9,332 (64.3)	9,348 (64.5)	4,594 (31.7)	4,675 (32.2)	5,513 (38.0)
2		9,364 (64.6)		4,756 (32.8)		
1	56	-	9,530 (65.7)	4,471 (30.8)	4,501 (31.0)	5,567 (38.4)
2		9,530 (65.7)		4,532 (31.2)		

Table 7.4: Compressive strength and E_c data, SCLC

Spec.	Age, Days	f'c psi (MPa)	Avg. f'c psi (MPa)	E_c ksi (GPa)	Avg. E_c ksi (GPa)	Pred. E_c (AASHTO) ksi (GPa)
1	28	7,901 (54.5)	7,641 (52.7)	3,636 (25.1)	3,608 (24.9)	3,604 (24.8)
2		6,826 (47.1)		3,580 (24.7)		
3		8,198 (56.5)		-		
1	56	7,053 (48.6)	7,921 (54.6)	3,531 (24.3)	3,370 (23.2)	3,669 (25.3)
2		9,167 (63.2)		3,140 (21.6)		
3		7,544 (52.0)		3,440 (23.7)		

Table 7.5: Compressive strength and E_c data, HESLC

Spec.	Age, Days	f'c psi (MPa)	Avg. f'c, psi (MPa)	E_c ksi (GPa)	Avg. E_c ksi (GPa)	Pred. E_c (AASHTO) ksi (GPa)
1	28	7,036 (48.5)	7,405 (51.1)	2,218 (15.3)	3,063‡ (21.1)	3,502 (24.1)
2		7,216 (49.8)		3,036 (20.9)		
3		7,964 (54.9)		-		
1	56	6,849 (47.2)	7,496 (51.7)	3,266 (22.5)	3,203 (22.1)	3,524 (24.3)
2		7,743 (53.4)		3,094 (21.3)		
3		7,896 (54.4)		3,249 (22.4)		

‡ = low value not used

Table 7.6: Suggested lightweight concrete mix design

Material Type	Mix Designation
	HESLC (suggested)
w/c Ratio	0.32
Cement, lb/yd^3	950
Fly Ash, lb/yd^3	0
Silica Fume, lb/yd^3	0
Stalite, lb/yd^3	608
Fine Sand, lb/yd^3	1,049
Int. Agg, lb/yd^3	523
Total Water, lb/yd^3	304
HRWR, oz/yd^3	as nec.
WR, oz/yd^3	as nec.
VMA, oz/yd^3	as nec.
AEA, oz/yd^3 (ml/m^3)	as nec.
Coarse/Fine Ratio	1.07‡
HRWR Type	Sika Viscocrete
Water Reducer Type	Sika Plastiment
Slump Flow, in	na
U-Box	na
L-Box	na
Air Content	4.5%
Unit weight (lbs/ft^3)	127
28 day f'c, psi	8,000 (target)

‡ CA = Stalite + Int. Agg.

Table 7.7: Tensile strength data, SCLC

Specimen	Age at Test, Days	Tensile Strength psi (MPa)	Avg. Tensile Strength psi (MPa)	AASHTO Pred. psi (MPa)	Modified Pred. psi (MPa)
1	28	570 (3.93)	505 (3.48)	541 (3.73)	442 (3.05)
2		474 (3.27)			
3		473 (3.26)			
1	56	450 (3.10)	480 (3.31)	550 (3.79)	450 (3.10)
2		520 (3.59)			
3		470 (3.24)			

Table 7.8: Tensile strength data, HESLC

Specimen	Age at Test, Days	Tensile Strength psi (MPa)	Avg. Tensile Strength psi (MPa)	AASHTO Pred. psi (MPa)	Modified Pred. psi (MPa)
1	28	408 (2.81)	406 (2.80)	532 (3.67)	435 (3.00)
2		407 (2.81)			
3		403 (2.78)			
1	56	464 (3.20)	450 (3.10)	536 (3.69)	438 (3.02)
2		460 (3.17)			
3		414 (2.85)			

Table 7.9: Rapid chloride permeability data

Concrete Mix	56 Day f'c psi (MPa)	Avg. Chloride Permeability (Coulombs)	Permeability Class
Batch No. 1	9,058 (62.5)	3,390	Moderate
Batch No. 2	6,782‡ (46.8)	4,323	High
Batch No. 3	9,530 (65.7)	2,645	Moderate
SCLC	7,921 (54.6)	4,390	High
HESLC	7,496 (51.7)	4,097	High

‡ = 14 day value used

Table 7.10: CLT evaluation - SCLC girder No. 1

	Repeatability Index (%)		Permanency (%)		IDL (%)	
	DWT-1	DWT-2	DWT-1	DWT-2	DWT-1	DWT-2
Loadset-1	95.66	92.01	1.27	0.82	0.00	0.00
					0.01	2.17
Loadset-2	98.18	99.45	1.85	1.12	21.17	17.36
					21.64	18.20
Loadset-3	96.99	98.55	1.41	0.13	22.55	19.66
					22.70	20.00
Loadset-4	101.57	106.19	0.59	3.01	19.45	10.52
					22.07	17.97
Loadset-5	97.17	100.19	2.44	2.21	26.91	20.03
					26.90	21.96
Loadset-6	96.05	100.84	1.82	0.28	27.03	22.55
					26.31	22.93
Loadset-7	109.11	105.88	0.58	2.21	43.02	44.63
					47.77	48.46
Loadset-8	100.93	99.32	0.66	1.97	NA	NA
					NA	NA
Loadset-9	98.98	98.76	0.82	0.80	47.42	47.77
					47.75	48.01
Loadset-10	93.11	87.90	2.17	7.88	NA	NA
					NA	NA

Table 7.11: CLT evaluation – SCLC girder No. 2 (fatigue girder)

	Repeatability Index (%)		Permanency (%)		IDL (%)	
Loadset	DWT-1	DWT-2	DWT-1	DWT-2	DWT-1	DWT-2
1	106.76	104.00	2.47	0.95	0.00	0.00
					0.54	0.81
2	100.00	103.60	0.00	0.29	1.54	5.78
					0.79	3.38
3	99.48	98.57	1.03	0.72	5.59	6.81
					5.96	7.51
4	102.33	101.68	2.06	2.33	6.69	7.14
					5.56	7.43
5	101.16	100.00	0.13	0.38	0.00	0.00
					0.67	1.01
6	101.65	100.51	0.37	0.38	1.07	0.63
					3.19	1.58
7	103.60	103.49	0.92	1.28	11.42	10.57
					14.05	13.44
8	101.63	101.06	0.48	0.17	NA	NA
					NA	NA
9	98.82	100.60	0.17	0.26	0.00	0.00
					1.27	0.41
10	100.63	100.67	0.62	0.83	NA	NA
					NA	NA
11	103.47	104.58	0.52	0.50	28.61	31.36
					31.32	34.61
12	102.81	102.00	0.41	2.41	51.73	54.44
					53.14	56.27

Table 7.12: CLT evaluation – HESLC girder

	Repeatability Index (%)		Permanency (%)		IDL (%)	
Loadset	DWT-1	DWT-2	DWT-1	DWT-2	DWT-1	DWT-2
1	93.58	100.87	4.61	9.89	0.00	0.00
					1.66	7.28
2	97.25	93.73	3.68	1.69	7.19	3.88
					8.38	1.05
3	98.51	103.33	0.03	2.24	3.94	1.67
					3.37	0.75
4	113.52	103.32	0.41	1.24	9.32	11.31
					6.07	9.28
5	100.28	101.91	0.81	1.34	1.55	6.12
					0.62	3.19
6	98.56	100.61	1.18	5.67	0.92	6.41
					0.07	3.09
7	106.27	113.74	1.61	0.60	23.88	24.53
					27.11	30.55
8	97.49	94.24	1.70	5.96	NA	NA
					NA	NA
9	98.67	96.50	1.64	2.84	28.29	30.44
					28.79	30.39
10	98.49	92.13	0.94	1.61	NA	NA
					NA	NA

Table 7.13: 24h load test deflection data (all girders)

Time, hours	SCLC No. 1 in. (mm)	HESLC in. (mm)	SCLC No. 2 in (mm)
0	0.00 (0.0)	0.00 (0.0)	0.00 (0.0)
0	0.56 (14)	0.53 (13)	1.54 (39)
24	0.52 (13)	0.52 (13)	1.49 (38)
24	0.01 (0.3)	0.04 (1.0)	0.04 (1.0)
48	0.01 (0.3)	0.03 (0.8)	0.00 (0.0)

Table 7.14: 24h load test evaluation (all girders)

	SCLC No. 1	HESLC	SCLC No. 2
Δmax/4, in. (mm)	0.14 (3.6)	0.13 (3.3)	0.38 (9.7)
Δr in. (mm)	0.01 (0.3)	0.04 (1.0)	0.04 (1.0)

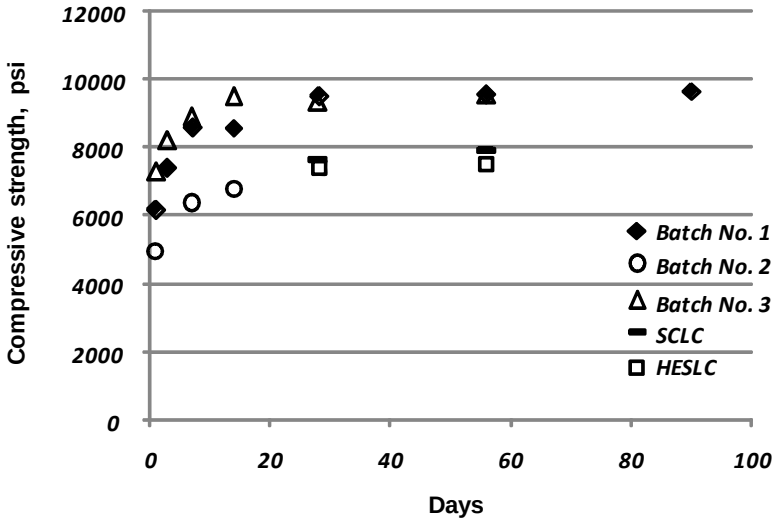

Figure 7.1: Compressive strength gain with time

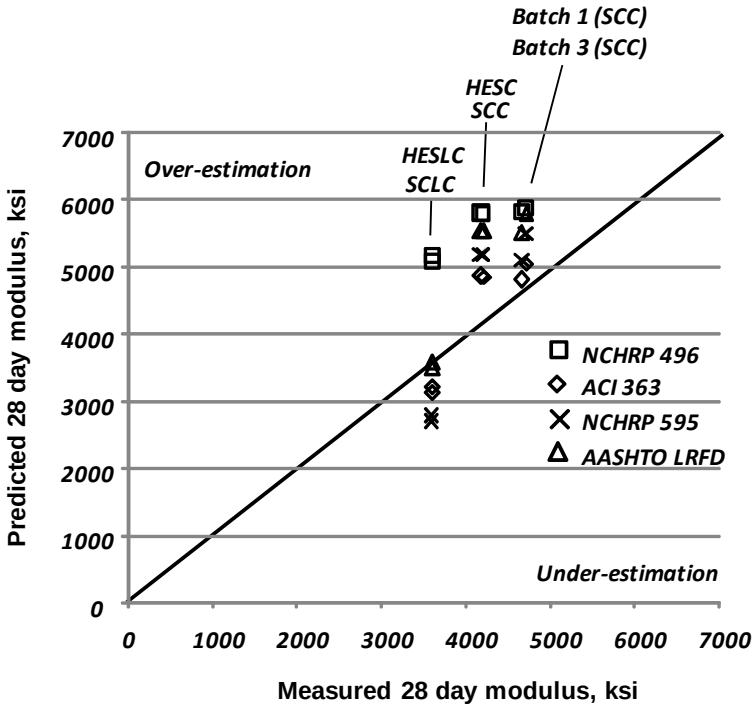

Figure 7.2: Predicted vs. measured E_c at 28 days

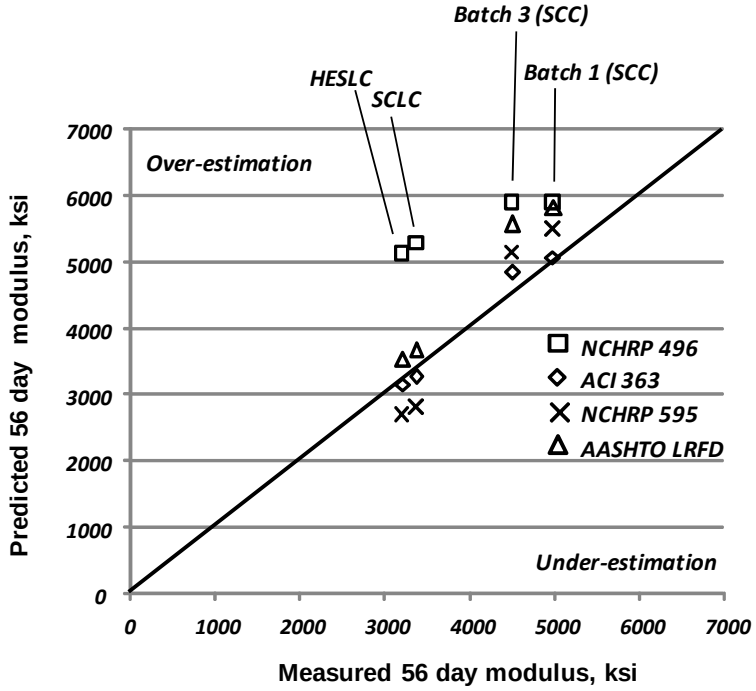

Figure 7.3: Predicted vs. measured E_c at 56 days

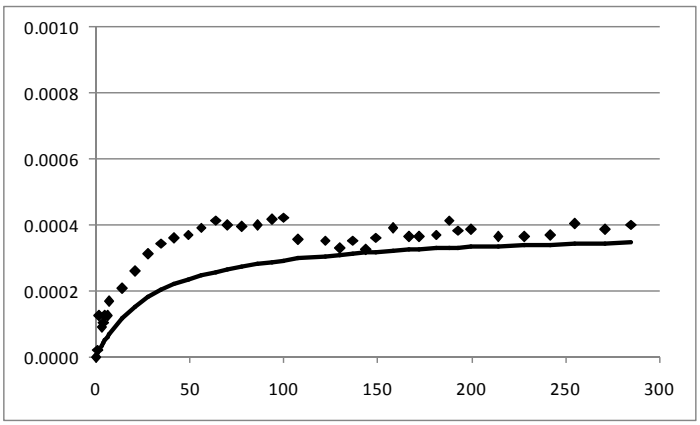

Figure 7.4: Shrinkage strain vs. time - Batch No. 1

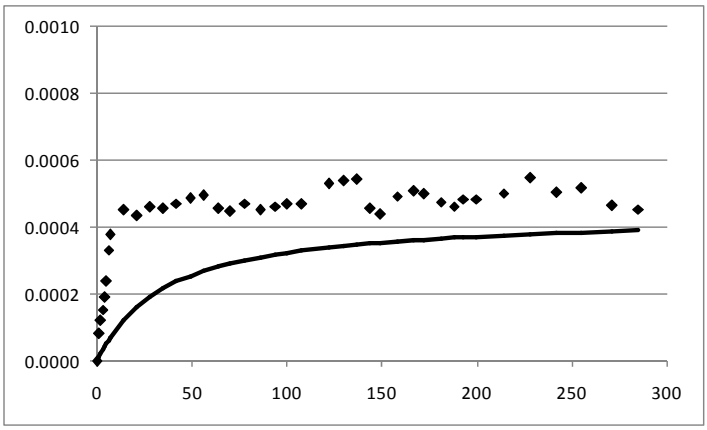

Figure 7.5: Shrinkage strain vs. time - Batch No. 2

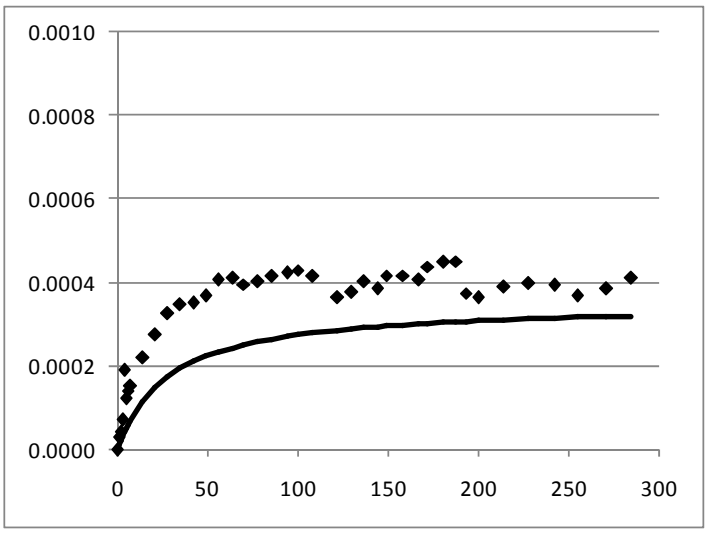

Figure 7.6: Shrinkage strain vs. time - Batch No. 3

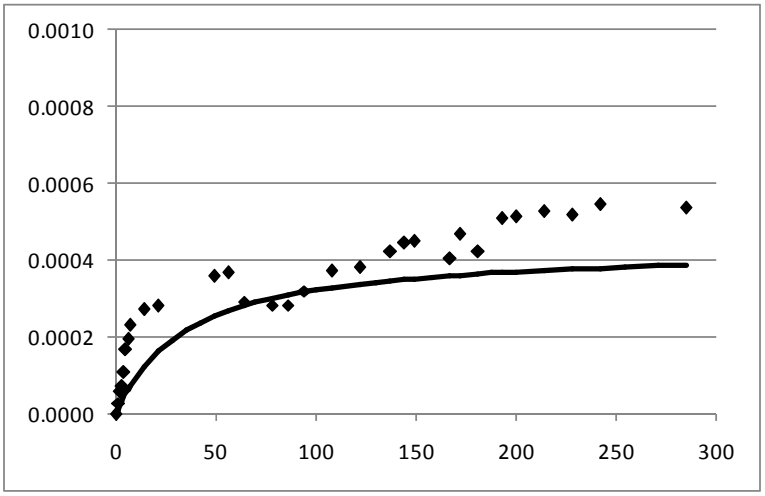

Figure 7.7: Shrinkage strain vs. time – SCC

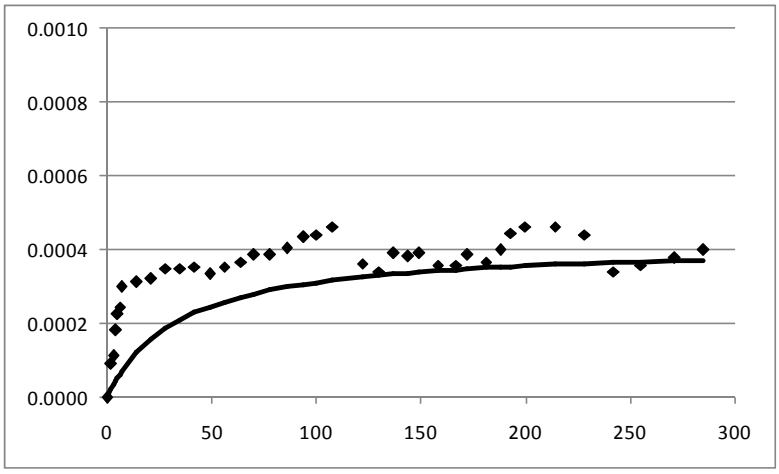

Figure 7.8: Shrinkage strain vs. time – HESC

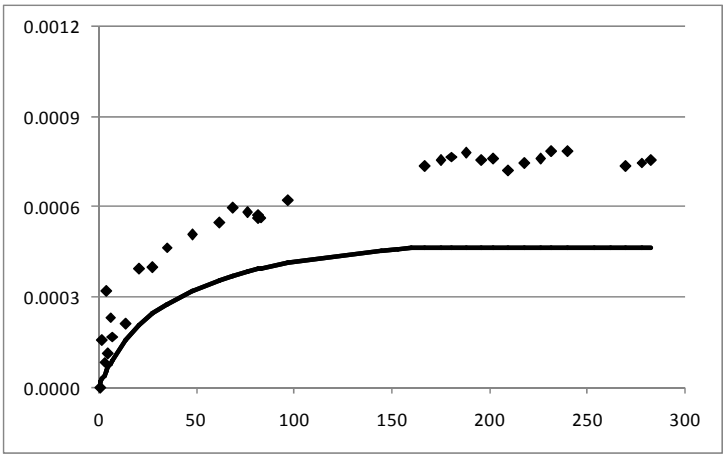

Figure 7.9: Creep strain vs. time - Batch No. 1

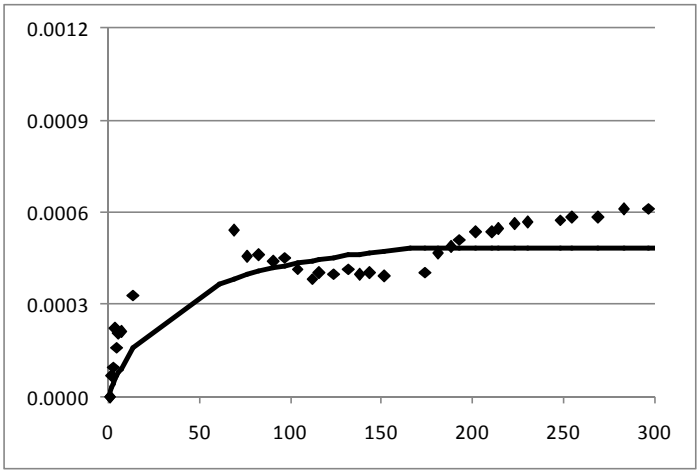

Figure 7.10: Creep strain vs. time – Batch No. 2

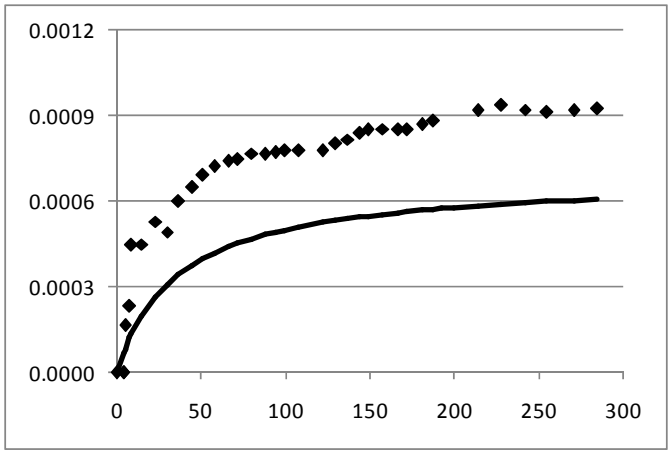

Figure 7.11: Creep strain vs. time, SCC

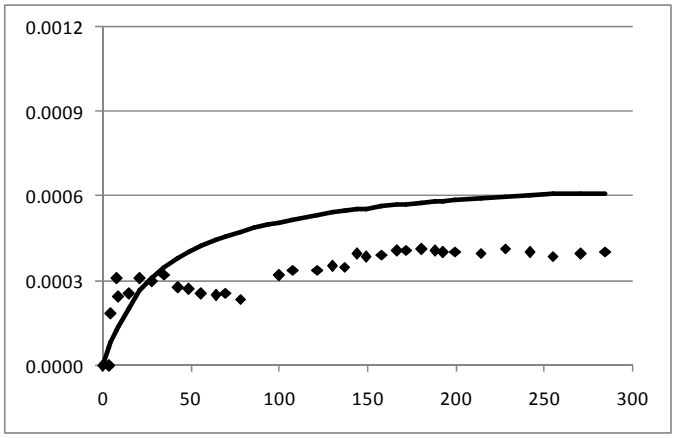

Figure 7.12: Creep strain vs. time, HESC

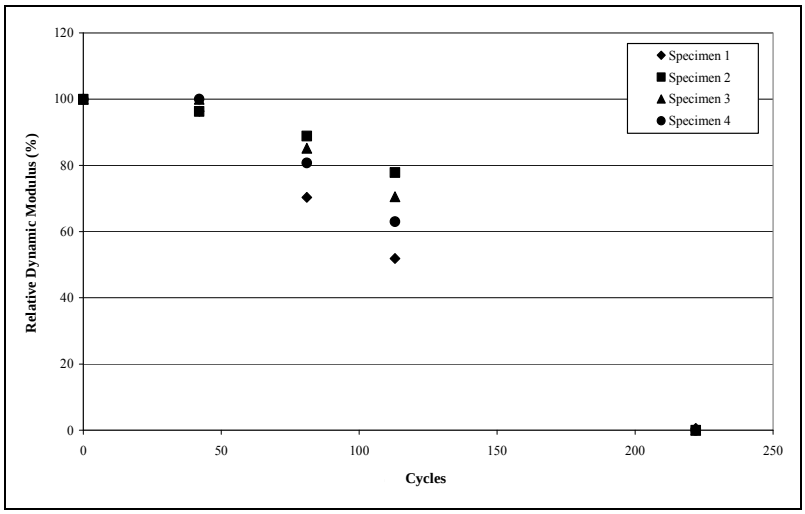

Figure 7.13: Freeze-thaw degradation – Batch No. 1

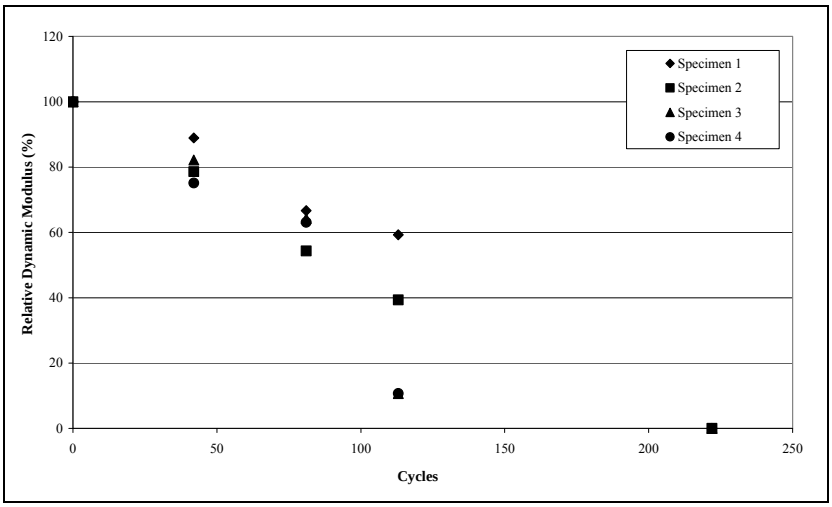

Figure 7.14: Freeze-thaw degradation – Batch No. 3

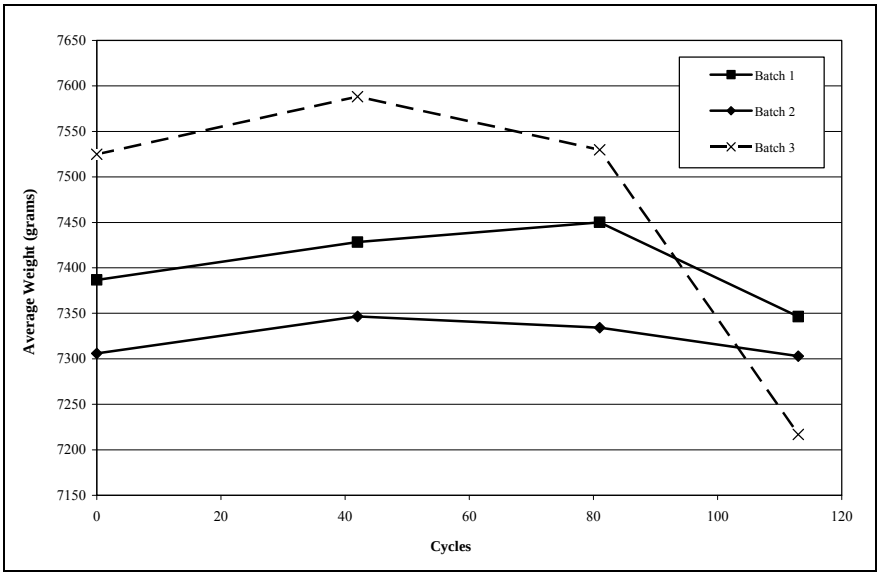

Figure 7.15: Freeze-thaw weight changes – Batch Nos. 1 - 3

Figure 7.16: Freeze-thaw setup and specimens

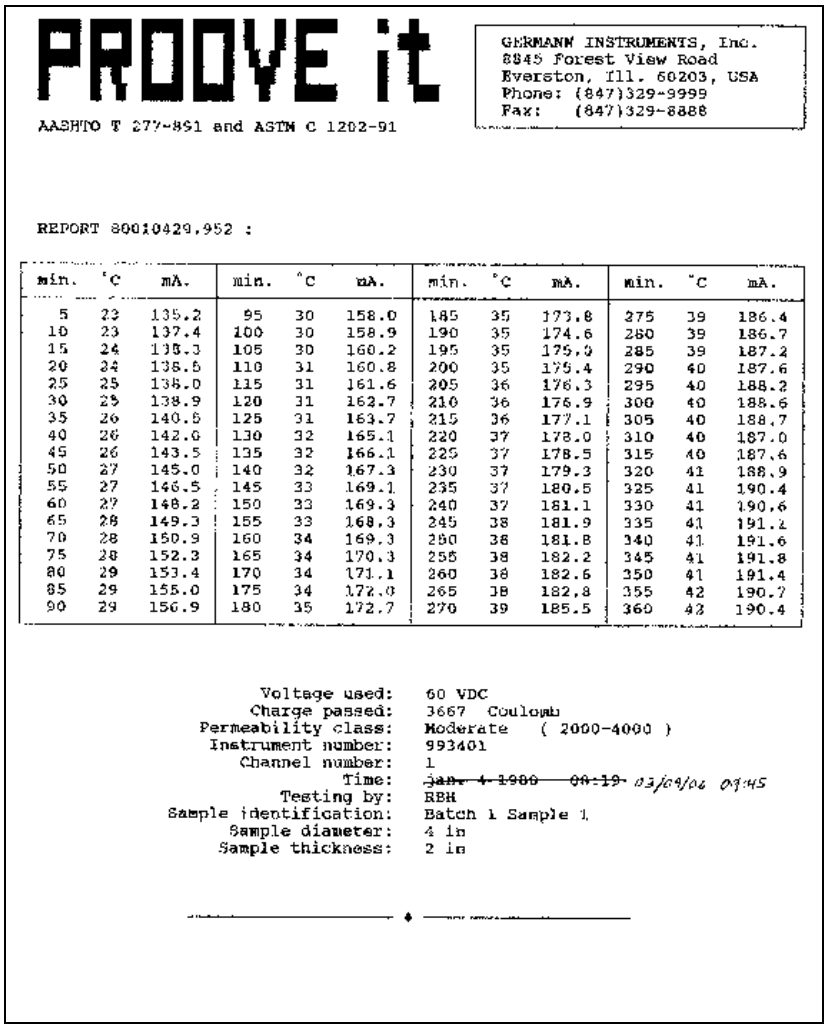

PROOVE it

AASHTO T 277-89 and ASTM C 1202-91

GERMANN INSTRUMENTS, Inc.
8845 Forest View Road
Everston, Ill. 60203, USA
Phone: (847)329-9999
Fax: (847)329-8888

REPORT 80010429.952 :

min.	°C	mA.	min.	°C	mA.	min.	°C	mA.	min.	°C	mA.
5	23	135.2	95	30	158.0	185	35	173.8	275	39	186.4
10	23	137.4	100	30	158.9	190	35	174.6	280	39	186.7
15	24	136.3	105	30	160.2	195	35	175.0	285	39	187.2
20	24	138.5	110	31	160.8	200	35	175.4	290	40	187.6
25	25	136.0	115	31	161.6	205	36	176.3	295	40	188.2
30	25	138.9	120	31	162.7	210	36	176.9	300	40	188.6
35	26	140.5	125	31	163.7	215	36	177.1	305	40	188.7
40	26	142.0	130	32	165.1	220	37	178.0	310	40	187.0
45	26	143.5	135	32	166.1	225	37	178.5	315	40	187.6
50	27	145.0	140	32	167.3	230	37	179.3	320	41	188.9
55	27	146.5	145	33	169.1	235	37	180.5	325	41	190.4
60	27	148.2	150	33	169.3	240	37	181.1	330	41	190.6
65	28	149.3	155	33	168.3	245	38	181.9	335	41	191.2
70	28	150.9	160	34	169.3	250	38	181.8	340	41	191.6
75	28	152.3	165	34	170.3	255	38	182.2	345	41	191.8
80	29	153.4	170	34	171.1	260	38	182.6	350	41	191.4
85	29	155.0	175	34	172.0	265	38	182.8	355	42	190.7
90	29	156.9	180	35	172.7	270	39	185.5	360	42	190.4

Voltage used:	60 VDC
Charge passed:	3667 Coulomb
Permeability class:	Moderate (2000-4000)
Instrument number:	993401
Channel number:	1
Time:	~~Jan. 4 1980 00:19~~ 03/04/04 09:45
Testing by:	REH
Sample identification:	Batch 1 Sample 1
Sample diameter:	4 in
Sample thickness:	2 in

Figure 7.17: Sample chloride permeability readout

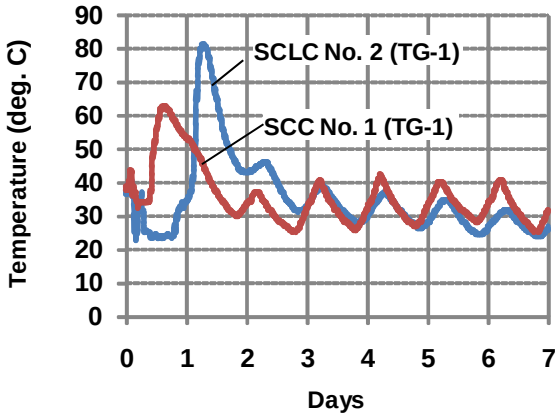

Figure 7.18a: Temperature profile – TG1

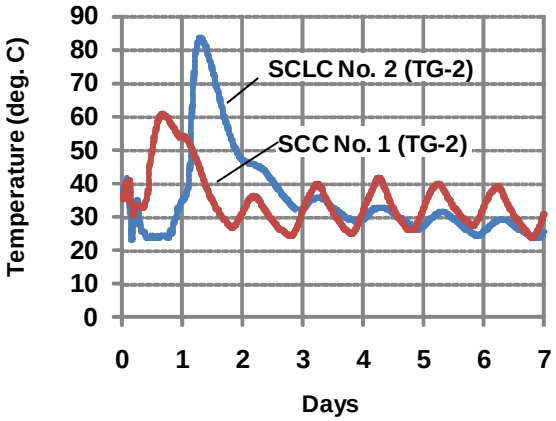

Figure 7.18b: Temperature profile – TG2

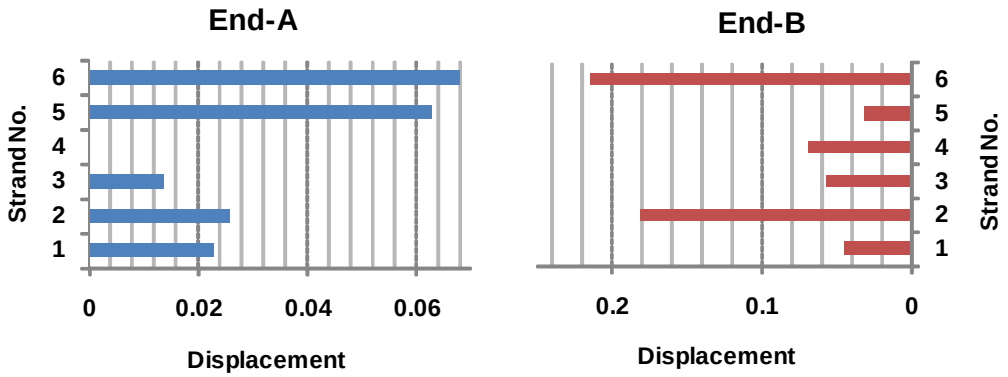

Figure 7.19a: End slip – SCLC girder No. 1

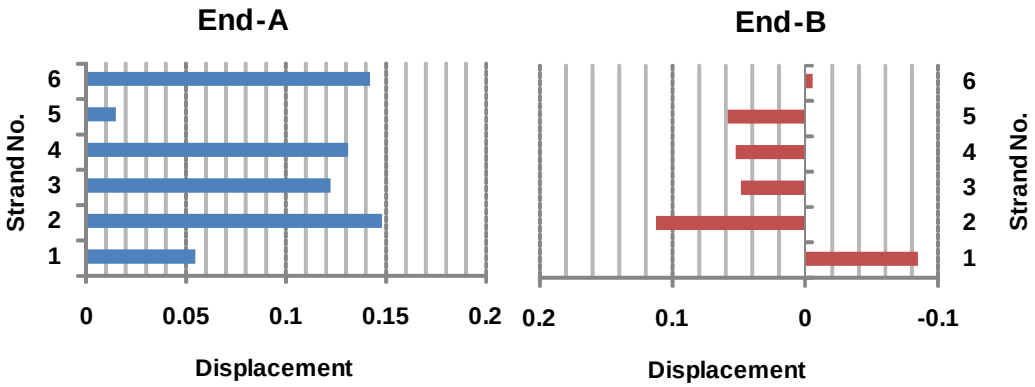

Figure 7.19b: End slip – SCLC girder No. 2

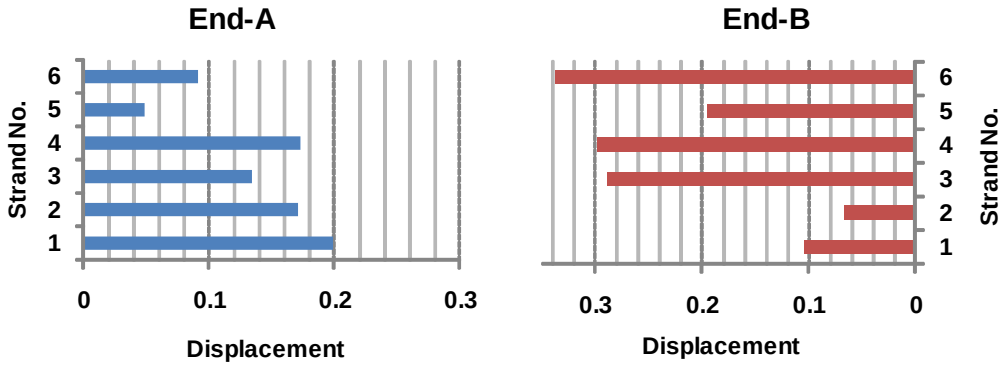

Figure 7.19c: End slip – HESLC girder

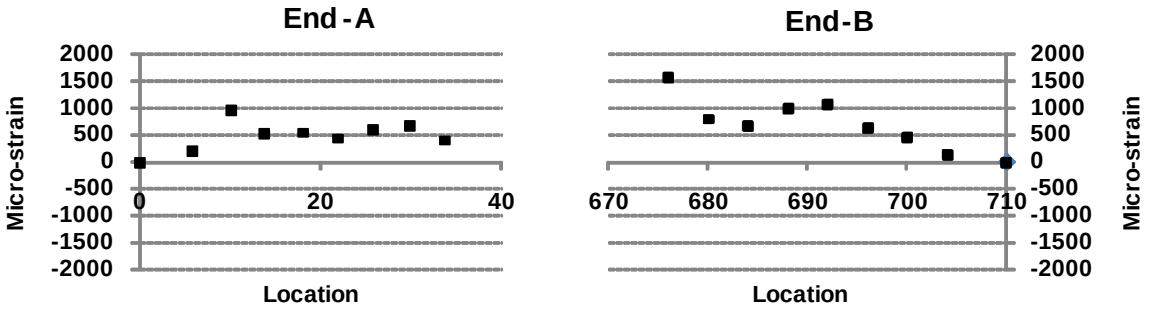

Figure 7.20a: Transfer length – SCLC girder No. 1

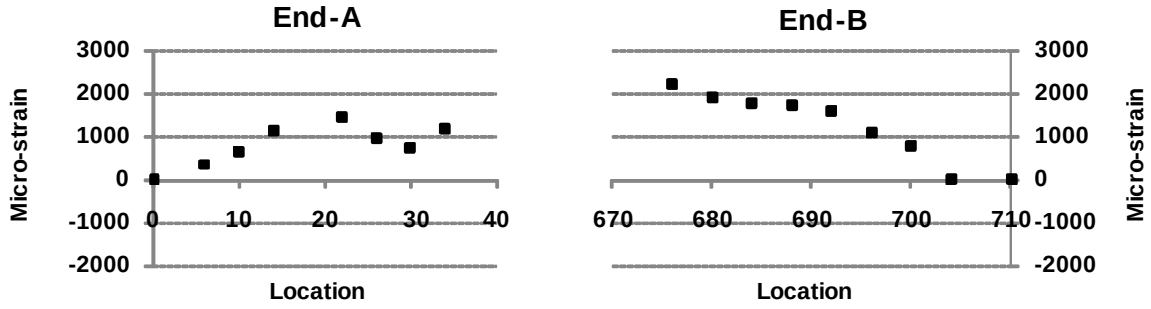

Figure 7.20b: Transfer length – SCLC girder No. 2

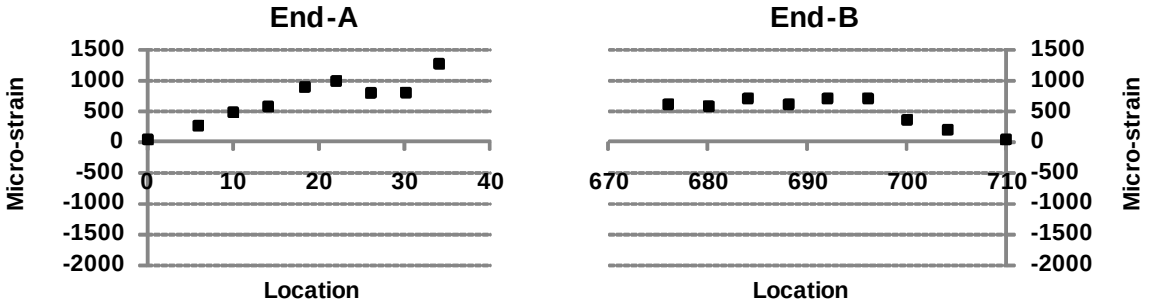

Figure 7.20c: Transfer length – HESLC girder

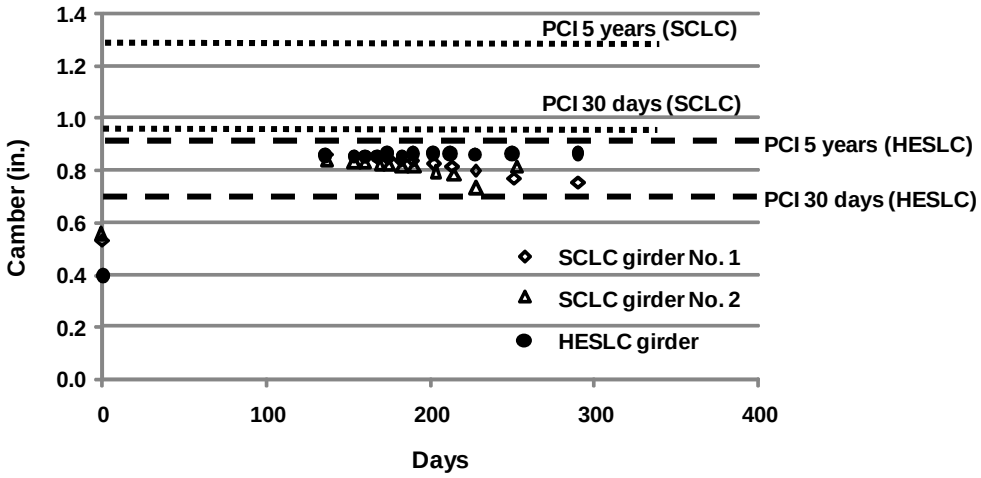

Figure 7.21: Camber – all girders

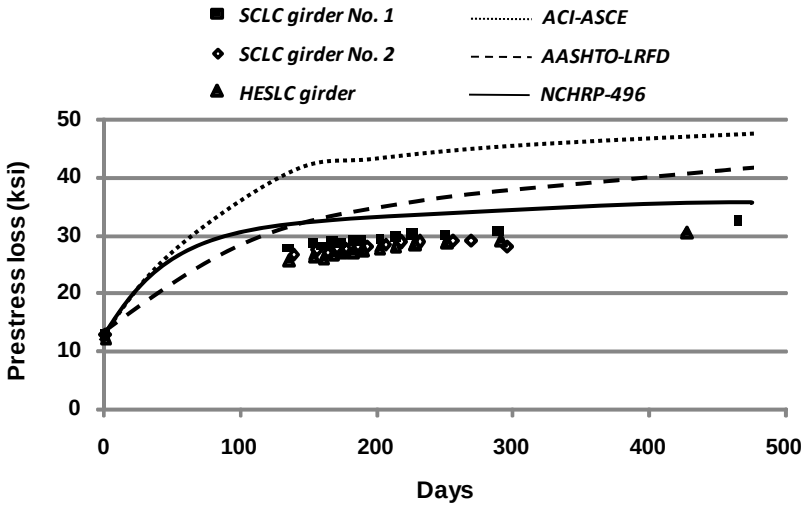

Figure 7.22: Prestress losses – all girders

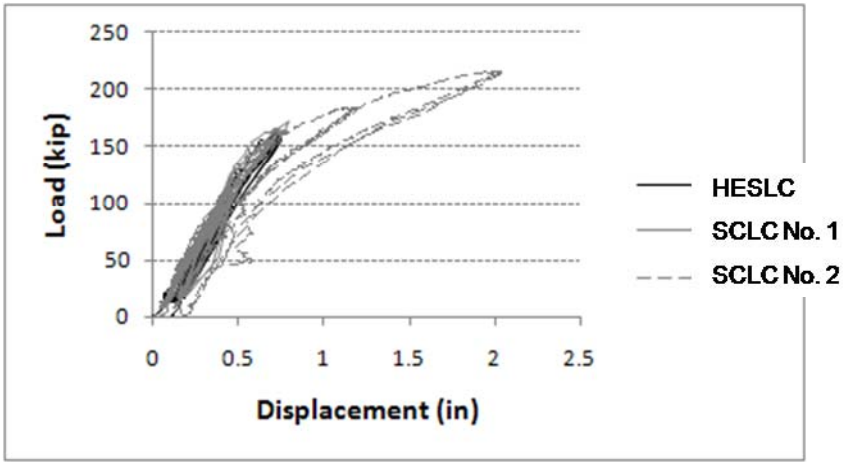

Figure 7.23: CLT method, load vs. displacement (all girders)

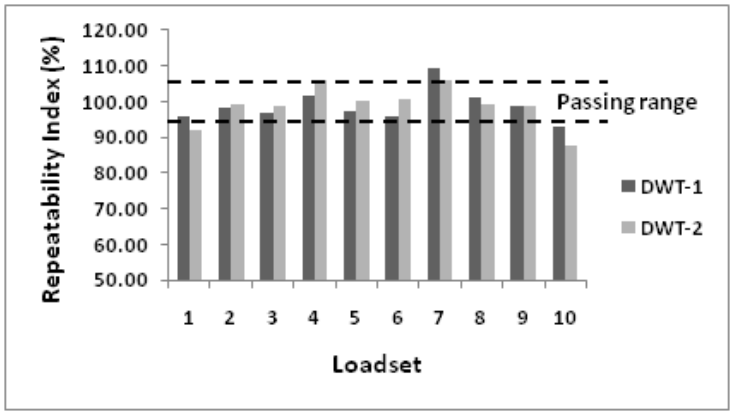

Figure 7.24a: CLT method, repeatability (SCLC girder No. 1)

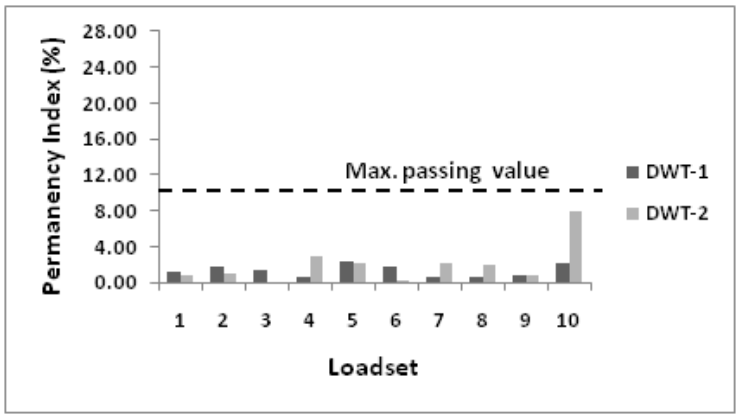

Figure 7.24b: CLT method, permanency (SCLC girder No. 1)

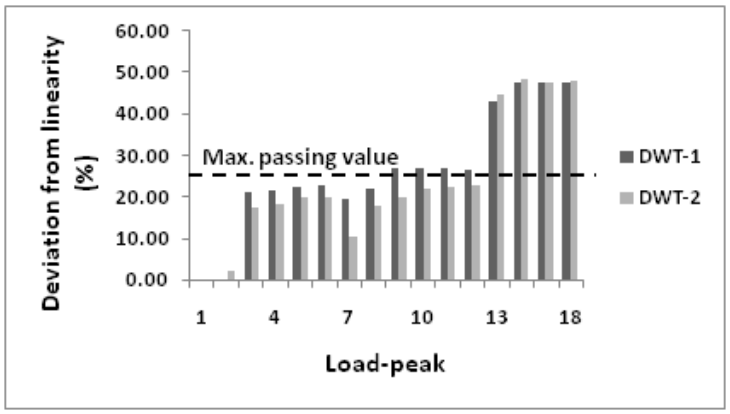

Figure 7.24c: CLT method, deviation from linearity (SCLC girder No. 1)

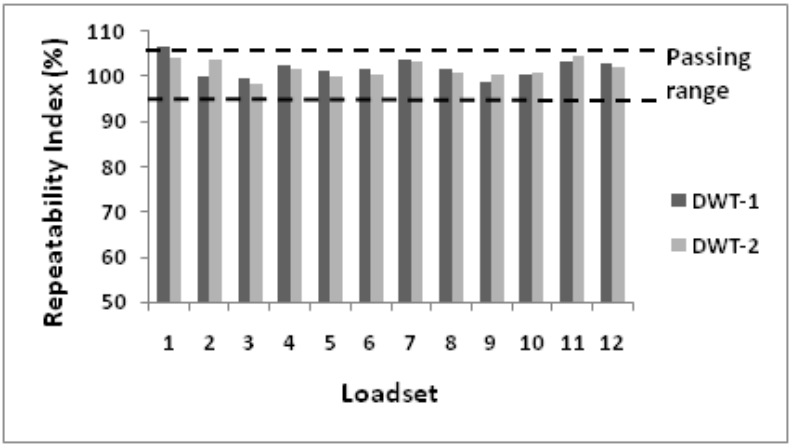

Figure 7.25a: CLT method, repeatability (SCLC girder No. 2)

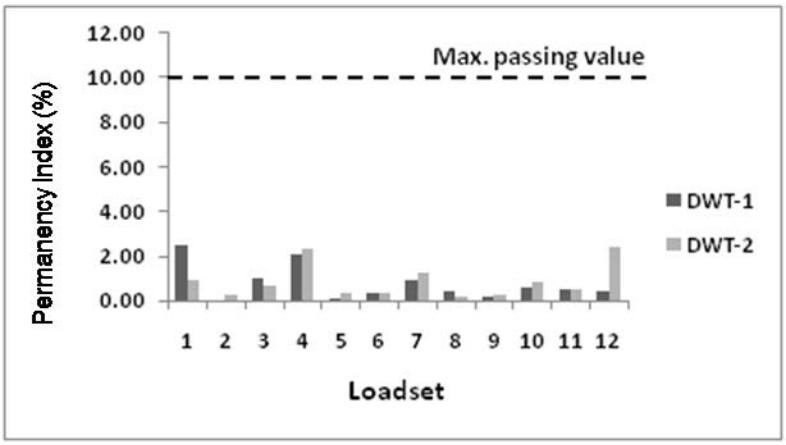

Figure 7.25b: CLT method, permanency (SCLC girder No. 2)

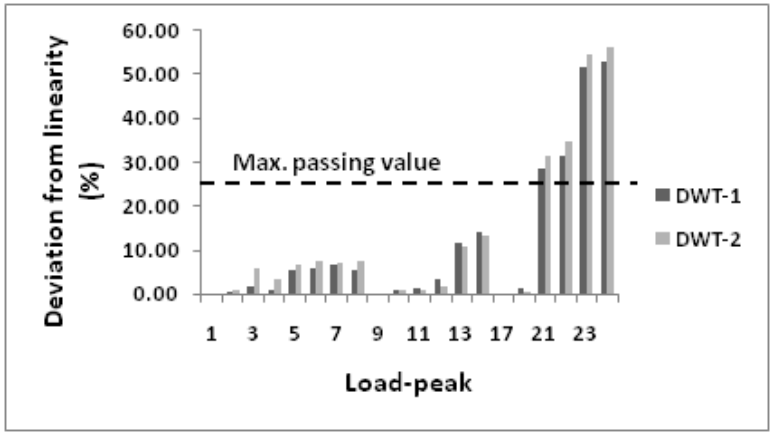

Figure 7.25c: CLT method, deviation from linearity (SCLC girder No. 2)

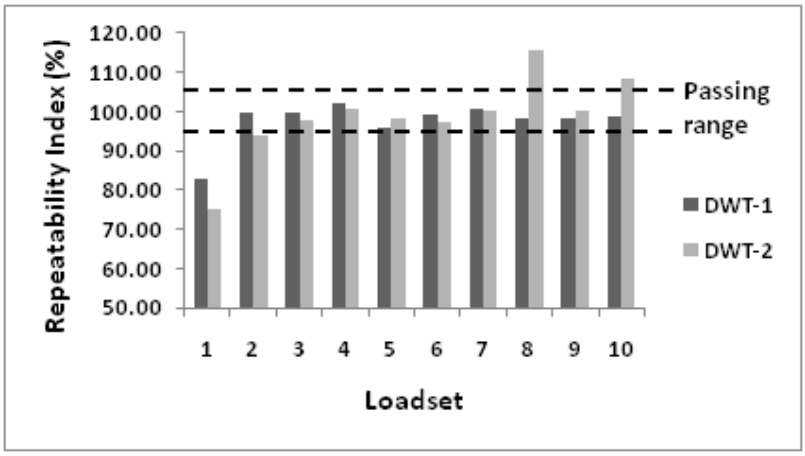

Figure 7.26a: CLT method, repeatability (HESLC girder)

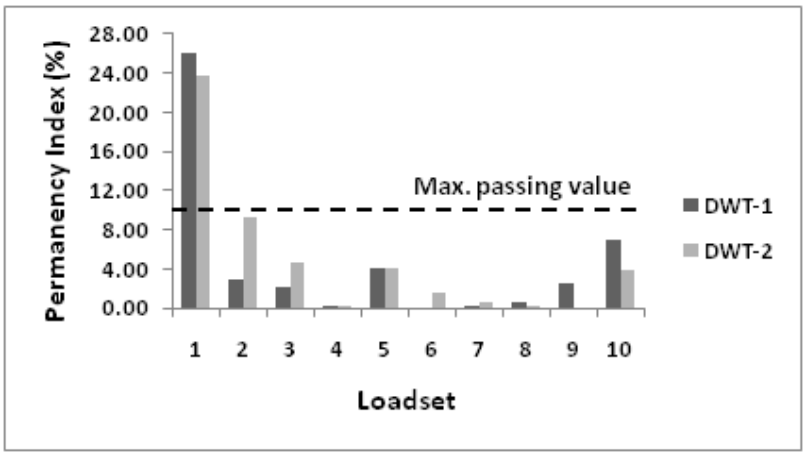

Figure 7.26b: CLT method, permanency (HESLC girder)

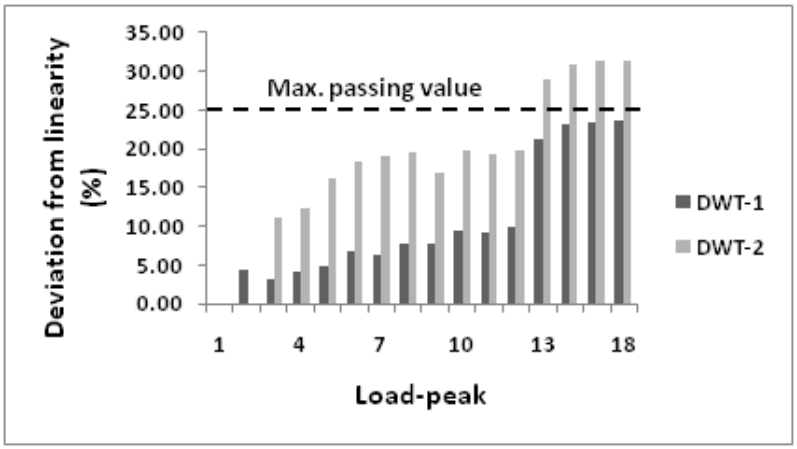

Figure 7.26c: CLT method, deviation from linearity (HESLC girder)

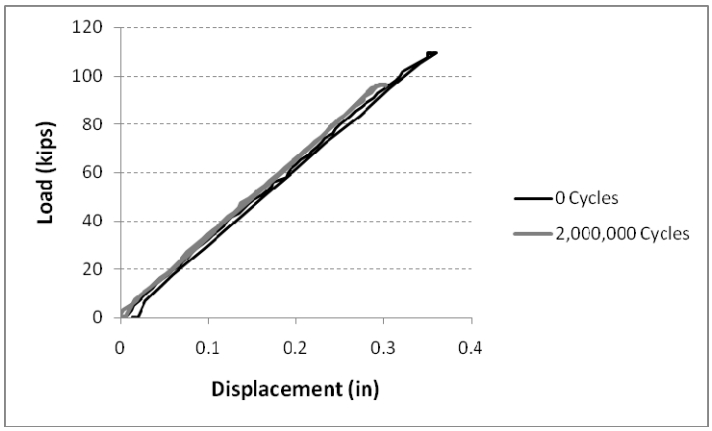

Figure 7.27a: Load versus displacement (SCLC girder No. 2)

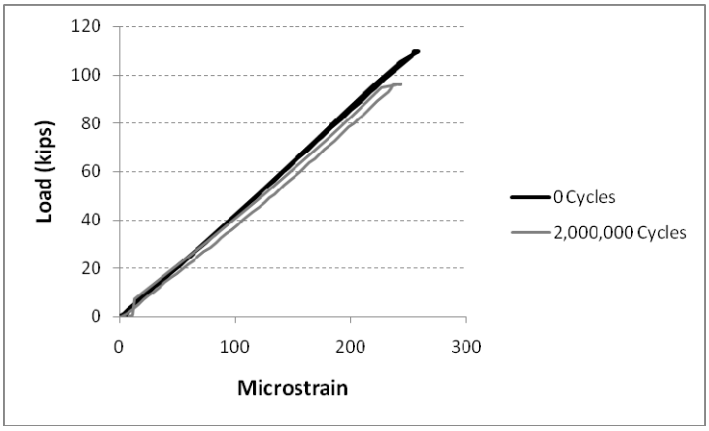

Figure 7.27b: Load versus strain (SCLC girder No. 2)

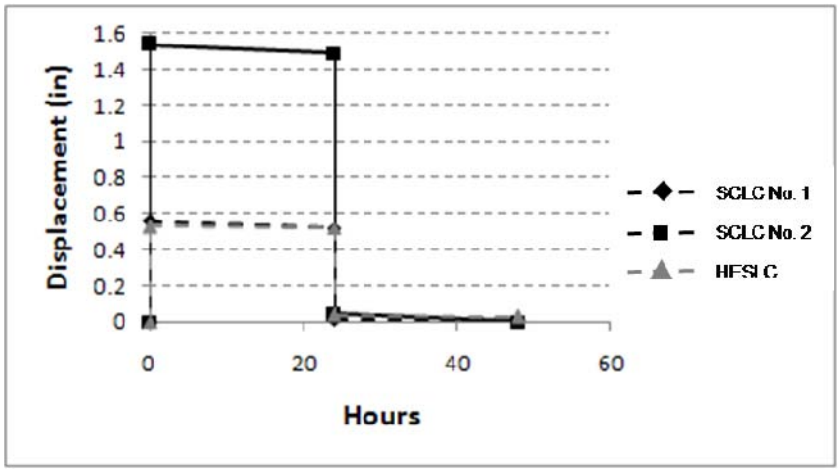

Figure 7.28: 24h load test – displacement vs. time (all girders)

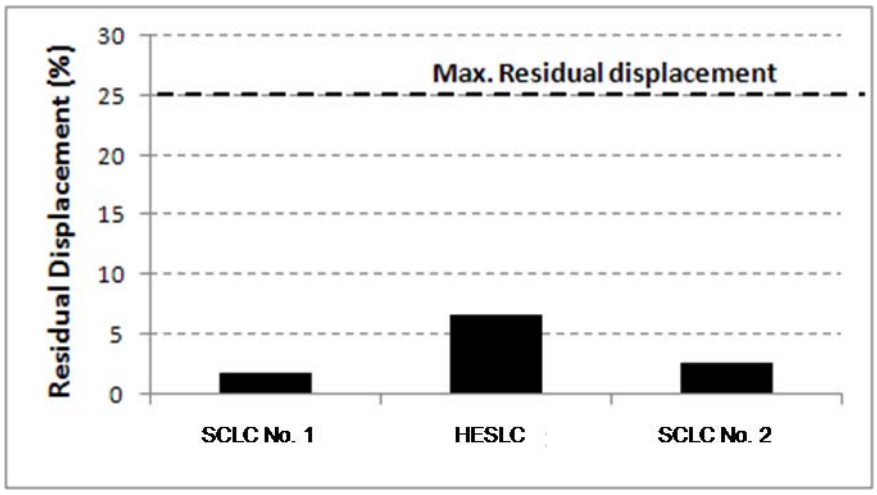

Figure 7.29: 24h load test - evaluation criteria (all girders)

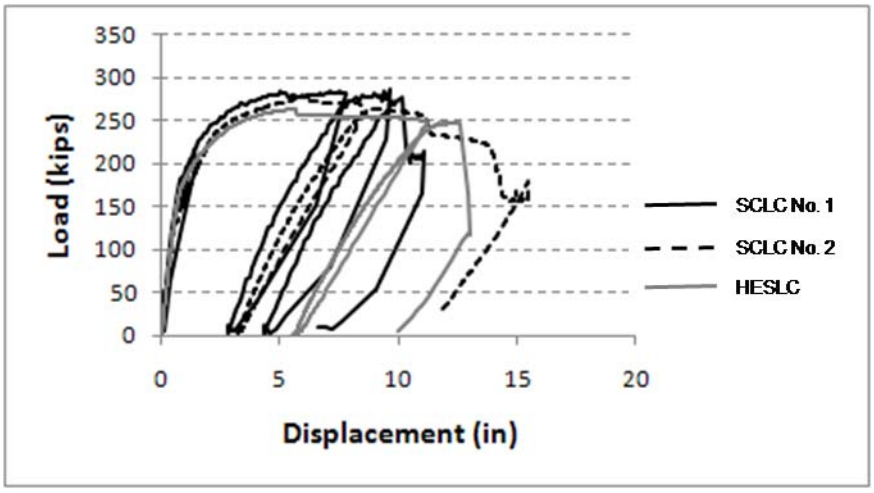

Figure 7.30: Load vs. displacement to failure (all girders)

Figure 7.31a: Failure mode - SCLC girder No. 1

Figure 7.31b: Failure mode - SCLC girder No. 1

Figure 7.32a: Failure mode - HESLC girder

Figure 7.32b: Failure mode - HESLC girder

Figure 7.33a: Failure mode - SCLC girder No. 2 (fatigue girder)

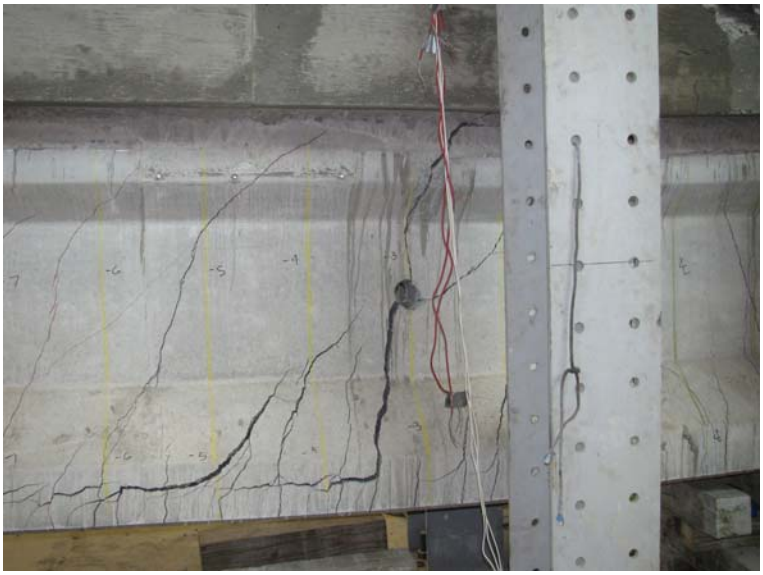

Figure 7.33b: Failure mode - SCLC girder No. 2 (fatigue girder)

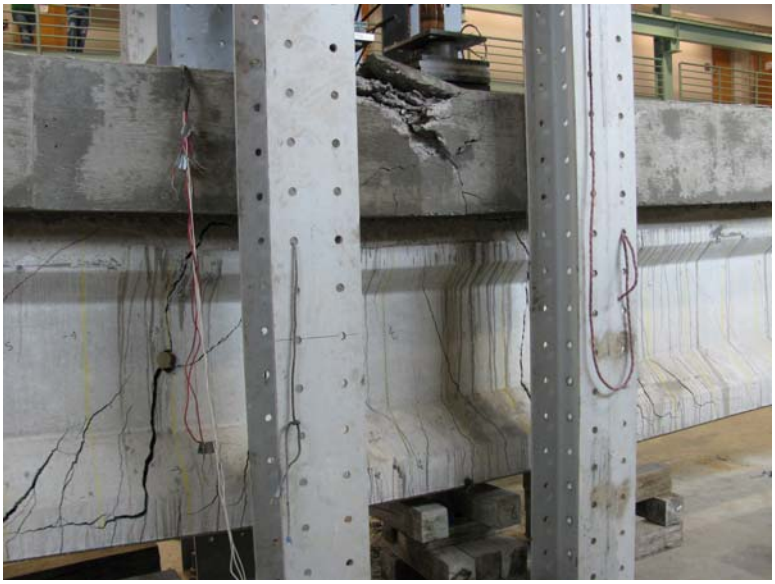

Figure 7.33c: Failure mode - SCLC girder No. 2 (fatigue girder)

Figure 7.33d: Failure Mode - SCLC girder No. 2 (fatigue girder)

Figure 7.33e: Failure mode - SCLC girder No. 2 (fatigue girder)

Figure 7.33f: Demolition - SCLC girder No. 2 (fatigue girder)

Figure 7.33g: Demolition - SCLC girder No. 2 (fatigue girder)

CHAPTER 8
SUMMARY AND CONCLUSIONS

8.1 Introduction

Self-consolidating concrete (SCC) is an alternative to conventional concrete that can reduce labor time, avoid poor consolidation, and add many benefits. As discussed in Chapter 2, SCC employs water-reducing admixtures and super-plasticizers to obtain highly workable concrete that eliminates or minimizes the need for mechanical vibration. The admixtures not only improve the workability of the mixture, but enable a lower water cement ratio leading to higher compressive strengths with reduced permeability. SCLC offers similar benefits while simultaneously reducing dead load of the structure. This is critical for areas where seismic activity is a foremost consideration and for longer spans in general.

The SCC mixes incorporated in this research program were typical of the SCC and SCLC that have been used for prestressed applications and other research in the Southeastern United States. The research effort included investigations into several different mix design approaches, characterization of hardened properties and durability characteristics of laboratory mix designs and those designed by a fabrication facility, and the loading and evaluation of three full-scale AASHTO type III lightweight concrete girders, two SCLC and one HESLC. Of these three girders, one SCLC girder was loaded cyclically to two million cycles prior to failing the specimen.

Items to consider in regard to implementation of both normal weight SCC and SCLC are related to the mix designs, characterization of the fresh and hardened properties of the mix, and differences in behavior of the fabricated girders when compared to HESC and HESLC girders. A recent NCHRP report related to normal weight SCC (NCHRP report 628, 2008) addresses many of the issues below and the findings of the NCHRP report are included in the discussion where appropriate. A summary of results related to the material properties of lightweight concrete for prestressed bridge girders can be found in Russell, 2009 and FHWA, 2007.

8.2 Fresh Properties

SCC in its fresh or “plastic” state exhibits much different characteristics than conventional concrete. Ideally it should be able to flow under its own weight without the need for mechanical vibration, completely fill formwork, and surround any steel reinforcement. The requirement for concrete to be considered an SCC in the plastic state is that it must exhibit adequate filling ability, passing ability, and stability (segregation resistance).

The slump flow for the laboratory test mixes was in the lower end of the design range, but many mixes had acceptable VSI and exhibited adequate passing ability when subjected to the L-Box and U-Box test.

The ability for an SCC to meet the performance criteria relies upon a number of factors including but not limited to coarse to fine aggregate ratio, aggregate gradation characteristics, type and amount of plasticizing agents used, and type and amount of viscosity modifying admixtures. While these factors are synergistic to some degree, it is possible to draw a few general conclusions regarding fresh properties of SCC and SCLC as summarized below:

- Well-graded aggregate is essential in producing a non-segregating workable SCC. Also, maximum aggregate size should be carefully selected depending on rebar and strand spacing. While SCC is sometimes thought of as having only #789 coarse aggregate in fact a blend of coarse aggregate to include #67 stone (or #67 stone alone) can be used. The laboratory mixes made with #67 stone generally demonstrated adequate fresh properties. The incorporation of larger aggregate may be beneficial in some cases for reduced cost and may also be beneficial in regard to creep and shrinkage behavior in some cases.

- The slump flow (spread) for the laboratory SCC test mixes and the SCLC mixes for the full-scale girders was in the lower end of the design range, but mixes had acceptable VSI and exhibited adequate passing ability when subjected to the L-Box and U-Box test.

- Several methods are currently used for assessing the fresh properties of SCC and SCLC, including the spread test, L-box, U-box, J-ring, and the visual stability index. Of these the most easily conducted is the spread test. This test is best used in combination with the visual stability index. For trial mixes, the L-box is well-suited and not difficult to perform. For production purposes, the J-ring test is more easily implemented than either the L-box or U-box tests.

- To attain adequate consolidation, the ideal of using no vibration whatsoever may not be practically achievable in actual field applications. For the case of the full-scale HESLC and SCLC girders, even though both mixes showed adequate fresh properties prior to casting external vibration was necessary in short (less than five second) bursts in order to avoid cold joints and voids. At the ends of the girder specimens, it was in some cases necessary to introduce conventional vibration in short (less than five second) bursts to preclude voids. While this is not ideal, some compromise away from the ideal of no vibration may be necessary to keep costs under control.

8.3 Hardened Properties

Engineers are often more concerned with the hardened properties such as strength and durability than they are with the fresh behavior of the mix. SCC and conventional mixes usually differ in fine/coarse aggregate ratios, water/cementitious ratios, aggregate sizes, and amount of chemical admixtures. These differences can have major effects on the strength and durability of the mix. For instance, many times self-consolidation is achieved by the use of super-plasticizers which allows for a reduced water/cementitious

material ratio, and thus, higher strength. On the other hand, because of the increased fines in SCC mixes, it is suspected that higher drying shrinkage and creep may occur in SCC than conventional concrete.

The mechanical properties of main interest are generally the compressive strength, f'_c, and the modulus of elasticity, E_c. Other properties such as tensile strength, shear strength, and bond strength are typically expressed in terms of the compressive strength (PCI, 1997). Results related to hardened properties are summarized below:

- ***Cement content:*** About 800 lbs/yd^3 of cementitious material was used in the SCC mixes developed at the University of South Carolina. SCC mixes commonly contain anywhere from about 600-900 lb/yd^3 of cementitious material since higher strengths are often needed for prestressed applications. For the HESC and SCLC mixes the cement content was 850 lb/yd^3 and the 28-day design strength was not obtained. A suggested mix provided by the producer indicated cement content of 950 lb/yd^3.

- ***Curing conditions:*** Curing conditions are critical for early strength development. All laboratory specimens were cured at elevated curing temperatures of about 105 - 110° F. This was to simulate internal curing temperatures of the AASHTO Type III Bridge girders.

- ***Compressive strength:*** The compressive strength for laboratory Batch No. 1 exceeded the design release strength of 6,400 psi at 3 days. Batch No. 3 exceeded the design release strength after 1 day. On average for these mixes, 72 % of the 28-day compressive strength was achieved in the first 32 hours after mixing. On the basis of compressive strength, Batch Nos. 1 and 3 met the FHWA HPC performance grade 2, while Batch No. 2 met HPC performance grade 1. With the correct air content and mix designs, SCC can gain adequate strength in the time required for prestressed applications and early strand releases.

  The HESC and SCLC mixes corresponding to the full-scale girders did not meet the 28 day design strengths but did qualify as FHWA HPC performance grade 1. These mixes had design unit weight in the range of 115 – 120 pcf. A revised mix design has been submitted for consideration with design unit weight in the range of 125 – 130 pcf and increased cement content.

- ***Modulus of elasticity*** values for the laboratory SCC test cylinders were lower than the corresponding predictions given by the AASHTO LRFD, NCHRP 496, and ACI 363 equations. The ACI 363 equations provided the best fit to the data. Batch Nos. 1 – 3 met the criteria for FHWA HPC performance grade 1. Data from a parallel research project on normal weight SCC was used to supplement the data from the laboratory mixes. The results were similar to the laboratory mixes in that the modulus was over-predicted by the commonly

used equations. When comparing similar SCC to HESC mixes there was no significant difference in measured modulus values.

Modulus of elasticity of the companion cylinders that were cast alongside the lightweight AASHTO Type III girders were essentially the same for the HESLC and SCLC girders. It is postulated that lightweight concrete modulus will be less affected by SCC because the modulus of the aggregate is closer to that of the paste for lightweight mixes. Therefore, the coarse/fine aggregate ratio is not expected to have as significant an effect on modulus as for normal weight concretes. The AASHTO LRFD predictive equations provided a relatively good fit to the measured data for the lightweight mixes. The NCHRP method is not intended for lightweight concretes and significantly over-predicted the modulus due to the relationship between strength and unit weight with this method. The lightweight mixes did not meet the FHWA HPC performance criteria for modulus.

NCHRP 628 mentions in the commentary that a reduction in modulus of up to 20 % may occur for SCC mixes in comparison to conventional high performance concrete. This is mainly attributed to lower coarse aggregate volume, increase in paste content, and higher content of ultra-fine materials. However, NCHRP 628 does not recommend a reduction factor for the prediction of modulus according to the AASHTO LRFD, 4th Edition.

- ***Tensile strength:*** The tensile strength of the companion cylinders that were cast alongside the lightweight AASHTO Type III girders indicated that SCLC had slightly higher tensile strength than the corresponding HESLC mix. The predictive equation given in the AASHTO LRFD, 4th Edition over-predicted tensile strength. Predictive equations as described in an FHWA synthesis report (FHWA, 2007: FHWA-HRT-07-053) provided a better fit to the data.

- ***Shrinkage:*** The shrinkage data for Batch Nos. 1 – 3 was in the range of 400 to 600 $\mu\varepsilon$. The AASHTO predictions marginally under-predicted the shrinkage strain but the estimate was reasonable. Data from a parallel research project related to SCC also indicated that shrinkage was within the range of 400 to 600 $\mu\varepsilon$. The SCC mixes qualified as FHWA HPC performance grade 3.

  NCHRP 628 recommends that the AASHTO LRFD, 4th Edition modified equation for shrinkage be multiplied by a factor of 0.918 for SCC with Type I/II cement and 1.065 for SCC with Type III cement + 20 % fly ash binder.

- ***Creep:*** Two of the laboratory mixes, Batch Nos. 1 and 2, were tested for creep. Creep was also measured for SCC and HESC specimens from the parallel research project related to normal weight SCC girders. The AASHTO equations under-predicted the creep for the SCC mixes. This was the most

significant for Batch No. 1 and the SCC plant mix. The HESC specimen had lower creep values than predicted with the AASHTO equation.

Batch No. 1, Batch No. 2 and the SCC mix from the producer had normalized creep values of 0.40, 0.38, and 0.45, respectively, and qualified as FHWA HPC performance grade 1. The HESC mix had significantly lower normalized creep of 0.19 and qualified as FHWA HPC performance grade 3.

NCHRP 628 recommends that the AASHTO LRFD, 4th Edition equation for prediction of creep be multiplied by a factor of 1.19 for SCC with Type I/II cement and 1.35 for SCC with Type III cement + 20% fly ash binder.

- ***Freeze-thaw:*** Freeze-thaw testing was conducted on Batch Nos. 1 – 3. For Batch Nos. 1 and 3, the dynamic modulus reduced to below 60 % of its original value in less than 125 cycles. Based on this data the mixes did not meet the FHWA HPC performance criteria.

  Large cracks were seen on the top faces of the concrete specimens. The air content of Batches 1 and 3 was approximately 3.5 % by volume for both mixes. While the air content is one important aspect for freeze-thaw durability the content alone may not be as important as the air void distribution.

  Results of freeze-thaw durability testing of specimens from a parallel research program related to normal weight SCC (and HESC) also failed to meet the FHWA HPC performance criteria.

  NCHRP 628 mentions that higher air content (6 – 9 %) may be necessary for more severe frost environments and the possibility of coalescence of small air bubbles, especially when polycarboxylate-based super-plasticizers are used. It also mentions that dosages of AEA in SCC with polycarboxylate-based super-plasticizers can be quite low compared to conventional concrete. This was noticed in most of the laboratory mixes, and in some cases high air content was achieved without the addition of AEA. NCHRP report 628 recommends the use of AEA to stabilize small, closely spaced, well-distributed voids. The AEA should be compatible with the super-plasticizers and other chemical admixtures. ASTM C 457 can be used for assessment of air void parameters in addition to ASTM C 666, procedure A for freeze-thaw.

- ***Rapid Chloride Permeability***: Rapid chloride permeability testing was conducted on Batch Nos. 1 - 3. Batch Nos. 1 and 3 had moderate chloride permeation ranging from 2,000 - 4,000 coulombs passed, while Batch No. 2 had high chloride permeation passing 4,323 coulombs. Both the SCLC and HESLC specimens showed high chloride permeation of greater than 4,000 coulombs.

Batch No. 3 met the criteria for FHWA performance grade 1. However, Batch Nos. 1 and 2 and the lightweight mixes (SCLC and HESLC) did not meet the FHWA performance criteria for HPC.

8.3 Full-scale Girders

Three full scale AASHTO Type III lightweight girders were cast at Florence Concrete Products in Sumter, South Carolina. Properties were measured before, during and after casting of the girders. The girders were delivered to the structures laboratory at the University of South Carolina and then tested to failure. Two of the girders were tested statically (SCLC girder No. 1 and the HESLC girder) and the third girder (SCLC girder No. 2) was cyclically loaded to two million cycles and then loaded to failure. The cyclic load test and 24 hour load test methods were used for evaluation along with investigation of the load vs. displacement behavior at ultimate. The results of the full-scale testing program are summarized below.

- ***Curing Temperature:*** When comparing to data recorded from a normal weight SCC mixture with the same design strength used in a parallel project, temperature values were found to reach higher levels for the SCLC girders. However, the normal weight SCC mixtures experienced a faster curing process since the peak of exothermal reactions occurred earlier in the process. The curing temperature for the SCLC girders was relatively high.

- ***End-slip***: The end-slip values were smaller in the SCLC girders compared to the HESLC girder.

- ***Transfer Length:*** Results indicated values between 14 in and 18 in (356 and 457 mm) for the HESLC girder and 16 in and 22 in (406 and 560 mm) for the SCLC girders. The maximum value registered in all girders in terms of the strand diameter is $44d_b$ which is less than the $50d_b$ value recommended by the AASHTO standard and the $60d_b$ recommended by the AASHTO LRFD. Based on these results either specification can be used to estimate the transfer length required for SCLC and HESLC prestressed bridge girders.

  NCHRP 628 also reports over-prediction of transfer length for SCC girders [AASHTO Type II, 29 ft (8.8 m) span].

- ***Camber:*** Camber was recorded immediately after release and continuously monitored upon arrival of the specimens at the University of South Carolina structures laboratory. The HESLC girder had smaller initial camber but exhibited similar long-term camber values to the two SCLC girders. Long-term camber growth was therefore less for the SCLC girders. The HESLC girder approached the predicted long-term value (PCI multiplier method) while the SCLC girders did not approach the predicted long-term value.

NCHRP 628 reported smaller cambers for SCC girders when compared to girders fabricated with conventional concrete of similar strength. This was attributed to lower elastic modulus and greater drying shrinkage for the SCC girders, leading to greater long-term loss of prestress.

- ***Prestress losses:*** Total prestress losses converged to an approximate value of 30 ksi (206 MPa) at 300 days for all specimens. Predicted losses were generally over-predicted. The NCHRP 496 method provided the closest match with 34 ksi (234 MPa) at 300 days.

- ***Cyclic Load Test***: For the first two specimens (SCLC girder No. 1 and the HESLC girder) all evaluation criteria were met below 125 % of the theoretical maximum test load, and even at this load level the girders failed only one of three criteria (deviation from linearity). As a consequence, two additional loadsets at 150 % and 175 % of the theoretical maximum test load were included in the CLT loading profile for the fatigue specimen (SCLC girder No. 2). Additionally, fatigue cycling for two million cycles was applied prior to the CLT loading of this specimen. Subsequent observation of the structural performance of the SCLC girder No. 2 girder (during CLT as well as failure) suggested no evidence of considerable stiffness degradation caused by fatigue cycling.

- ***24 Hour Load Testing:*** A 24h load test was performed on each of the girders following the cyclic load test (CLT). Following the same approach taken for the CLT method, the maximum load level for the 24h load test was increased to 150 % of the maximum test load. Despite the considerable increase in the applied load and the significant amount of cracking present in SCLC girder No. 2, this girder still passed the evaluation criteria with less than 5 % of $\boldsymbol{\Delta}_{max}$ as residual deflection.

- ***Load versus displacement behavior to failure:*** This data indicates that all specimens had a similar initial stiffness and ultimate capacity. All girders behaved similarly during reloading stages on the load versus deflection curves. Additionally, all specimens were able to attain significant midspan deflection [$\boldsymbol{\Delta} > 10$ in. (254 mm)] prior to collapse.

  The ultimate capacity of the girders was marginally over-predicted for both the HESLC girder (approximately 10 %) and the SCLC girders (approximately 5 %). This may be attributable to the failure mode which consisted of longitudinal splitting along the bottom flange at the level of the prestressing strand.

  NCHRP 628 reported higher ductility for HPC girders in relation to SCC girders. Predicted capacities of SCC girders according to AASHTO LRFD, 4th Edition, were within 1.5 % of measured values. An FHWA report related

to lightweight concrete girders (FHWA, 2003) documents under-prediction of flexural capacity for lightweight AASHTO Type II girders.

- ***Failure modes:*** The failure modes for all three girders were similar. Failure was in all cases initiated by yielding of the strands followed by propagation of nearly vertical cracks near midspan. Once the cracks reached the deck, significant crushing of the concrete deck appeared simultaneously with horizontal splitting cracks close to the bottom of the girder and following the prestressing strands.

CHAPTER 9
RECOMMENDATIONS AND GUIDELINES

9.1 Introduction

Based on the results of the literature review and the results and conclusions of this project, guidelines have been developed for the acceptance of the materials (both SCC and SCLC) as a recommendation to the South Carolina Department of Transportation for adoption into the State's Standard Specifications (SCDOT, 2006).

North Carolina and Georgia have developed their own specifications for SCC. As a general statement the North Carolina approach is more performance based while the Georgia approach is more prescriptive. The recommended guidelines suggested for South Carolina are more performance based than prescriptive. This approach is taken due to the very significant variation in how SCC can be achieved. A performance based approach in general allows the producer greater flexibility to deal with changing market conditions, such as the availability of fine and coarse aggregate and changes in admixture suppliers. However, a performance based approach results in the need for more testing to assure that the necessary quality is consistently achieved.

9.2 Guidelines

The guidelines below apply to normal weight Self-Consolidating Concrete (SCC) and Self-Consolidating Lightweight Concrete (SCLC) for prestressed concrete bridge girders. Guidelines that are appropriate for only SCC or SCLC are noted.

Definition: Self-consolidating concrete is concrete designed to flow under its own weight, maintain homogeneity and completely fill the formwork, even in the presence of dense reinforcement.

Vibration: While it is not desirable, it may be necessary in some cases for SCC to be form vibrated. This need should be an exception and form vibration should be used sparingly. If external vibration is used, it should only be used in short bursts of less than 5 seconds in duration. Internal vibration of self-consolidating concrete is not recommended.

Placement: Self-Consolidating Concrete (SCC) should be placed as noted on the plans or with the permission of the Engineer.

Materials:

- Cement – For SCC a minimum of 650 lbs. per cubic yard and a maximum of 850 lbs. per cubic yard is recommended. For SCLC and HESLC increased cement content (up to 950 lbs. per cubic yard) may be required to achieve design strength.

- Pozzolan – With permission of the Engineer, a pozzolan such as fly ash, ground granulated blast furnace slag, silica fume, limestone powder, or metakaolin may be substituted for a portion of the cement.

- Coarse and fine aggregate – A fine aggregate content of 40 % to 60 % of the combined coarse and fine aggregate weight is recommended.

- Water – A quantity of water that produces a water-cementitious material ratio no greater than 0.40 and in accordance with other provisions of the standard specification for prestressed concrete is recommended.

- Admixtures – Viscosity modifier admixtures are allowed as a way to enhance the homogeneity and flow of the mix.

Proposed mix designs should be submitted for evaluation. Supporting data from trial batches conducted by an approved testing laboratory should be provided to aid in this process. The following test methods and criteria are recommended for the trial mix designs:

Trial batches (Fresh Properties):

- Slump flow (ASTM C 1611) – Slump flow should be within the range of 24 inches to 30 inches spread. Slump flow should be used in combination with the Visual Stability Index.

- L-Box test – Refer to PCI guidelines for design of the L-box and conducting the test. The ratio of H2 to H1 should be within the range of 0.8 to 1.0.

- J-Ring test (ASTM C 1621) – The difference in spread between tests with and without the ring should not exceed 2 inches.

- Air content (ASTM C 231) – Test the air content of the plastic concrete. Air content should be in the range for conventional concrete for prestressed concrete girders (0 – 4.5 %).

Trial batches (Hardened Properties):

The following tests are highly recommended:

- Compressive strength (ASTM C 39) – It is recommended that 28-day compressive strength be greater than 6,000 psi (41.3 MPa). Compressive strength of concrete cylinders should be reported at 3, 7, 14, 28 and 56 days. The strength should meet the requirements of the project. The cylinder molds should be filled in one layer with no rodding, vibration or other consolidation. Cylinders should be cured in similar curing conditions to those encountered for production. 4 x 8 in. (102 x 204 mm) cylinders are recommended.

- Modulus of elasticity (ASTM C 469) – It is recommended that the 56-day modulus of elasticity be greater than 4,000 ksi (27.6 MPa). The modulus of concrete specimens should be reported at 3, 28, and 56 days. Cylinders should be cured in similar curing conditions to those encountered for production. 6 x 12 in. (152 x 304 mm) cylinders are recommended.

The following tests are recommended. These tests may be waived in the event that past positive performance can be demonstrated for similar mix designs.

- Creep (ASTM C 512) – It is recommended that the normalized creep at 300 days be less than 0.52. Creep of concrete specimens should be reported over a period of 300 days. To expedite decision making and in the absence of a more exact analysis, the 100 day value of normalized creep can be assumed to have reached 80 % of the 300 day value.

  Cylinders should be cured alongside the girders and in similar curing conditions. For concrete strengths above 10,000 psi (69.0 MPa) at 28 days it is recommended that the cylinders be match cured. 6 x 12 in. (152 x 304 mm) cylinders are recommended. The effect of shrinkage should be separated from creep experimentally through the use of companion specimens of the same size and storage conditions.

- Shrinkage (ASTM C 157) - It is recommended that shrinkage be less than 0.04 % at 28 days. Steel molds should be used and the SCC should not be rodded, vibrated or otherwise consolidated. It is important that the specimens be handled and cured in accordance with the ASTM specification. Length change of each specimen should be recorded to the nearest 0.001 % of the effective gage length at 3, 7, 14, 28, and 56 days.

- Rapid Chloride Permeability (ASTM C 1202) – It is recommended that chloride permeability at 56 days not exceed 3,000 coulombs. Cylinders should be cured alongside the girders and in similar curing conditions. For concrete strengths above 10,000 psi at 28 days it is recommended that the cylinders be match cured. 4 x 8 in. (102 x 204 mm) cylinders are recommended.

- Freeze-thaw (ASTM C 666) – It is recommended that the relative dynamic modulus be greater than 60 % after 300 cycles. Specimens should be cured in similar curing conditions to those encountered for production. If freeze-thaw criteria are not met, ASTM C 457 (determination of air void parameters) can be used to provide insight into the air void distribution.

- Tensile Strength (lightweight concrete only) (ASTM C 496/C 496M) – For lightweight concretes (both SCLC and HESLC) it is recommended that the 56 day tensile strength exceed 390 psi (2.69 MPa). Specimens should be cured and stored according to ASTM specifications.

Mock-up Specimen:

Before beginning production, it is recommended that the producer demonstrate competence in using SCC by casting a mock item of like or similar design in the presence of the Engineer. A mock item or production item being cast for another state or agency could be substituted. The recommendation for a mock-up specimen does not apply to the case of a producer having substantial previous experience including successful mock-up specimens.

Production (General):

It is recommended that a representative of the admixture supplier be present during casting of the demonstration item and all production items. After production begins, this recommendation may be waived.

It is recommended that self-consolidating concrete remain plastic and within the specified range of slump flow during placement. Concrete delivery shall be timed such that consecutive lifts will combine completely without creating segregation, visible pour lines or cold joints. No more than 20 minutes should elapse between placements of consecutive lifts.

Concrete should be placed from one point and be allowed to flow outward, or pumped from the bottom upward so as not to encapsulate air. Opposing flow of concrete should be avoided.

The distance of horizontal flow should not exceed 30 feet and the vertical free fall distance should not exceed 10 feet.

Production (Fresh Properties):

The following field tests are recommended on the plastic concrete using the standards and modifications listed above and the sampling rates listed:

- Slump flow (ASTM C1611 / C1611M) – The slump flow should range between 22 and 30 inches spread. Test the first batch and whenever cylinders are made. Test each 10 cubic yards after the first batch. Whenever testing occurs, retest if the initial test fails. The visual stability index should be equal to 1 or better.

- J-Ring test – Follow the "Interim Guidelines for the Use of Self-Consolidating Concrete in Precast/Prestressed Concrete Institute Member Plants (TR-6-03)" published by PCI. The difference in spread between tests with and without the ring should not exceed 2 inches.

- Air Content (ASTM C 231) – Test the first batch and whenever cylinders are made. Test each 10 cubic yards after the first batch. When testing occurs, retest if

the initial test fails. The air content requirements should be the same as those required for conventional prestressed girders (range of 0 to 4.5 %).

- Concrete temperature – As stated in the standard specifications.

Production (Hardened Properties):

- Compressive strength (ASTM C 39) – It is recommended that the compressive strength of concrete cylinders be reported for 3, 7, 28 and 56 days. The strength should meet the requirements shown on the plans or in the Standard Specifications. The cylinder molds should be filled in one layer with no rodding or vibration of the sample. Cylinders should be cured alongside the girders and in similar curing conditions. For concrete strengths above 10,000 psi at 28 days it is recommended that the cylinders be match cured. 4 x 8 in. (102 x 203 mm) cylinders are recommended. It is recommended that cylinders be made and tested at the same rate as for conventional prestressed girder applications.

9.3 Design Considerations

There are a significant number of different approaches for the development of SCC and SCLC. In general it can be stated that most SCC mix designs rely upon well-graded aggregates and an increased fine to coarse aggregate ratio when compared to conventional concretes. Because the coarse aggregate is generally of higher modulus and is less susceptible to creep and shrinkage than the paste, increased fine to coarse aggregate ratios have the general effect of decreasing modulus and increasing creep and shrinkage. Creep appears to be more significantly affected than shrinkage. As a general statement, the modulus can be expected to be marginally reduced (approximately 5 to 10 %) for like SCC mixes. For predictions of creep and shrinkage of SCC it is recommended that the NCHRP 496, 595 and 628 equations for high strength concrete be considered for 28 day concrete strengths in excess of 6,000 psi.

Because lightweight concrete relies upon coarse aggregates of reduced modulus, changes to the fine to coarse aggregate ratio for lightweight concretes are not expected to result in the same magnitude of changes in the modulus and creep. Shrinkage, however, may be similarly affected.

While modulus, creep and shrinkage are known to affect camber the results of the girders measured in the laboratory did not show significant differences between the SCLC and HESLC girders. It is possible that camber is less affected by differences between conventional and SCC for lightweight compared to normal weight girders due to the reasons mentioned above. Prestress losses were also similar for all three girders.

In terms of the ultimate strength and fatigue performance of the full-scale girders, there appeared to be no significant differences between SCLC and HESLC girders used in this testing program. The stiffness of the SCLC girder tested in fatigue did not significantly decrease after two million cycles. Therefore, the fatigue considerations for SCLC girders

may be similar to those for HESLC girders. It is important to note that the fatigue testing performed was limited to a single specimen.

Specific recommendations for consideration in design are given below. These recommendations are intended for use until additional information related to SCC, HESLC and SCLC becomes available. Additional information will become available as more literature related to these materials is released and as trial batches are submitted. Recommendations should then be modified accordingly. Where deviations from standard practice are recommended these are generally based on differences in measured behavior from specimens of similar type (such as SCC compared to HESC) as described in this report.

- Creep – It is recommended that creep values as predicted by standard practice (AASHTO LRFD, 4th edition) be increased by 20 % for SCC (normal weight only). If fly ash is used as a supplementary cementitious material, it is recommended that creep values as predicted by standard practice be increased by 25 %.

  It is noted that creep can be minimized through later loading (later strand release), increasing the amount of coarse aggregate, and increasing the modulus of the coarse aggregate.

  Where creep is a critical design consideration close monitoring of the results of the trial batches is recommended. In such cases it is also recommended that the values described in NCHRP 628 be consulted.

  The recommendations above do not apply to SCLC or HESLC. Actual field projects (Davis, 2009) have shown that creep for structural lightweight concrete is not substantially increased relative to normal weight concrete. The modulus of lightweight coarse aggregates is generally reduced in comparison to that of normal weight aggregates. Therefore, significantly increased creep due to increased fines is not necessarily expected for SCLC. Due to the novelty of the material, close attention to the results of the trial batches is recommended for creep of SCLC and HESLC.

- Tensile strength – It is recommended that the following equation be used for the prediction of splitting tensile strength for lightweight concrete (both SCLC and HESLC):

$$f_{ct} = 0.16\sqrt{f'_c} \qquad \text{(eqn. 9.1)}$$

  The equation above represents a deviation from standard practice, where a value of 0.23 (multiplied by 0.85 for sand-lightweight concrete) is used in place of 0.16.

The recommendation above does not apply to SCC or HESC. Where splitting tensile strength is a critical design parameter close monitoring of the results of the trial batches is recommended.

- Modulus of elasticity – No deviation from standard practice (AASHTO LRFD, 4th Edition) is recommended for the prediction of modulus of elasticity of SCC concretes (applies to both SCC and SCLC).

  It is noted that for normal weight concretes the AASHTO LRFD, 4th Edition, significantly over-predicted the modulus of elasticity. This was true regardless of whether the concrete was SCC or conventional HESC. For lightweight concretes (both SCLC and HESLC) this equation provided a fairly good fit to the measured data. The ACI 363 equations also provided a fairly good fit to the measured data.

  It is also noted that other studies have mentioned reduced modulus for SCC and that this has some physical basis due to increased fine aggregate content. NCHRP 628 mentions that reductions in modulus up to 20 % are possible but does not recommend a reduction factor on modulus. Where modulus is a critical design parameter close monitoring of the results of the trial batches is recommended.

- Shrinkage – No deviation from standard practice (AASHTO LRFD, 4th Edition) is recommended for the prediction of shrinkage for SCC concretes (applies to both SCC and SCLC).

  Actual field projects (Davis, 2009) have shown that shrinkage for structural lightweight concrete is not substantially increased relative to normal weight concrete. Due to the novelty of the materials, close attention to the results of the trial batches is suggested for shrinkage of SCC, SCLC and HESLC.

  It is noted that NCHRP 628 recommends modifiers for shrinkage prediction of SCC. In cases where shrinkage is a critical design parameter close monitoring of the results of the trial batches is recommended.

- Transfer length - No deviation from standard practice (AASHTO LRFD, 4th Edition) is recommended for the prediction of transfer length for SCLC or HESLC girders.

  SCC and HESC girders were not a part of this project and therefore the recommendations above are restricted to SCLC and HESLC girders. NCHRP 628 addresses SCC girders and does not recommend deviations from standard practice for transfer length.

- Prestress losses - No deviation from standard practice (AASHTO LRFD, 4th Edition) is recommended for the prediction of prestress losses for SCLC or HESLC girders.

SCC and HESC girders were not a part of this project and therefore the recommendations above are restricted to SCLC and HESLC girders. NCHRP 628 addresses SCC girders and does not recommend deviations from standard practice for prestress losses.

- Camber – No deviation from standard practice is recommended for the prediction of camber for SCLC or HESLC girders.

  SCC and HESC girders were not a part of this project and therefore the recommendations above are restricted to SCLC and HESLC girders. NCHRP 628 addresses SCC girders and does not recommend deviations from standard practice for prediction of camber.

  It is noted that camber is related to modulus of elasticity, creep, and shrinkage. Therefore, it may be expected that SCC girders could exhibit increased camber values in relation to HESC girders. This effect may be lessened for SCLC girders compared to HESLC girders because the modulus of the aggregate is closer to that of the paste for lightweight concretes. Increased long-term camber was not observed in the SCLC test girders. This may be partially attributed to the fact that the girders were of relatively short length (59 ft. 2 in.) and contained prestressing strands in the top flange.

- Flexural capacity – No deviation from standard practice (AASHTO LRFD, 4th Edition) is recommended for the prediction of nominal flexural capacity for SCLC or HESLC girders.

  SCC and HESC girders were not a part of this project and therefore the recommendations above are restricted to SCLC and HESLC girders. NCHRP 628 addresses SCC girders and does not recommend deviations from standard practice for prediction of ultimate flexural capacity.

  It is noted that the girders used in this study approached but did not achieve the nominal flexural capacity. The use of an unconventional deck system may have contributed to this effect and the failure mode that was observed was related to splitting of the bottom flange along the prestressing strands. Lightweight girders in other studies have been shown to exceed the nominal flexural capacity (FHWA, 2003). In that study the support conditions were mentioned as a consideration that may have contributed to increased measured flexural capacity.

- Fatigue behavior – No deviation from standard practice (AASHTO LRFD, 4th Edition) is recommended for the prediction of fatigue behavior for SCLC girders. However, due to the measured reduction in splitting tensile strength (both SCLC and HESLC) it is recommended that the service state tensile stress limit be reduced by 15 % for both SCLC and HESLC girders. This is consistent with the

factor of 0.85 recommended for reduction of splitting tensile strength for sand-lightweight girders in the AASHTO LRFD, 4th Edition.

SCC and HESC girders were not a part of this project and therefore the recommendations above are restricted to SCLC and HESLC girders. NCHRP 628 does not address fatigue behavior of SCC girders. Where fatigue is a critical design consideration close monitoring of the results of the trial batches in regard to splitting tensile strength (or modulus of rupture) is recommended.

It should be carefully noted that the fatigue testing in this project was limited to a single specimen (SCLC) under a single set of conditions (stress state, number of cycles, cyclic loading rate, girder geometry, prestressing configuration, etc.). This recommendation should be interpreted accordingly and further fatigue testing of SCLC and HESLC girders is recommended. It is noted that fatigue behavior of high strength prestressed concrete girders is an item of interest as noted in other studies, including Tanner and Ziehl, 2005 and the related publication of Roller et al., 2007.

REFERENCES CITED

American Association of State Highway and Transportation Officials, (2004), "AASHTO LRFD Bridge Design Specifications – 3rd Edition including 2005 and 2006 Interim Revisions," Washington, DC (2004).

American Association of State Highway and Transportation Officials, (2007), "AASHTO LRFD Bridge Design Specifications – 4th Edition with 2008 and 2009 Interim Revisions," Washington, DC.

ACI Committee 209 (1997) "Prediction of Creep, Shrinkage, and Temperature effects in Concrete Structures." (ACI 209R-97) American Concrete Institute, Farmington Hills, MI.

ACI Committee 318 (2002) "Building Code Requirements for Structural Concrete (ACI 318-02) and Commentary (ACI 318-02)," American Concrete Institute, Farmington Hills, MI.

ACI Committee 318 (2005) "Building Code Requirements for Structural Concrete (ACI 318-05) and Commentary (ACI 318-05)," American Concrete Institute, Farmington Hills, MI.

ACI Committee 363, (1998), "Guide to Quality Control and Testing of High-Strength Concrete", ACI 363.2R-98, American Concrete Institute, Farmington Hills, MI.

ACI Committee 437, (2007), "Test Load Magnitude, Protocol and Acceptance Criteria", (ACI 437.1R-07), American Concrete Institute, Farmington Hills, MI, 2006, 83 pp.

ASTM International, (2004) "C39/C39M - 05e2 - Compressive Strength of Cylindrical Concrete Specimens," American Society for Testing and Materials, West Conshohocken, PA.

ASTM International, (2003) "C143/C143M - Standard Test Method for Slump of Hydraulic Cement Concrete," American Society for Testing and Materials, West Conshohocken, PA.

ASTM International, (1999) "C157/C157M - Standard Test Method for Length Change of Hardened Hydraulic-Cement Mortar and Concrete," American Society for Testing and Materials, West Conshohocken, PA.

ASTM International, (1997) "C215/C215M - Standard Test Method for Fundamental Transverse, Longitudinal, and Torsional Resonant Frequencies of Concrete Specimens," American Society for Testing and Materials, West Conshohocken, PA.

ASTM International, (2009), "C231 - Standard Test Method for Air Content of Freshly Mixed Concrete by the Pressure Method," American Society for Testing and Materials, West Conshohocken, PA.

ASTM International, (2009), "ASTM C457 - Standard Test Method for Microscopical Determination of Parameters of the Air-Void System in Hardened Concrete", American Society for Testing and Materials, West Conshohocken, PA.

ASTM International, (2002), "C469 - Standard Test Method for Static Modulus of Elasticity and Poisson's Ratio of Concrete in Compression," American Society for Testing and Materials, West Conshohocken, PA.

ASTM International, (2004), "ASTM C496/C 496M Standard Test Method for Splitting Tensile Strength of Cylindrical Concrete Specimens", American Society for Testing and Materials, West Conshohocken, PA.

ASTM International, (1994) "C512 - Standard Test Method for Creep of Concrete in Compression," American Society for Testing and Materials, West Conshohocken, PA.

ASTM International, (2008) "C666 - Standard Test Method for Resistance of Concrete to Rapid Freezing and Thawing," American Society for Testing and Materials, West Conshohocken, PA.

ASTM International, (2001) "C1202 – Standard Test Method for Electrical Indication of Concrete's Ability to Resist Chloride Ion Penetration," American Society for Testing and Materials, West Conshohocken, PA.

ASTM International, (2009a), "C1611 / C1611M - 09b Standard Test Method for Slump Flow of Self-Consolidating Concrete", American Society for Testing and Materials, West Conshohocken, PA.

ASTM International, (2009b), "ASTM C1621 / C1621M - 09b, Standard Test Method for Passing Ability of Self-Consolidating Concrete by J-Ring", American Society for Testing and Materials, West Conshohocken, PA.

Attiogbe, E., Daczko, J., (2003) "Engineering Properties of Self-Consolidating Concrete," *First North American Conference on the Design and Use of Self-Consolidating Concrete,* Evanston, Il. pp. 331-336.

Badman, C., et al, (2003) "Interim Guidelines for the Use of Self-Consolidating Concrete in PCI Member Plants," PCI Journal, Chicago, IL, April, 88p.

Bailey, J., Schindler, A., Brown, D., (2005) "An Evaluation of the Use of Self-Consolidating Concrete (SCC) for Drilled Shaft Applications.",Report No. 1, Auburn, AL., July, pp. 4-18.

Bardhan-Roy, (1993), "Structural Lightweight Aggregate Concrete – Chapter 7, Lightweight Concrete for Special Structures", Edited by J. L. Clarke, Chapman and Hall.

Berke, N., Cornman, C., Jeknavorian, A., Knight, G., Wallevik, O. (2003) "The Effective Use of Superplasticizers and Viscosity Modyfying Agents in Self-Consolidating Concrete," *First North American Conference on the Design and Use of Self-Consolidating Concrete,* Evanston, Il. pp. 165-170.

Brite EuRam (2000), "Rational Production and Improved Working Environment Through Using Self Compacting Concrete," http://www.civeng.ucl.ac.uk/ research/concrete/ Final%20technical%20report,%20ver% 207%20(001020)%20.PDF, July 2000.

Casadei, P., Parretti, R., Heinze, T., and Nanni, A. (2005), "In-Situ Load Testing of Parking Garage RC Slabs: Comparison Between 24-Hour and Cyclic Load Testing", ASCE, Practice Periodical on Structural Design and Construction, Vol. 10, No. 1, February 1, pp. 40-48.

Chandra, S., and Berntsson, L., (2002), "Lightweight Aggregate Concrete - Science, Technology, and Applications", William Andrew Publishing/Noyes.

Choi, Y., Kim, Y., Shin, H., Moon, H., (2006), "An experimental research on the fluidity and mechanical properties of high-strength lightweight self-compacting concrete," Cement and Concrete Research, Vol. 36, pp. 1595–1602.

Davis, R., (2008**), "**Creep and Shrinkage of Structural Lightweight Concretes", HPC Bridge Views, Issue 49, May/June, http://www.hpcbridgeviews.com/i49/ Article4.asp

EFCA, (2005), "The European Guidelines for Self-Compacting Concrete, Specification, Production and Use," Web Site: http://www.efca.info/pdf/SCC%20Guidelines% 20May%202005.pdf, May 2005.

EFNARC, (2002), Specification and Guidelines for Self-Compacting Concrete. EFNARC (European Federation of Producers and Applicators of Specialist Products for Structures), 2002 (February). http://www. efnarc.org/pdf/SandGforSCC.PDF.

FHWA, (1996), "Implementation Program on High Performance Concrete - Guidelines for Instrumentation of Bridges," FHWA SA-96-075, August 1996 Web Site: http://www.fhwa.dot.gov/bridgehpcinstr.htm (October 6, 2003), 18 pp.

FHWA (2003), “Investigation of Transfer Length, Development Length, Flexural Strength, and Prestress Losses in Lightweight Prestressed Concrete Girders”, Authors: Cousins, T., and Nassar, A., Final Contract Report – FHWA/VTRC 03-CR20, 44 pp.

FHWA, (2005), “High Performance Concrete Structural Designer’s Guide” by the High Performance Concrete Technology Delivery Team, US Department of Transportation, Federal Highway Administration, FHWA-RCBAL-05-007, 120 pp.

FHWA, (2007), “Synthesis of Research and Provisions Regarding the Use of Lightweight Concrete in Highway Bridges”, Author: Russell, H., FHWA-HRT-07-053, 114 pp.

Galati, N., Casadei, P., Lopez, A., and Nanni, A., (2004), “Load Test Evaluation of Augspurger Ramp Parking Garage, Buffalo, NY”, Report No. 04-50, Center for Infrastructure Engineering Studies, University of Missouri-Rolla, Rolla, Missouri 65409-0710, 21 pp.

Galati, N., Nanni, A., Tumialan, G., and Ziehl, P., (2008), "In-Situ Evaluation of Two RC Slab Systems – Part I: Load Determination and Loading Procedure ", ASCE Journal of Performance of Constructed Facilities, Volume 22, No. 4, pp. 207-216.

Gold, W., and Nanni, A., (1998), “In-situ Load Testing to Evaluate New Repair Techniques”, Proceedings of the NIST Workshop on Standards Development for the Use of Fiber Reinforced Polymers for the Rehabilitation of Concrete and Masonry Structures, Dat Duthinh Editor, Tucson, Arizona, pp. 102-112.

Hwang, C., Hung, M., (2005), “Durability design and performance of self-consolidating lightweight concrete,” Elsevier, 619-626.

Hwang, S., Khayat, K., and Bonneau, O., (2006), “Performance-Based Specifications of Self-Consolidating Concrete Used in Structural Applications,” ACI Materials Journal, Vol. 103, Issue 2, pp. 121 – 129.

International Code Council (2003), “International Building Code,” International Code Council, Inc., Country Club Hills, IL.

Kahn, L. and Lopez, M., (2005), “Prestress Losses in High Performance Lightweight Concrete Pretensioned Bridge Girders”, PCI Journal, September – October 2005, pp. 84 – 94.

Khayat, K., Hu, C., Laye, J., (2003) "Importance of Aggregate Packing Density on Workability of Self-Consolidating Concrete," *First North American Conference on the Design and Use of Self-Consolidating Concrete,* Evanston, Il. pp. 55-62.

Kolzos R., (2000), "Transfer and Development Length of Fully Bonded l/2-inch Prestressing Strand in Standard AASHTO Type I Pretensioned High Performance Lightweight Concrete (HPLC) Beams. Thesis, University of Texas at Austin, 2000.

Lo, T., Tang, P., Cui, H., and Nadeem, A., (2007), "Comparison of workability and mechanical properties of self-compacting lightweight concrete and normal self-compacting concrete" Materials research innovations, 45-50.

Lydon, F.D., and Balendran, R. V., "Some Properties of Higher Strength Lightweight Concrete under Short-Term Tensile Stress", Journal of Lightweight Concrete, September, No. 3, 2 (1980) 125-139.

Martin, David J., (2003) "Economic Impact of SCC in Precast Applications," *First North American Conference on the Design and Use of Self-Consolidating Concrete,* Evanston, Il. pp. 147-152.

Mettemeyer, M., (1999), "In situ rapid load testing of concrete structures." Master's thesis, Dept. of Civil Engineering, Univ. of Missouri-Rolla, Rolla, Mo.

Mettemeyer, M., and Nanni, A. (1999), "Guidelines for Rapid Load Testing of Concrete Structural Members", Report No. 99-5, Center for Infrastructure Engineering Studies, University of Missouri-Rolla, Rolla, Missouri 65409-0710, 99 pp.

Meyer, K. and Kahn, L., (2002), "Lightweight concrete reduces weight and increases span length of pretensioned concrete bridge girders", PCI Journal, 2002, vol. 47, no. 1, pp. 68 – 75.

Melby, K., Jordet, E., and Hansvold, C., (1996), "Long-span bridges in Norway constructed in high-strength LWA concrete" Elsevier, 845-849.

Myers, J. J. and Carrasquillo, R. L., "Production and Quality Control of High Performance Concrete in Texas Bridge Structures," Research Report 580/589-1, Center for Transportation Research, University of Texas, Austin, TX (1999) 176 pp.

Naito, C., Brunn, G., Parent, G., Tate, T., (2005) "Comparative Performance of High Early Strength and Self-Consolidating Concrete for Use in Precast Bridge Beam Construction," ATLSS Report No. 05-03, Bethlehem, PA.

Nanni, A., and Gold, W., (1998a), "Evaluating CFRP Strengthening Systems In-situ", Concrete Repair Bulletin, International Concrete Repair Institute, Vol. 11, No. 1, January-February, pp. 12-14.

Nanni, A., and Gold, W., (1998b), "Strength Assessment of External FRP Reinforcement", Concrete International, American Concrete Institute, June, pp. 39-42.

Meyer, K., Buchberg, B., and Kahn, L., (2006), "High-Strength Lightweight Concrete for Application in Highway Girders," SP-234: Seventh CANMET/ACI International Conference on Durability of Concrete, Editor: V.M. Malhotra.

NCHRP Report 496, (2003), "Prestress Losses in Pretensioned High-Strength Concrete Bridge Girders," authors: Tadros, M., Al-Omaishi, N., Seguirant, S., and Gallt, J., Transportation Research Board, Washington, D. C.

NCHRP Report 595, (2007), "Application of the LRFD Bridge Design Specifications to High-Strength Structural Concrete: Flexure and Compression Provisions," Authors: Rizkalla, S., Mirmiran, A., Zia, P., Russell, H., and Mast, R., Transportation Research Board, Washington, D.C.

NCHRP Report 628, (2008), "Self-Consolidating Concrete for Precast, Prestressed Concrete Bridge Elements", Authors: Khayat, K., and Mitchell, D., Transportation Research Board, Washington, D.C.

Ohno, H., Kawall, Kuroda, Y., and Ozawa, K. (1993). "Development of vibration free high strength lightweight concrete and its application," Proceedings FIP Symposium, Kyoto, Vol I. 297-304.

PCI (1997), "Precast Prestressed Bridge Design Manual," (MNL-133-97), Chicago, IL.

PCI (2003a), "Interim Guidelines for the Use of Self-Consolidating Concrete in Precast /Prestressed Concrete Institute Member Plants".

PCI (2003b), "PCI Bridge Design Manual".

Peterman R., Ramirez J., and Olek, J. *Evaluation ofStrand Transfer and Development Lengths in Pretensioned Girders with Semi-Lightweight Concrete.* FHWA-IN-JTRP-99/3, Federal Highway Administration, Washington, D.C., July 1999.

Pfeifer, D., (1968), "Sand Replacement in Structural Lightweight Concrete", ACI Journal, Vol. 65, No. 2, pp. 131 – 139.

Quiroga, P. and Fowler, D., (2004) "Guidelines for Proportioning Concrete Mixtures with High Microfines," Research Report # ICAR 104-2.

Raghaven, K., Sarma, B., and Chattopadhay, D., (2003) "Creep, Shrinkage, and Chloride Permeability of Self-Consolidating Concrete," Conference Proceedings: *First North American Conference on the Design and Use of Self-Consolidating Concrete*, Evanston, Il. pp. 307-311.

Ridge, A., and Ziehl, P., (2006), "Nondestructive Evaluation of Strengthened RC Beams: Cyclic Load Test and Acoustic Emission Methods", ACI Structural Journal, Volume 103, Issue 6, pp. 832-841.

Roller, J., Russell, H., Bruce, R., (2007), "Fatigue Endurance of High-Strength Prestressed Concrete Bulb-Tee Girders," *PCI Journal*, May-June, pp. 30-42

Russell, H., (2009), "Lightweight Concrete – Material Properties for Structural Design", International Bridge Conference, Lightweight Concrete Bridges Workshop, pp. 1-21 (*paper was first presented at the ESCSI Special Workshop on Lightweight Aggregate Concrete Bridges, May, 2008 in conjunction with the 2008 Concrete Bridge Conference and appeared as Paper 141 of the Proceedings).*

SCDOT, (2006), "Bridge Design Manual (2006), South Carolina Department of Transportation, http://www.scdot.org/doing/bridge/pdfs/BD_manual/Files/Cover.pdf

SCDOT, (2008), "Bridge Design Memorandum – DM0108, Design of Prestressed Concrete Girders.

Swedish Ceramic Institute (SCI), (2003), "Surface Chemistry and Rheology," http://www.keram.se/eng/pdf/surface_chemistry.pdf, May.

Swedish Ceramic Institute (SCI), (2004), "Summary Report on Work package 3.2 – Test Methods for Passing Ability," http://www.civeng.ucl.ac.uk/research/concrete/Testing%2DSCC/WP3.2-Summary%20report.pdf, October.

Shadle, R. and Somerville, S., (2003) "The Benefites of Utilizing Fly Ash in Producing Self-Consolidating Concrete," First North American Conference on the Design and Use of Self-Consolidating Concrete, Evanston, Il. pp. 217-220.

Slate, F. O., Nilson, A. H., and Martinez, S., 1986, "Mechanical Properties of High-Strength Lightweight Concrete," ACI Journal, *Proceedings*, Vol. 83, No. 4, July-August, pp. 606-613.

Tanner, C., and Ziehl, P., (2005), "An Evaluation of the Fatigue Behavior of High Performance Concrete Bulb Tee Girders", *Seventh International Symposium on Utilization of High Strength/High Performance Concrete*, Special Publications-228, June 20-24, Washington, D.C.

Waldron, C.; Thomas E. Cousins, T., Nassar, A., and Gomez, J., (2005), "Demonstration of Use of High-Performance Lightweight Concrete in Bridge Superstructure in Virginia," ASCE Journal of Performance of Constructed Facilities, Vol. 19, No. 2, pp. 146 – 154.

Wu, Z., Zhang, Y., Zheng, J, and Ding, Y., (2009), “An experimental study on the workability of self-compacting lightweight concrete”, Construction and Building Materials, Vol. 23, pp. 2087–2092.

Zhang, M.H. and Gjorv, O.E., (1991), “Characteristics of Lightweight Aggregate for High-strength Concrete,” ACI Materials Journal 88 2, pp. 150–158.

Zhang, M.H. and Gjorv, O.E., (1991), “Mechanical Properties of High-strength Lightweight Concrete,” ACI Materials Journal 88 3, pp. 240–247.

Zia, P., Nunez, R., Mata, L, Dwairi, H. (2005) “Implementation of Self-Consolidating Concrete for P restressed Concrete Girders.” *Seventh International Symposium on the Utilization of High-Strength/High-Performance Concrete,* Washington, D.C., pp 297-316.

Ziehl, P., Galati, N., Tumialan, G., and Nanni, A., (2008), "In-Situ Evaluation of Two RC Slab Systems – Part II: Evaluation Criteria", ASCE Journal of Performance of Constructed Facilities, Volume 22, No. 4, pp. 217-227.

APPENDIX

TEC Services
Testing • Engineering • Consulting

March 17, 2009

Dr. Paul Ziehl
University of South Carolina
300 Main Street
Columbia, South Carolina 29208

Phone: 803-777-0671
email: zhiel@engr.sc.edu

Subject: **Freezing and Thawing Test Results – ASTM C 666-03 (*Procedure A*)**
TEC Services Project No: TEC 08-0684
TEC Services Laboratory ID: 08-550

Dear Dr. Ziehl:

As requested, Testing, Engineering and Consulting, Inc. (TEC Services) has performed laboratory rapid freezing and thawing testing on 4 specimens sent to us by your office. The samples were tested it in accordance with ASTM C 666-03 *Resistance of Concrete to Rapid Freezing and Thawing – Procedure A (freezing and thawing in water)*. The results of our testing are reported below.

Sample ID	Total Cycles Completed	Start Fundamental Transverse Frequency, KHz	Final Fundamental Transverse Frequency, kHz	Relative Dynamic Modulus, Percent	Pass/Fail**
Normal 1	153	1.484	0.781	28	Fail
Normal 2	153	2.148	1.719	92	NA
SCC 1	153	1.387	0.645	22	Fail
SCC 2	153	1.484	0.371	6	Fail

***Note:** The testing was halted after 153 cycles due to extensive cracking of the samples.
** **Note:** Per ASTM C666, any sample with a relative dynamic modulus less than 60% after 300 cycles is considered failing.

We appreciate the opportunity of providing our services to you. If you have any questions pertaining to this report or need any additional information, please do not hesitate to call us.

Sincerely,

TESTING, ENGINEERING, AND CONSULTING SERVICES, INC.

Anne Miller
Staff Engineer

Shawn McCormick
Lab Manager

Attachments: Photos 1 – 5: Cracking of the freeze thaw beams.

Photo 1 – Cracking visible on the side of beam Normal 1

Photo 2 – Cracking visible on the top of beam Normal 1

Photo 3 –Normal 2 (no visible cracking)

Photo 4 –Normal 2 (no visible cracking)

Photo 5 – Cracking visible on the side of beam SCC 1

Photo 6 – Close-up of cracking visible on the side of beam SCC 1

Photo 7 – Cracking visible on the top of beam SCC 1

Photo 8 – Cracking visible on the side of beam SCC 2

Photo 9 – Cracking visible on the top of beam SCC 2